UNIVERSITAT DE BARCELONA

Grosor de la pared auricular en la ablación por catéter de fibrilación auricular y otras aplicaciones del angioTAC de la aurícula izquierda

Cheryl Terés Castillo

GROSOR DE LA PARED AURICULAR EN LA ABLACIÓN POR CATÉTER DE FIBRILACIÓN AURICULAR

Y otras aplicaciones del angiotac de la aurícula izquierda

Memoria de tesis doctoral presentada por **Cheryl Terés Castillo** para optar al grado de doctora por la Universidad de Barcelona.

Dirigida por:
Antonio Berruezo Sánchez, MD, PhD, Instituto del Corazón, Centro Médico Teknon
José Tomás Ortiz Pérez MD, PhD, Hospital Clínic; Institut d'Investigació August Pi i Sunyer; Instituto del Corazón, Centro Médico Teknon, Barcelona, Spain.

Tutor: **José Tomás Ortiz Pérez**, Instituto del Corazón, Centro Médico Teknon; Hospital Clínic; Institut d'Investigació August Pi i Sunyer, Barcelona, Spain.

Programa de Doctorado Medicina e Investigación Traslacional.

Facultad de Medicina y Ciencias de la Salud. Universidad de Barcelona.

Septiembre 2023.

UNIVERSITAT DE BARCELONA

Facultat de Medicina i Ciències de la Salut – Campus Clínic

Informe director/s /tutor sobre l'autorització del dipòsit de la tesi

Dr./a.Antonio Berruezo Sánchez, com a director/tutor de la tesi doctoral titulada "GROSOR DE LA PARED AURICULAR EN LA ABLACIÓN POR CATÉTER DE FIBRILACIÓN AURICULAR Y OTRAS APLICACIONES DEL ANGIOTAC DE LA AURÍCULA IZQUIERDA"
i, d'acord amb el que s'estableix a l'article 35 Normativa reguladora del Doctorat a la Universitat de Barcelona, emeto el següent:

INFORME

(Informe detallat i motivat sobre el contingut de la tesi i sobre l'autorització de dipòsit de la tesi que s'ha demanat)

Aval de tesis doctoral de Cheryl Teres Castillo

Escribo para avalar con entusiasmo la tesis doctoral de Cheryl Teres Castillo, titulada "Grosor de la pared auricular en la ablación por catéter de fibrilación auricular y otras aplicaciones del angiotac de la aurícula izquierda". Habiendo seguido de cerca el recorrido académico de la doctoranda, es evidente que esta obra es el resultado de un extenso esfuerzo investigador, un entendimiento exhaustivo de la fibrilación auricular.

A lo largo del proceso de investigación, Cheryl ha demostrado una determinación destacable, habilidades analíticas y una capacidad para pensar de forma innovadora sobre los desafíos a los cuales nos enfrentamos durante las intervenciones de ablación de fibrilación auricular. Las metodologías empleadas fueron rigurosas y los conocimientos derivados fueron tanto originales como significativos.

Está claro que esta tesis expande nuestros conocimientos actuales en el campo de la ablación de fibrilación auricular proporcionando herramientas que mejoran la eficiencia y la seguridad del procedimiento, y estoy seguro que será una referencia valiosa tanto para académicos como para profesionales en los próximos años.

Desde mi punto de vista, la tesis doctoral de Cheryl Teres Castillo, es un brillante ejemplo de investigación innovadora. No solo cumple, sino supera las expectativas de una disertación doctoral en Medicina. En consecuencia, en calidad de co-director, recomiendo su aceptación y espero presenciar el impacto positivo que tendrá en la comunidad académica.

UNIVERSITAT DE BARCELONA

Facultat de Medicina i Ciències de la Salut – Campus Clínic

Barcelona, 4 d'/de Septiembre de 2023.

(signat)

Dr./a **Antonio Berruezo Sánchez**.

Un cop s'hagi emplenat l'informe, s'ha d'adjuntar i s'ha de fer arribar al doctorand o al president de la Comissió Acadèmica del programa de doctorat responsable de la tesi.

UNIVERSITAT DE BARCELONA

Facultat de Medicina i Ciències de la Salut – Campus Clínic

Informe director/s /tutor sobre l'autorització del dipòsit de la tesi

Dr./a. José Tomás Ortiz Pérez, com a director/tutor de la tesi doctoral titulada "ROSOR DE LA PARED AURICULAR EN LA ABLACIÓN POR CATÉTER DE FIBRILACIÓN AURICULAR Y OTRAS APLICACIONES DEL ANGIOTAC DE LA AURÍCULA IZQUIERDA " i, d'acord amb el que s'estableix a l'article 35 Normativa reguladora del Doctorat a la Universitat de Barcelona, emeto el següent:

INFORME

(Informe detallat i motivat sobre el contingut de la tesi i sobre l'autorització de dipòsit de la tesi que s'ha demanat)

Escribo este informe para respaldar la tesis doctoral de Cheryl Teres Castillo, titulada "Grosor de la pared auricular en la ablación por catéter de fibrilación auricular y otras aplicaciones del angiotac de la aurícula izquierda". En calidad de co-director, he supervisado la evolución de la tesis que tras varios años de investigación ha resultado en una disertación completa, clara y estructurada que demuestra la capacidad de la doctoranda para transmitir sur conocimientos extensivos en el campo de la fibrilación auricular.

La tesis redactada por la doctoranda y las publicaciones científicas que la componen se han realizado siguiendo una metodología científica adecuada en aspectos innovadores de la aplicación de la tomografía computerizada en el campo de la fibrilación auricular y de la evaluación de las intervenciones de ablación por catéter. El resultado es un trabajo que combina principios teóricos con implicaciones clínicas prácticas. Esta tesis refleja y confirma la capacidad de la doctoranda como investigadora, resaltando su pensamiento crítico aplicado al campo de la fibrilación auricular, y contribuye al conocimiento científico general para inspirar y profundizar otras futuras investigaciones. De esta manera reconozco el calibre académico emergente de Cheryl Teres Castillo y doy mi aval con confianza a su doctorado.

Barcelona, 4 d'/de Septiembre de 2023.

UNIVERSITAT DE BARCELONA

Facultat de Medicina i Ciències de la Salut – Campus Clínic

(signat)

Dr./a **José Tomás Ortiz Pérez**

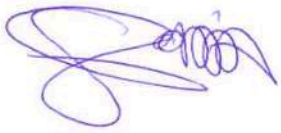

Un cop s'hagi emplenat l'informe, s'ha d'adjuntar i s'ha de fer arribar al doctorand o al president de la Comissió Acadèmica del programa de doctorat responsable de la tesi.

Los abajo firmantes, Dres Antonio Berruezo Sánchez y Dr José Tomás Ortiz Pérez en calidad de codirectores y Dra Cheryl Terés Castillo en calidad de doctoranda,

MANIFESTAMOS

que la presente tesis no contiene plagio y que conocemos y consentimos que la tesis podrá ser sometida a procedimientos para comprobar su originalidad, y que en este trabajo de investigación se han seguido los códigos éticos, y de buenas prácticas.

En Barcelona, a primero de septiembre de 2023.

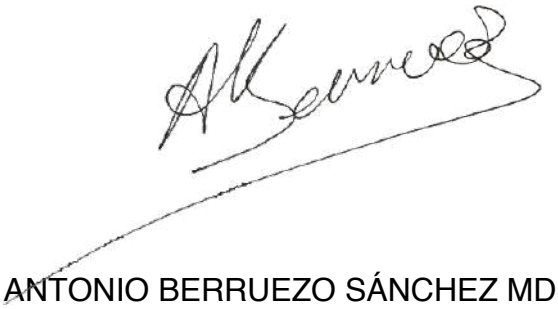

ANTONIO BERRUEZO SÁNCHEZ MD, PhD

JOSÉ TOMÁS ORTIZ PÉREZ MD, PhD

CHERYL TERES CASTILLO MD

Yo, Cheryl Terés Castillo con DNI [redacted], estudiante en el programa de doctorado de la Facultad de Medicina de la Universidad de Barcelona, como autora de la Tesis doctoral con título:

“Grosor de la pared auricular en la ablación por catéter de fibrilación auricular y otras aplicaciones del angiotac de la aurícula izquierda”

DECLARO QUE:

La tesis es una obra original que no infringe los derechos de propiedad intelectual ni los derechos de propiedad industrial u otros, de acuerdo con el ordenamiento jurídico vigente, en particular, la Ley de Propiedad Intelectual (R.D. legislativo 1/1996, de 12 de abril, por el que se aprueba el texto refundido de la Ley de Propiedad Intelectual, modificado por la Ley 2/2019, de 1 de marzo, regularizando, aclarando y armonizando las disposiciones legales vigentes sobre la materia), en particular, las disposiciones referidas al derecho de cita.

Del mismo modo, asumo frente a la Universidad cualquier responsabilidad que pudiera derivarse de la autoría o falta de originalidad del contenido de la tesis presentada de conformidad con el ordenamiento jurídico vigente.

En Barcelona, a primero de septiembre de 2023.

A mi familia por su apoyo incondicional y a mis mentores por sus invaluables conocimientos.

Financiamiento

El trabajo de investigación no contó con financiamiento público. La Dra Cheryl Terés financió su Fellowship en Barcelona gracias a la Beca de la fundación *Schweizeriche Herzrhythmus Stiftung* para jóvenes electrofisiólogos del 2018. https://shrs.ch/de/stiftung/stipendien/bisherige-stipendien/

ÍNDICE

MATERIAL, MÉTODOS Y RESULTADOS – PUBLICACIONES

ÍNDICE DE FIGURAS

ÍNDICE DE TABLAS

ABREVIATURAS Y ACRÓNIMOS

FA fibrilación auricular
RF radiofrecuencia
VP venas pulmonares

Tesis en formato de compendio de publicaciones

La tesis consta de 4 artículos:

1. **Teres C**, Soto-Iglesias D, Penela D, Jáuregui B, Ordoñez A, Chauca A, Huguet M, Ramírez-Paesano C, Oller G, Jornet A, Palet J, Santana D, Panaro A, Maldonado G, de Leon G, Gualis B, Jimenez-Britez G, Evangelista A, Carballo J, Ortiz-Perez JT, Berruezo A. Left atrial wall thickness of the pulmonary vein reconnection sites during atrial fibrillation redo procedures. Pacing Clin Electrophysiol. 2021 May;44(5):824-834. **IF 1.9 Q2**

2. **Teres C**, Soto-Iglesias D, Penela D, Jáuregui B, Ordoñez A, Chauca A, Carreño JM, Scherer C, San Antonio R, Huguet M, Roque A, Ramírez C, Oller G, Jornet A, Palet J, Santana D, Panaro A, Maldonado G, de Leon G, Jiménez G, Evangelista A, Carballo J, Ortíz-Pérez JT, Berruezo A. Personalized paroxysmal atrial fibrillation ablation by tailoring ablation index to the left atrial wall thickness: the 'Ablate by-LAW' single-centre study-a pilot study. Europace 2022 Mar 2;24(3):390-399. **IF 6.1 Q1**

3. **Teres C**, Soto-Iglesias D, Penela D, Jáuregui B, Ordoñez A, Chauca A, Carreño JM, Scherer C, Huguet M, Ramírez C, Mandujano JT, Maldonado G, Panaro A, Carballo J, Cámara Ó, Ortiz-Pérez JT, Berruezo A. Relationship between the posterior atrial wall and the esophagus: Esophageal position during atrial fibrillation ablation. Heart Rhythm O2. 2022 Feb 13;3(3):252-260. **IF 1.9 Q2**

4. **Teres C**, Soto-Iglesias D, Penela D, Falasconi G, Viveros D, Meca-Santamaria J, Bellido A, Alderete J, Chauca A, Ordoñez A, Martí-Almor J, Scherer C, Panaro A, Carballo J, Cámara Ó, Ortiz-Pérez JT, Berruezo A. Relationship between the posterior atrial wall and the esophagus: esophageal position and temperature measurement during atrial fibrillation ablation (AWESOME-AF). A randomized controlled trial. J Interv Card Electrophysiol. 2022 Dec;65(3):651-661. **IF 1.8 Q2**

INTRODUCCIÓN

La fibrilación auricular (FA) es la arritmia más frecuente en el ser humano (1). A pesar del progreso en el manejo de pacientes con FA, ésta sigue siendo una de las principales causas de accidente cerebrovascular, insuficiencia cardíaca, muerte súbita y morbilidad cardiovascular en el mundo. Además, se prevé que el número de pacientes con FA aumente considerablemente en los próximos años. En consecuencia, la FA supone una carga importante para los pacientes, los médicos y los sistemas de salud a nivel mundial.

Los enfoques terapéuticos actuales para la FA todavía tienen limitaciones importantes con respecto a la eficacia y la probabilidad de efectos adversos significativos. Estas limitaciones han inspirado esfuerzos sustanciales para desarrollar nuestra comprensión de los mecanismos subyacentes a la FA, con la premisa de que una mejor comprensión de los mecanismos conducirá a enfoques terapéuticos innovadores y mejorados. Por otra parte, las terapias ablativas evolucionan constantemente gracias a los avances tecnológicos de manera que hoy en día existen numerosos tipos de energía disponibles para realizar las terapias intervencionistas de la FA.

1. Definición de fibrilación auricular

Una arritmia es cuando el corazón late demasiado lento, demasiado rápido o de manera irregular. La fibrilación auricular es una taquiarritmia supraventricular en la que la activación eléctrica de las aurículas (las cavidades superiores del corazón) es descoordinada e irregular, perdiendo así la aurícula su capacidad contráctil resultando en una contracción auricular ineficaz en la que la sangre no fluye tan bien como debería desde las aurículas a los dos ventrículos.

Las características electrocardiográficas de la FA incluyen:

- Intervalos R-R irregularmente irregulares (cuando la conducción auriculoventricular no está alterada),
- Ausencia de ondas P repetitivas distintas, y
- Activaciones auriculares irregulares.

La fibrilación auricular puede ocurrir en episodios breves o puede ser una condición permanente. Los documentos de consenso sobre la ablación quirúrgica y con catéter definen la fibrilación auricular (FA) como una arritmia que dura ≥30 s, asumiendo que un evento de FA breve se correlaciona con eventos de FA más prolongados o con una alta prevalencia.

2. Epidemiología de la fibrilación auricular

En todo el mundo, la FA es la arritmia cardíaca sostenida más común en adultos. Se calcula que en 2016 43,6 millones de individuos presentaban una FA. En la Unión Europea, la prevalencia de FA en adultos mayores de 55 años se estimó en 8,8 millones (IC 95 %, 6,5–12,3 millones) en 2010 y se proyectó que aumentaría a 17,9 millones en 2060 (IC 95 %, 13,6 millones–23,7 millones) (2). Fig 1 y 2. Los factores de riesgo asociados a la ocurrencia de FA son: hipertensión arterial, diabetes mellitus (tipo 1 o 2), sobrepeso, tabaquismo, consumo de alcohol y antecedentes de infarto de miocardio o insuficiencia cardíaca. La tasa de incidencia varía según la raza en el Reino Unido, la tasa de incidencia por 1000 años-persona estandarizada fue 8,1 (IC 95 %, 8,1–8,2) en blancos versus 5,4 (IC 95 %, 4,6–6,3) en asiáticos y 4,6 (IC 95 %, 4,0–5,3) en pacientes afrodescendientes (3).

Figura 1. Prevalencia global de la FA(4).

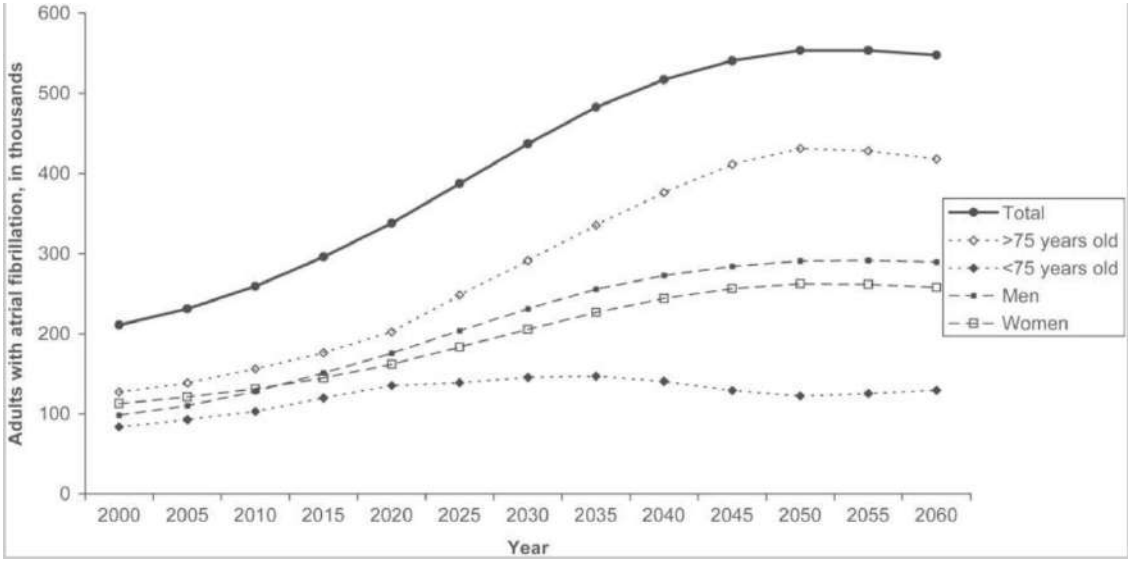

Figura 2. Número proyectado de adultos con fibrilación auricular en la Unión Europea entre 2000 y 2060(2).

3. Etiopatogenia de la fibrilación auricular

Varios factores provocan alteraciones auriculares complejas, como fibrosis inducida por estiramiento, hipocontractilidad, infiltración grasa, inflamación, remodelado vascular, isquemia, disfunción de los canales iónicos e inestabilidad del calcio. Todos magnifican la ectopia y las alteraciones de la conducción, aumentan la propensión auricular a desarrollar/mantener la FA y facilitan el estado de hipercoagulabilidad que se asocia. La hipocontractilidad reduce la tensión de cizallamiento endotelial local, lo que aumenta la expresión del inhibidor del activador del plasminógeno, y la inflamación inducida por isquemia aumenta la expresión de moléculas de adhesión endotelial o promueve el desprendimiento de células endoteliales, lo que da como resultado la exposición del factor tisular al torrente sanguíneo. La FA por sí misma agrava muchos de estos mecanismos, lo que puede explicar su carácter progresivo.

3.1. Remodelación eléctrica

En general, la FA se asocia con una variedad de patologías y factores de riesgo cardiovascular establecidos que pueden causar remodelación estructural y/o eléctrica (canales iónicos). Algunas son: la edad, la presencia de cardiopatías preexistentes (coronaria, valvular), hipertensión, diabetes,

tabaquismo, obesidad, apnea obstructiva del sueño, consumo de alcohol y ejercicio físico intenso. Además, la propia FA provoca una remodelación de la corriente iónica que desempeña un papel importante en la fisiopatología de la FA. Las propiedades eléctricas auriculares se modifican al afectar la expresión y función de los canales iónicos, las bombas y los intercambiadores, creando así un sustrato propenso a la reentrada y promoviendo la arritmia. Este concepto, conocido como remodelación de la taquicardia auricular, se describió por primera vez en modelos animales y demostró que la estimulación auricular rápida a largo plazo o el mantenimiento de la FA favorece la aparición y el mantenimiento de la FA (5). El mecanismo molecular consiste en una serie de modificaciones que dan como resultado un acortamiento del período refractario debido un acortamiento de la duración del potencial de acción i) disminución de la corriente de Ca2+ tipo L, ii) aumento del rectificador interno corriente de K+, y iii) expresión/distribución anormal de los hemicanales de conexinas de las uniones gap intercelulares (6). La actividad automática anormal ocurre cuando un aumento en las corrientes despolarizantes internas dependientes del tiempo transportadas por Na^+ o Ca_2^+ (haciendo que el interior celular sea más positivo) o una disminución en las corrientes externas repolarizantes transportadas por K^+ (que mantienen el interior celular negativo) provoca una despolarización celular progresiva tiempo-dependiente. Cuando se alcanza el umbral de potencial, la célula dispara, produciendo una actividad automática. Si se produce una descarga automática antes del siguiente latido normal (sinusal), tiene lugar una activación auricular ectópica (7). Se cree que los focos auriculares ectópicos de ciclo corto clínicamente típicos (P sobre T) surgen a través de la actividad desencadenada, más típicamente causada por posdespolarizaciones retardadas (PDR), pero en algunos casos por posdespolarizaciones tempranas (PDT). Las PDR son oscilaciones del potencial de membrana que se producen después de la repolarización completa del potencial de acción desencadenante. Constituyen el mecanismo más importante de las arritmias auriculares focales y se ven favorecidas por condiciones que producen sobrecarga de Ca2+, como isquemia, estimulación betaadrenérgica, baja concentración extracelular de K^+ y taquicardia (8,9). Son

el resultado de una fuga diastólica anormal de Ca2+ desde el retículo sarcoplásmico (RS) a través de los canales de liberación de Ca_2^+ conocidos como receptores de rianodina (10). El exceso de Ca_2^+ diastólico es manejado por el intercambiador Na+/Ca_2^+ de la membrana celular que transporta tres iones Na+ a la célula por cada ion Ca_2^+ extruido, creando una corriente despolarizante neta (llamada corriente de entrada transitoria, o Iti) que produce PDR, lo suficientemente grande como para alcanzar el umbral de descarga ectópica. Las PDR repetitivas causan taquicardias auriculares focales. Por el contrario, las PDT son oscilaciones de membrana que ocurren durante la fase 2 o 3 del potencial de acción. Se originan cuando la duración del potencial de acción es excesivamente prolongada y las corrientes de Ca_2^+ de la membrana celular se recuperan de la inactivación y permiten que el Ca_2^+ se mueva hacia adentro, generando así un nuevo potencial de acción ascendente (11). Los miofibroblastos pueden aumentar el potencial de reentrada de las células miocárdicas adyacentes, acercándolas al umbral de disparo e iniciando la actividad focal. La actividad ectópica puede ser transitoria, manifestándose como latidos ectópicos aislados o taquicardia sostenida.

3.2. Remodelación estructural

La remodelación estructural se caracteriza por un agrandamiento auricular y una fibrosis tisular. Morillo, et al. describieron por primera vez modificaciones estructurales en un modelo canino de taquiarritmia auricular (12). La microscopía electrónica mostró un aumento en el número y tamaño de las mitocondrias y la ruptura del retículo sarcoplásmico. También se observaron núcleos agrandados y dilatación del retículo endoplásmico rugoso. Un modelo ovino encontró desdiferenciación con agotamiento del material contráctil (sarcómeros) y acumulación de glucógeno, pero más bien múltiples mitocondrias pequeñas. Las células no presentaban atrofia, por el contrario, estaban agrandadas y no se observaban cambios degenerativos ni alteraciones en la matriz extracelular (13). Sin embargo, los estudios realizados en aurículas de perros y humanos mostraron cambios degenerativos y evidencia de muerte celular necrótica y apoptótica de los cardiomiocitos (14–

16). La implicación clínica de esta diferencia sería la reversibilidad en el caso de desdiferenciación en comparación con la irreversibilidad para la degeneración. La fibrosis auricular es una característica común de muchos precursores de la fibrilación auricular, como la insuficiencia cardíaca congestiva, la cardiopatía isquémica, la valvulopatía, la senescencia y la propia fibrilación auricular. La implicación clínica de esta diferencia sería la reversibilidad en el caso de desdiferenciación en comparación con la irreversibilidad para la degeneración. De hecho, la persistencia de la FA se correlaciona con la cantidad de fibrosis y contribuye a la resistencia terapéutica en la arritmia persistente (17–19). La fibrosis consiste básicamente en el depósito de proteínas de la matriz extracelular por parte de los fibroblastos, que son células no excitables y las que se encuentran con mayor frecuencia en el corazón (20). Esta matriz extracelular crea una barrera para la propagación del impulso. Además, las interacciones entre los cardiomiocitos y los fibroblastos a través de la creación de uniones comunicantes pueden causar cambios arritmogénicos en la bioelectricidad y las propiedades de conducción de los cardiomiocitos (21–23). Asimismo, se ha comprobado que la rápida activación de los cardiomiocitos auriculares induce fibrosis, creando así un ciclo de arritmia y fibrosis (24). La remodelación estructural solo parece ser reversible durante las primeras fases del trastorno arrítmico, pero su extensión es crucial porque puede alcanzar un umbral más allá del cual ya no se puede restaurar el ritmo sinusal. El agrandamiento auricular está muy a menudo presente en la FA y es un fuerte predictor independiente para el desarrollo de esta (25). De hecho, puede ser una causa o una consecuencia de la FA y puede revertirse parcialmente después de la restauración del ritmo sinusal (26,27).

Estudios histopatológicos han demostrado infiltración de adipocitos en el miocardio de pacientes con FA, cuya extensión se correlaciona con el volumen de tejido adiposo epicárdico. De hecho, se ha observado, en pacientes obesos, que el tejido adiposo epicárdico infiltra la pared de la aurícula izquierda, lo que resulta en una reducción del voltaje endocárdico. Además, el volumen de tejido adiposo epicárdico se correlaciona significativamente con la localización de electrogramas auriculares fraccionados, que son un marcador del

enlentecimiento local de la conducción en pacientes con FA. Por lo tanto, el tejido adiposo epicárdico juega un papel importante en la alteración de las propiedades electrofisiológicas de los tejidos cardíacos (28–30).

3.3. Remodelación autonómica

El sistema nervioso autónomo cardíaco (SNA) se ha implicado en la fisiopatología de varias arritmias, incluida la FA. El papel del SNA en la patogenia de la FA fue reconocido por primera vez por Coumel y colaboradores en 1978(31). En particular, las ramas simpática y parasimpática del sistema nervioso autónomo pueden afectar la actividad eléctrica del corazón, lo que lleva al desarrollo de la fibrilación auricular. La activación simpática puede aumentar la actividad eléctrica en las aurículas, mientras que la activación parasimpática puede disminuir la frecuencia cardíaca y aumentar la variabilidad de la frecuencia cardíaca. Por lo tanto, los desequilibrios en el sistema nervioso autónomo pueden conducir a una mayor susceptibilidad a la fibrilación auricular. Estudios previos demostraron que la hiperactividad del sistema nervioso autónomo cardíaco (SNA) es fundamental en el inicio y mantenimiento de la FA. En un modelo canino de fibrilación auricular paroxística simulada mediante estimulación auricular rápida, la actividad neural en los plexos ganglionares cardíacos aumentó progresivamente a medida que continuaba la estimulación (32,33). La remodelación autonómica progresiva se traduce en con un aumento de la densidad de los nervios simpático y vagal que resulta en una hiperinervación y un cambio del equilibrio simpático/vagal en las primeras 24 horas de FA simulada por estimulación auricular rápida. Trabajando sinérgicamente con la remodelación eléctrica y la remodelación estructural, la remodelación autonómica puede ser un elemento crítico en el mantenimiento de la FA en las primeras 24 horas después de su inicio (34).

4. Mecanismos de iniciación de la fibrilación auricular

4.1. Actividad ectópica focal desencadenada – inicio de la FA

Los estudios clínicos han demostrado que hasta el 94 % de los desencadenantes auriculares que inician paroxismos frecuentes de FA se originan en una de las venas pulmonares (VP), de hecho, desde los manguitos miocárdicos que se extienden más allá de la unión venoauricular hacia las VP (35). Estos manguitos son más extensos alrededor de las VP superiores que alrededor de las inferiores (36). Esta disposición coincide con la distribución de focos de despolarizaciones auriculares prematuras para el inicio espontáneo de FA en las series clínicas publicadas (37). Las propiedades altamente arritmogénicas de las venas torácicas se han relacionado con una anisotropía debida a fibras miocárdicas discontinuas separadas por tejido fibrótico, lo que promueve la excitación reentrante, la automaticidad y la actividad desencadenada. Además, las VP y los *ostia* de las VP de los pacientes con FA muestran con frecuencia propiedades de conducción anormales (fragmentación, alta frecuencia dominante) que promueven aún más la arritmogénesis (38). Curiosamente, también se han encontrado patrones histológicos congruentes en las uniones entre las células del miocardio auricular y la musculatura lisa vascular en el seno coronario, la vena cava superior y las válvulas AV, donde bajo condiciones fisiológicas, se observa actividad eléctrica sincrónica, mientras que se producen posdespolarizaciones y actividad desencadenada durante la estimulación con catecolaminas, la estimulación auricular rápida y/o aumento de la presión intra-auricular(38). Esto explica que las fuentes desencadenantes de la FA puedan localizarse en la pared posterior de la aurícula izquierda, la vena cava superior, el ligamento de Marshall, el ostium del SC, el tabique interauricular, la cresta terminal y la región adyacente al anillo de las válvulas atrioventriculares. Incluso las anomalías congénitas raras, como una vena cava superior izquierda persistente, pueden desencadenar una FA (39–41).

4.2. Reentrada – Mantenimiento de la FA

La reentrada requiere tanto un sustrato vulnerable adecuado, como un disparador que actúa sobre el sustrato para iniciar la arritmia. Dichos sustratos pueden ser causados por alteraciones de las propiedades eléctricas (reentrada

funcional) o por cambios estructurales (reentrada anatómica) (42). Numerosas patologías cardíacas pueden causar sustratos estructurales para reentrada básicamente mediada por el agrandamiento auricular y la fibrosis. De hecho, el tamaño auricular afecta la cantidad de tejido disponible para acomodar los circuitos de reentrada y es un determinante mayor de la aparición de reentradas relacionadas con la FA al hacer disponibles vías anatómicas de mayor dimensión (43). La inducción y mantenimiento de la reentrada requieren un equilibrio crítico entre periodo refractario y propiedades de conducción. En consecuencia, un acortamiento del período refractario y/o una conducción más lenta son los principales mecanismos que contribuyen a la perpetuación de ya sea uno o múltiples circuitos de reentrada. La combinación de todos los componentes eléctricos y los procesos de remodelación estructural promueve el acortamiento del periodo refractario del tejido auricular y por lo tanto disminuye la longitud de onda de los circuitos de reentrada, ya que esta última es el producto del período refractario y la velocidad de conducción. Es fundamental tener en cuenta que cualquier propagación de frente de onda depende de una interacción crítica entre la "fuente" y el "sumidero" de una corriente despolarizante. Si el sumidero, que actúa como una especie de tejido aguas abajo del frente de onda de activación, es demasiado grande, la propagación falla porque la corriente de la fuente es demasiado débil para su excitación. Sin embargo, si ocurre lo contrario, un gran número de células se encuentran con una dimensión más pequeña de tejido corriente abajo, lo que resulta en una mayor velocidad de conducción (44). Múltiples mecanismos de reentrada han sido postulados. Allessie y colaboradores fueron los primeros en demostrar que la actividad de reentrada es funcional y, por lo tanto, existe sin la necesidad de un obstáculo anatómico. Con base en sus observaciones de una taquicardia, que fue inducida en la aurícula izquierda de un conejo por estimulación prematura que mostraba excitación por ondas giratorias, introdujeron su concepto de “círculo principal” (45). Su teoría consiste en un circuito de reentrada que se establece en un bucle lo más pequeño posible que permite que la onda se propague. Dentro del círculo principal, múltiples impulsos que se propagan centrípetamente vuelven refractario el tejido central

y lo extinguen. Por el contrario, la propagación centrífuga de impulsos en el borde de ataque del círculo despolariza el tejido adyacente lo más rápido posible, antes durante el período refractario relativo (46).

El otro mecanismo que ha sido descrito es la reentrada de onda espiral. Estos estudios postulan que la reentrada relacionada con la FA es el resultado de la actividad periódica ininterrumpida de una reentrada de onda espiral estable, serpenteante y autosostenida que adopta la forma de un rotor, la onda espiral gira alrededor de un circuito microrreentrante (47). Las ondas espirales son conocidas por observaciones de reacciones químicas en medios excitables y se han adaptado a fenómenos electrofisiológicos después de experimentos con modelos matemáticos de propagación eléctrica intercelular (modelo Fitzhugh-Nagumo) y han sido reproducidos en modelos de tejido cardiaco (48,49). Como resultado de una activación ectópica prematura dentro de la aurícula que inicia un frente de onda, que choca con el latido sinusal anterior (y, por lo tanto, encuentra su frente refractario y de recuperación), esto puede servir como un escenario típico: la propagación del frente de onda ectópico puede chocar y bloquear tarde o temprano en el borde del tejido no recuperado y por lo tanto refractario. En el momento en que éste recupera la excitabilidad es activado por el frente de onda prematuro, generando una curva que sigue continuamente al frente de recuperación hasta lograr una revolución completa. El punto en el que los tejidos excitados y refractarios chocan se denomina "singularidad de fase". Cabe destacar que el radio de la curvatura del frente de onda disminuye hacia el vórtice del rotor, donde la velocidad de conducción es infinitesimal debido a un desajuste fuente-sumidero. Esta hipótesis se considera el mecanismo de reentrada más popular en la FA. Algunos estudios postularon que la ablación de dichos rotores se asocia con una ausencia sostenida de FA cuando se realiza su ablación con éxito (50) aunque los estudios multicéntricos no demostraron el mismo resultado. Además, también se cree que estos rotores actúan como focos de fondo periódicos que generan frentes de onda, que pueden romperse en múltiples ondas al encontrar obstáculos anatómicos como orificios o tejido cicatricial. El progreso en los

sistemas electroanatómicos de mapeo de la superficie corporal podría permitir pronto su verificación o identificación confiable.

Nuestra comprensión actual de los mecanismos de mantenimiento de la FA también se basa en parte en las observaciones obtenidas a través de modelos informáticos y experimentos clave a principios de la década de 1960. Moe et al. describieron probablemente la vía final común más frecuente en la FA sostenida, es decir, un frente de onda irregular que se fracciona y divide en ondículas hijas independientes y finalmente inestables después de haber chocado con islotes o hebras de tejido refractario (51). Estas ondículas hijas muestran una actividad muy rápida con una duración de ciclo variable y muy corta, pueden volver a dividirse, chocar entre sí y/o extinguirse al encontrar tejido refractario (bloqueo funcional) o sitios de conducción lenta. Finalmente, numerosas wavelets garantizan el sustento de la FA, particularmente cuando están presentes procesos avanzados de remodelación estructural y eléctrica, favoreciendo su "supervivencia". Finalmente, numerosas ondículas garantizan el sustento de la FA, particularmente cuando están presentes procesos de remodelación estructural y eléctrica avanzados, favoreciendo su "supervivencia". Sin embargo, demostrar que múltiples wavelets pueden ser el mecanismo principal para la reentrada relacionada con la FA es un desafío, ya que esto básicamente requeriría una diferenciación de otros mecanismos como los mencionados anteriormente o la conducción fibrilatoria remota del sitio de interés (ver más abajo). Hasta el momento, no podemos identificar todas las fuentes locales de reingreso relacionado con la FA, razón por la cual este concepto mantiene su naturaleza hipotética.

Con menos frecuencia, un único foco de disparo muy rápido (PV o no PV) puede identificarse como el mecanismo de inicio y mantenimiento de la FA. En estos casos, se ha demostrado que una actividad focal ectópica se propaga hacia las aurículas y se encuentra con tejido parcialmente recuperado y refractario. Cabe señalar que la duración del ciclo de dicho conductor es, por definición, más corta que los períodos refractarios del tejido adyacente, razón por la cual no todo el tejido de esa cámara cardíaca puede despolarizarse de

manera regular 1: 1 y con conducción irregular y fibrilatoria por lo que puede producirse una activación fragmentada (44).

4.3. Implicaciones clínicas de los conceptos fisiopatológicos

Vincular la diversidad de factores de riesgo y mecanismos que conducen a la FA y la comprensión de los conceptos fisiopatológicos involucrados puede mejorar la prevención y el tratamiento de la FA. En consecuencia, seguimos implementando enfoques diagnósticos y terapéuticos cada vez más innovadores, dirigidos a objetivos específicos.

Los enfoques actuales se basan en sistemas tridimensionales de mapeo electroanatómico. Estos métodos pueden ser no invasivos y analizar la actividad eléctrica del corazón desde la superficie corporal con una resolución espacial y temporal creciente o invasivos basándose en la información adquirida con catéteres diagnósticos multipolares y catéteres de ablación. En el campo farmacológico no se han desarrollado novedades por ejemplo para el bloqueo específico de los canales de Na^+ o K^+.

Por el contrario, los métodos de imagen son una fuente de información en pleno desarrollo. Estas son múltiples siendo las más importantes la resonancia magnética nuclear, la tomografía computarizada y la ecografía intracardiaca.

Estas nuevas herramientas invasivas y no invasivas actualmente disponibles no permiten el conocimiento completo de los mecanismos relacionados con la FA, al menos pueden allanar el camino para una mejora adicional en vistas de desarrollar terapias selectivas y personalizadas.

5. Diagnóstico y clasificación de la fibrilación auricular

El diagnóstico de FA requiere la documentación del ritmo con un trazado de electrocardiograma (ECG) que muestre FA. Por convención, un episodio que dura al menos 30 s es diagnóstico de FA clínica. Además, existe la denominada FA subclínica en la que se incluyen episodios de alta frecuencia auricular confirmados como FA, flutter auricular o taquicardia auricular. Dichos episodios de FA detectados por un monitor cardíaco insertable o un monitor

portátil y confirmados por electrogramas intracardiacos revisados visualmente o con el ritmo registrado en un ECG. En general se definen como episodios de alta frecuencia auricular aquellos que duran más de 5 minutos, aunque aún no disponemos de estudios robustos que prueben cual es la actitud clínica que se debe tener ante los mismos en pacientes asintomáticos que requerirían una anticoagulación si su riesgo cardioembólico es elevado.

La clasificación está basada en la presentación, duración y terminación espontánea de los episodios de FA:

FA inaugural	FA no diagnosticada antes, independientemente de su duración o de la presencia/gravedad de los síntomas
FA paroxística	FA que termina espontáneamente o con intervención dentro de los 7 días del inicio.
FA persistente	FA que se mantiene continuamente más de 7 días, incluidos los episodios terminados por cardioversión (medicamentos o cardioversión eléctrica) después de ≥7 días
FA persistente de larga duración	FA continua de > 12 meses de evolución cuando se decide adoptar una estrategia de control del ritmo.
FA permanente	FA aceptada por el paciente y el médico, en la que no se realizarán más intentos de restaurar/mantener el ritmo sinusal. La FA permanente representa una actitud terapéutica del paciente y del médico más que un atributo fisiopatológico inherente de la FA

Tabla 1. Clasificación de la fibrilación auricular

Esta clasificación es una simplificación excesiva de la naturaleza compleja de la FA, pero en ella se basa gran parte de nuestra evidencia actual puesto que es la utilizada para los estudios clínicos.

6. Presentación clínica de la FA

Algunas personas que tienen FA no saben que la tienen y no tienen ningún síntoma. Otros pueden experimentar uno o más de los siguientes síntomas (52–54): palpitaciones del corazón (rápidas o fuertes), aturdimiento, fatiga extrema, dificultad para respirar, dolor torácico, poca tolerancia al esfuerzo. En algunos casos se pueden observar manifestaciones clínicas severas como

síncope, hipotensión, insuficiencia cardíaca aguda con edema pulmonar, isquemia miocárdica y shock cardiogénico.
Además, la presencia de una FA se asocia con los siguientes problemas:

6.1. Disminución de la calidad de vida

Más del 60% de los pacientes con FA tienen una calidad de vida significativamente deteriorada, siendo el problema más grave en pacientes de sexo femenino, aquellos más jóvenes o que presentan comorbilidades (55–57). Sin embargo, en una población con fibrilación auricular con función sistólica del VI conservada, solo el funcionamiento psicológico predice sistemáticamente tanto los síntomas relacionados con la fibrilación auricular como la calidad de vida relacionada con la salud con mayor prevalencia de la personalidad tipo D (58). Los síntomas y la calidad de vida son importantes para identificar el tratamiento óptimo de la FA. También es importante confirmar que los síntomas están relacionados con la FA o, en su defecto, excluir una adaptación a vivir con una capacidad física subóptima interrogando al paciente por disnea o fatiga de esfuerzo y registrando posibles mejoras después de la cardioversión.

6.2. Accidente cerebrovascular o tromboembolismo periférico

El riesgo anual de accidente cerebrovascular relacionado con la FA en pacientes con FA depende de las comorbilidades. Los accidentes cerebrovasculares cardioembólicos asociados con la FA suelen ser graves, muy recurrentes, a menudo fatales o con discapacidad permanente (59,60). La FA de inicio reciente también se asocia a la incidencia de embolias sistémicas (61).

6.3. Insuficiencia cardiaca

Múltiples mecanismos asociados a la FA pueden conducir a una disfunción ventricular izquierda e insuficiencia cardíaca, lo que resulta en una alta prevalencia e incidencia de insuficiencia cardíaca entre los pacientes con FA. Compartiendo factores de riesgo comunes, la FA y la insuficiencia cardíaca a menudo coexisten, pudiendo exacerbarse entre sí, lo que resulta en una

mortalidad significativamente mayor que cualquiera de las dos por separado (62,63).

6.4. Hospitalización

Aproximadamente el 30 % de los pacientes con FA tienen al menos uno, y el 10 % tiene ⩾ 2, ingresos hospitalarios al año (64–66), con el doble de probabilidades de ser hospitalizados que las personas sin FA de la misma edad y sexo (37,5 % frente a 17,5 %, respectivamente). En una cohorte nacional, la FA fue la principal causa de ingreso en el 14% de los pacientes hospitalizados, pero su mortalidad intrahospitalaria fue <1%. Las razones más comunes de hospitalización de los pacientes con FA fueron los trastornos cardiovasculares (49%), causas no cardiovasculares (43%) y sangrado (8%).

6.5. Deterioro cognitivo y demencia vascular

La FA puede causar dificultad cognitiva que va desde un leve deterioro hasta la demencia (67). Esto puede ocurrir a través de un accidente cerebrovascular clínico o silencioso, o a través de vías independientes del accidente cerebrovascular que no se comprenden completamente. Estudios de imagen por resonancia magnética (MRI) han demostrado que la AF se asocia con un aumento de más del doble de las probabilidades de tener isquemia cerebral silenciosa (68).

6.6. Muerte

La FA se asocia de forma independiente con un aumento del doble del riesgo de mortalidad por todas las causas en mujeres y un aumento del 1,5 en hombres, con un aumento general del riesgo de mortalidad de 3,5 veces.(69) Si bien la explicación mecanicista de esta asociación es multifacética, las comorbilidades asociadas juegan un papel importante.(70) Un estudio mostró que las causas más comunes de muerte entre los pacientes con FA fueron la insuficiencia cardíaca (14,5%), el cáncer (23,1%) y la infección/sepsis (17,3%), mientras que la mortalidad por accidente cerebrovascular fue solo del 6,5%.(71) Estos y otros datos recientes indican que, además del tratamiento

anticoagulante y el tratamiento de la insuficiencia cardíaca, es necesario tratar de forma activa las condiciones comórbidas en el esfuerzo por reducir la mortalidad relacionada con la AF.

7. Anatomía de la aurícula izquierda

La aurícula izquierda es una de las cuatro cámaras principales del corazón, situada en el lado posterior izquierdo. Se conecta proximalmente con las venas pulmonares, que devuelven sangre oxigenada de los pulmones y distalmente con el ventrículo izquierdo, forma la mitad sistémica del corazón, que es responsable de hacer circular la sangre oxigenada por todo el cuerpo.

La pared de la aurícula izquierda es una estructura delgada con un grosor heterogéneo, que va desde < 1 mm hasta > 5 mm, con una importante variabilidad inter e intrapaciente. Esta variabilidad en el grosor de la pared es el resultado de una serie compleja de fibras musculares tridimensionales (36,72,73).

7.1. Grosor de la pared como determinante de la lesión

Un estudio prospectivo demostró que el aislamiento de las VP tras la primera línea de ablación circunferencial (el “primer paso”) estaba limitado por la incapacidad de crear lesiones transmurales en ciertos sitios anatómicos donde se ha descrito que el grosor auricular es mayor en los corazones ex vivo (36,73,74). El grosor de la pared auricular fue un predictor independiente de reconexión (75), conducción latente (76) y recurrencia de FA después de 12 meses de seguimiento (77) e incluso podría ser un predictor de transición de FA paroxística a crónica (78).

8. AngioTAC cardíaco

Las máquinas modernas de tomografía axial computarizada multidetector (TAC) permiten una resolución submilimétrica. De hecho, las mediciones del grosor de la pared auricular por TAC se han validado de forma fiable en un modelo porcino (79). Ya se han generado mapas de grosor de la pared

auricular en 3D a partir de imágenes de angioTAC (TAC con contraste) (80), aunque su integración en un sistema de mapeo anatómico 3D para uso clínico aún no se ha descrito.

9. Tratamiento de la fibrilación auricular

El tratamiento de la fibrilación auricular tiene como objetivo restablecer el ritmo cardíaco normal o controlar la frecuencia cardíaca en función de cada paciente y, además, prevenir el accidente cerebrovascular y aliviar los síntomas.
El estudio EAST-AFNET 4 fue un ensayo clínico aleatorizado controlado que investigó la efectividad del control del ritmo temprano en pacientes con FA recién diagnosticada. Incluyó a 2400 pacientes diagnosticados dentro de un año de la inclusión randomizados para recibir control del ritmo precoz o atención habitual. La atención habitual consistió el control de la frecuencia cardíaca. Los resultados del estudio mostraron que el control del ritmo precoz se asocia con un menor riesgo de resultados cardiovasculares adversos. Concretamente, los pacientes en el grupo de control del ritmo precoz tuvieron un menor riesgo de accidente cerebrovascular (riesgo 29% menor), insuficiencia cardíaca (riesgo 29% menor) y muerte (riesgo 22% menor) (81). En consecuencia, el control del ritmo es preferible al control de la frecuencia.

El control de la frecuencia se reserva a un grupo seleccionado de pacientes para los cuales restablecer el ritmo sinusal se considera inoperante porque la remodelación auricular se estima avanzada o bien por las comorbilidades del paciente. En este grupo de pacientes existen dos estrategias para controlar la frecuencia. La primera es el tratamiento farmacológico que se realiza principalmente con betabloqueantes o antagonistas de los canales del calcio no dihidropiridínicos (diltiazem o verapamilo). La digoxina se emplea, aunque cada vez menos, en combinación con los anteriores en casos resistentes. La segunda estrategia de control de la frecuencia es el implante de un dispositivo de estimulación cardíaca seguido de la ablación por radiofrecuencia del nodo aurículo-ventricular. Esta última opción es muy eficaz, pero tiene la desventaja

de hacer que el paciente dependa del dispositivo en cuestión lo cual no está exento de complicaciones.

El control del ritmo, que tiene por objetivo reestablecer el ritmo sinusal, puede obtenerse por varios medios: cardioversión eléctrica, medicamentos y tratamiento invasivo por catéter.
La cardioversión eléctrica se reserva a dos situaciones, la primera es la inestabilidad hemodinámica por conducción atrioventricular rápida por lo cual se prioriza un control inmediato del ritmo cardíaco; la segunda es cuando previa introducción de un tratamiento farmacológico antiarrítmico, se desea reestablecer el ritmo sinusal bien sea para una farmacoterapia a mediano-largo plazo o bien en espera de una intervención o incluso para evaluar la presencia de síntomas que hubiesen pasado desapercibidos o que hubiesen sido subestimados por el paciente.

La eficacia del tratamiento con fármacos antiarrítmicos de primera línea es limitada y hace que una proporción sustancial de pacientes suspenda el tratamiento debido a los efectos tóxicos/indeseables de los mismos (82,83). Por esta ineficacia o intolerancia de los fármacos antiarrítmicos, la ablación con catéter ha demostrado ser superior a un tratamiento antiarrítmico adicional para prevenir la recurrencia de la FA (84,85).

9.1. Evidencia sobre el aislamiento de venas pulmonares

En los últimos años, varios ensayos clínicos han proporcionado evidencia robusta de la superioridad de la ablación con respecto a los medicamentos antiarrítmicos para mantener un ritmo sinusal (RS) duradero y revertir el riesgo de complicaciones tromboembólicas asociado con la FA (86). En particular, el aislamiento circunferencial completo de las VP mediante ablación por radiofrecuencia es frecuentemente efectivo para curar a muchos pacientes afectados por FA paroxística. Sin embargo, el éxito de este procedimiento es limitado en aquellos pacientes con una evolución más larga en el tiempo que ya están en fase de FA persistente/permanente, probablemente debido a una

remodelación auricular más extensa ya que pueden identificarse desencadenantes de la arritmia fuera de las venas pulmonares en un número significativo de estos pacientes remitidos para ablación por catéter (40,87). Los sitios más frecuentes de desencadenantes auriculares fuera de las VP incluyen la pared posterior de la aurícula izquierda, la vena cava superior, el seno coronario, el ligamento de Marshall y la región adyacente al anillo de la válvula mitral. Además, los plexos ganglionares auriculares pueden desempeñar un papel importante en la patogenia de la FA. Sin embargo, la evidencia que apoya la ablación de los focos desencadenantes fuera de las venas es escasa e incluso contradictoria. Por esta razón, la presente tesis se centra en el aislamiento exclusivo de las VP.

Existen varias técnicas para el aislamiento de las VP. Las más frecuentes son la radiofrecuencia (lesión térmica por calor punto a punto) y la crioablación (lesión térmica por balón frío). Un metaanálisis reciente mostró que, aunque el tiempo de procedimiento fue más corto en el grupo de criobalón, la eficacia y la seguridad fueron similares en ambos grupos (88).

9.2. Recidivas post aislamiento de las venas pulmonares

La conducción latente y las reconexiones de las VP son responsables de las recurrencias de FA/taquicardia auricular (TA) debido a lesiones de ablación no transmural incompletas que generan brechas en las líneas de ablación (89–91). La atenuación del electrograma local, la temperatura de la punta del catéter y la caída de la impedancia se han utilizado como indicadores de la formación de lesión tisular. Sin embargo, estos se correlacionan mal con la fuerza de contacto y por lo tanto constituyen malos predictores del tamaño de la lesión (92). Se ha demostrado que la potencia de radiofrecuencia (RF), la duración de la aplicación de energía de RF, la impedancia de base y la fuerza de contacto son determinantes de la formación de lesiones (93–95).

Se han desarrollado fórmulas más complejas para evaluar el efecto en tiempo real de la RF y así establecer los valores de umbral que deben alcanzarse para

reducir las reconexiones y lograr un aislamiento de las VP permanente. A saber, Integral Fuerza-Tiempo (FTI), que se calcula en gramos por segundo (gs) y representa el área bajo la curva fuerza de contacto/tiempo (96,97); y el índice de ablación (IA), que es una fórmula ponderada compleja que integra FC, tiempo de RF y potencia de RF (98,99). Para minimizar la reconexión de las VP, se han estudiado los valores de umbral de FTI y AI. En general, estos valores deben ser mayores en el techo y la pared anterior en comparación con la pared inferior y posterior, probablemente en relación con un menor espesor de la pared (98).

9.3. Indicaciones para el aislamiento de venas pulmonares

Para decidir la estrategia se tienen en cuenta los riesgos del procedimiento y los principales factores de riesgo de recurrencia de la FA después del procedimiento de común acuerdo con el paciente.
El nivel de evidencia más elevado para el aislamiento de VP se encuentra en los pacientes jóvenes con fibrilación auricular paroxística sintomática resistente al tratamiento antiarrítmico puesto que numerosos estudios han demostrado una mejora significativa de los síntomas (100,101).

A continuación, se sitúan los pacientes con insuficiencia cardiaca con fracción de eyección del ventrículo izquierdo (FEVI) disminuida. La FA y la insuficiencia cardiaca se asocian frecuentemente mediante varios mecanismos como la activación neurohormonal y el remodelaje estructural. La incidencia de FA en pacientes con insuficiencia cardíaca aumenta de forma paulatina con la progresión de la disfunción y con la edad. En el grupo de pacientes en que la FA con respuesta ventricular taquicárdica es la causa de la disfunción ventricular izquierda (conocido como taquimiocardiopatía), el pronóstico parece ser mejor.

Varios registros, han demostrado consistentemente una reducción de la mortalidad y del riesgo de accidente cerebrovascular isquémico en comparación con los medicamentos antiarrítmicos(102,103). Igualmente, los

datos de varios ensayos clínicos aleatorizados(104–106) y un metaanálisis de estos ensayos(107) indican claramente que la ablación es superior al control de frecuencia farmacológico o basado en marcapasos y ablación del nodo atrioventricular en términos de mejora en la fracción de eyección del ventrículo izquierdo, capacidad de ejercicio y calidad de vida.

9.4. Complicaciones potenciales e implicación de la posición esofágica.

El aislamiento de las VP se ha convertido en un procedimiento de rutina en numerosos centros hospitalarios, esto ha permitido la disminución de las complicaciones de forma significativa puesto que se han implementado diferentes estrategias para aumentar el nivel de seguridad.

Recientemente se publicó un metaanálisis de ensayos controlados aleatorizados que evaluaron las complicaciones relacionadas con el procedimiento de ablación con catéter para la fibrilación auricular (FA). El estudio incluyó datos de 15701 pacientes que se sometieron a un primer procedimiento de ablación por FA usando radiofrecuencia o ablación con criobalón.

Los principales hallazgos del estudio fueron una tasa global de complicaciones relacionadas con el procedimiento del 4,51 % (IC del 95 %: 3,76 %-5,32 %). Las complicaciones vasculares fueron las más frecuentes (1,31%). Otras complicaciones frecuentes incluyeron derrame pericárdico/taponamiento (0,78 %) y el accidente cerebrovascular/ataque isquémico transitorio (0,17 %). La tasa de complicaciones relacionadas con el procedimiento fue menor en el período de publicación de 5 años más reciente (3,77 % frente a 5,31 %; P = 0,043).

No hubo diferencias significativas en la tasa de complicaciones según el patrón de FA, la modalidad de ablación o las estrategias de ablación más allá del aislamiento de las VP (108).

Un tratamiento por aislamiento de VP implica inevitablemente, lesiones de ablación en la pared posterior de la aurícula izquierda, que se relaciona

estrechamente con el esófago que es una estructura tubular de ancho variable que discurre de arriba abajo del tórax. Esta relación anatómica depende principalmente de la anatomía y posición del arco aórtico y su influencia en la posición esofágica (109). La estrecha relación entre el esófago y la pared auricular izquierda y las VP puede dar lugar a varias complicaciones durante la intervención que van desde lesiones esofágicas asintomáticas hasta perforación con fístula atrio-esofágica (AEF), que puede ser letal. Además, otras posibles complicaciones incluyen daño a los plexos nerviosos peri-esofágicos que pueden resultar en complicaciones gastrointestinales posteriores a la ablación como gastroparesia, espasmo pilórico y reflujo gastroesofágico (110). Para mejorar la seguridad, se debe evitar la lesión térmica esofágica absteniéndose de aplicar radiofrecuencia en la pared posterior de la aurícula, adyacente al esófago.

El mecanismo exacto de la fístula atrio-esofágica no se conoce, pero la precede una lesión térmica. Las lesiones térmicas esofágicas asintomáticas detectadas por endoscopia se encontraron en el 18% de los pacientes durante la ablación en un análisis retrospectivo en el cual el único predictor independiente de lesión fue un aumento de la temperatura esofágica por encima de 40,5 °C (111). Algunos estudios han reportado lesiones hasta en el 47% de los pacientes después del aislamiento de VP (112,113). Por tanto, consideramos la temperatura esofágica alta como un buen marcador del riesgo de lesión térmica.

Se ha reportado información contradictoria referente a la interacción atrio-esofágica puesto que podría ser dinámica debido a la movilidad del esófago. Un estudio con imágenes cinefluoroscópicas del esófago obtenidas tras la deglución de bario mostró una relativa estabilidad de la posición esofágica en la reintervención realizada 7 ± 2 meses después de una primoablación (114). En otro estudio realizado con resonancia magnética cardíaca (RMC) seriada en 50 pacientes, se observó un desplazamiento lateral de al menos 1 cm en el 32% de los pacientes con un intervalo de tiempo medio entre RMC de 90,2 ± 100,5 días (115). Starek y colegas también analizaron la posición esofágica

antes y después de la ablación utilizando angiografía rotacional 3D para las VP y visualización del esófago mediante la administración per oral de un agente de contraste. Las posiciones del esófago se determinaron al inicio del procedimiento y, en parte de los pacientes, también al final del procedimiento con el mismo método. Se encontró que la posición esofágica antes y después del procedimiento era relativamente estable dentro del procedimiento de ablación y los cambios de posición significativos eran raros con una estabilidad del esófago en la mayoría de los pacientes (95%) (116). Sin embargo, se desconoce si el movimiento esofágico es estimulado por la ingestión de bario y si la anestesia general tiene alguna influencia sobre la motilidad esofágica. Una observación en tiempo real de la posición esofágica es factible con ecocardiografía intracardíaca, pero esta costosa opción no está ampliamente disponible en Europa.

HIPÓTESIS

La hipótesis de este proyecto se basa en observaciones previas de análisis *post mortem* que demuestran una gran variabilidad inter e intrapersonal en el grosor de la pared auricular. Por otra parte, el avance tecnológico que permitió una mejora en la calidad del TAC cardíaco permitiendo una resolución espacial inferior a 0,5 mm de manera que hipotéticamente permitiría la creación de mapas de grosor en 3D que se puedan integrar vía un módulo especial al sistema de navegación 3D utilizado para la ablación por radiofrecuencia de FA y apreciar así cual es el grosor de la pared en cualquier punto de la aurícula izquierda. Por otra parte, estudios previos el análisis offline de las reconexiones de las venas pulmonares sugerían que estas se reconectan más frecuentemente en las zonas de mayor grosor. La justificación de esta hipótesis se sustenta en que las reconexiones post ablación se relacionan con lesiones no transmurales directamente en relación con un grosor de la pared más importante.

A continuación, se plantea la hipótesis de que conocer el grosor de la pared en cualquier punto de la aurícula izquierda durante el procedimiento permite dos cosas. Por una parte, una adaptación de la energía administrada (calculada mediante una fórmula compleja llamada *Ablation Index*) con el fin de crear una lesión transmural más eficiente permitiendo disminuir la energía administrada en gran proporción sin que esto represente un aumento en la tasa de reconexiones y por ende en las recidivas. Por otra parte, de mejorar el perfil de seguridad del procedimiento puesto que no se administran sobredosis de energía en puntos donde el grosor es extremadamente delgado (< 1mm).

Dado que la evidencia respecto a la posición esofágica es contradictoria. Se plantea, además, la hipótesis por una parte que es posible derivar la posición esofágica del angioCT cardíaco preoperatorio y por otra que la posición esofágica no se modifica de forma significativa entre diferentes procedimientos en un mismo paciente. Con la hipótesis postulada de que el esófago tiene una

posición de reposo, especialmente en pacientes operados bajo anestesia general.

Finalmente, se plantea la hipótesis que adaptar las líneas de ablación en la pared posterior de la aurícula izquierda durante el aislamiento de las VP de acuerdo con la posición esofágica derivada del angioTAC, gracias a una herramienta desarrollada recientemente llamada huella esofágica para evitar aumentos locales de temperatura esofágica causados por la aplicación de radiofrecuencia (RF) durante la ablación de FA paroxística, podría ayudar a desarrollar estrategias de ablación más seguras al evitar el calentamiento del esófago. Dichos aumentos de temperatura se miden gracias a una sonda de temperatura esofágica y se han relacionado con lesiones esofágicas que a la postre pueden resultar en complicaciones graves. De manera que una intervención que contribuya a disminuir el calentamiento esofágico se traducirá en una mejor seguridad del procedimiento.

OBJETIVOS

Objetivos principales

- Determinar si el grosor de la pared de la aurícula izquierda es mayor en los segmentos de reconexión de PV observados durante las intervenciones de rehacer, en comparación con los sitios no reconectados.
- Determinar si adaptar el *Ablation Index* al espesor de la pared es factible, eficaz y seguro.
- Determinar si el esófago se encuentra ubicado en la misma posición anatómica en diferentes momentos:
    - Entre una primera ablación de FA y la reablación en pacientes que presentan recurrencias.
    - Entre el momento en que se realiza el angioCT previo al procedimiento y el procedimiento de ablación, como se observa con el MÓDULO CARTOUNIVU™.
    - Entre el inicio del procedimiento como se ve con el MÓDULO CARTOUNIVU™ y el final como se ve en el mapa anatómico rápido esofágico (FAM).
- Validar la utilidad de la impresión esofágica para evitar aumentos de temperatura causados por la aplicación de RF en la pared posterior de la AI durante la ablación de la fibrilación auricular.

Objetivos secundarios

- Analizar otras variables que podrían estar relacionadas con las reconexiones, como el espesor de pared normalizado, el espesor medio de la pared y la variabilidad del espesor de la pared alrededor de un sitio de ablación determinado.
- Determinar cuáles son los sitios más comunes de reconexiones en las VP, evaluados utilizando un modelo de segmentos de VP ya definido.
- Recopilar otros criterios de valoración del procedimiento disponibles
    - Tiempo de procedimiento

    - Tiempo de radiofrecuencia
    - Complicaciones periprocedimiento
- Estimar la tasa de recurrencia con este novedoso enfoque.
- Identificar los determinantes de la reconexión aguda de PV.
- Evaluar la tasa de complicaciones con el método *ablate By-LAW*.
- Evaluar la aparición de complicaciones gastrointestinales después de la ablación de la fibrilación auricular.
- Establecer el papel de los factores anatómicos como determinantes de las complicaciones gastrointestinales.
- Establecer si existe una relación lineal entre la distancia auriculo-esofágica calculada por la impresión esofágica derivada del angioTAC y el aumento de la temperatura esofágica medida por sonda endoesofágica.
- Analizar la necesidad de modificación de la línea de ablación.
- Analizar la necesidad de modificación de los parámetros de ablación con el fin de evitar una elevación de la temperatura esofágica.
- Desarrollar un nuevo enfoque multimodal para la monitorización esofágica durante la ablación de FA/AT.

MATERIAL, MÉTODOS Y RESULTADOS

Artículo 1

Grosor de la pared auricular izquierda de los sitios de reconexión de las venas pulmonares durante los procedimientos de reablación de fibrilación auricular

Este trabajo investigó la relación entre el grosor de la pared auricular izquierda y los sitios de reconexión las venas pulmonares durante procedimientos de reablación de fibrilación auricular. El objetivo principal fue establecer si el grosor puede desempeñar un papel predictivo en la identificación de posibles sitios de reconexión. Los resultados indicaron que los sitios de reconexión de las venas pulmonares durante los procedimientos frecuentemente se correlacionaban con regiones de mayor espesor de la pared auricular, lo que sugiere que estas regiones podrían no haber sido abordadas adecuadamente durante la ablación inicial. Esta idea enfatiza la importancia de considerar el grosor de la pared auricular en la planificación y ejecución de procedimientos de ablación de FA para mejorar la probabilidad de una intervención única exitosa y reducir la necesidad de repetir los procedimientos.

Received: 9 November 2020 | Revised: 16 February 2021 | Accepted: 14 March 2021

DOI: 10.1111/pace.14222

ORIGINAL - ELECTROPHYSIOLOGY

PACE WILEY

Left atrial wall thickness of the pulmonary vein reconnection sites during atrial fibrillation redo procedures

Cheryl Teres MD | David Soto-Iglesias MSc, PhD | Diego Penela MD, PhD | Beatriz Jáuregui MD, MSc | Augusto Ordoñez MD, PhD | Alfredo Chauca MD | Marina Huguet MD, PhD | Carlos Ramírez-Paesano MD | Guillermo Oller MD, PhD | Agustí Jornet MD, PhD | Jordi Palet MD, PhD | David Santana MD | Alejandro Panaro MD | Giuliana Maldonado MD | Gustavo de Leon MD | Belen Gualis MD | Gustavo Jimenez-Britez MD, PhD | Arturo Evangelista MD, PhD | Julio Carballo MD | José T. Ortiz-Perez MD, PhD | Antonio Berruezo MD, PhD

Heart Institute, Teknon Medical Center, Barcelona, Spain

Correspondence
Antonio Berruezo, MD, Heart Institute, Teknon Medical Center, C/Vilana 12, 08022 Barcelona, Spain.
Email: antonio.berruezo@quironsalud.es

Abstract

Background: Left atrial wall thickness (LAWT) has been related to pulmonary vein (PV) reconnections after atrial fibrillation (AF) ablation. The aim was to integrate 3D-LAWT maps in the navigation system and analyze the relationship with local reconnection sites during AF-redo procedures.

Methods: Consecutive patients referred for AF-redo ablation were included. Procedure was performed using a single catheter technique. LAWT maps obtained from multidetector computerized tomography (MDCT) were imported into the navigation system. LAWT of the circumferential PV line, the reconnected segment and the reconnected point, were analyzed.

Results: Sixty patients [44 (73%) male, age 61 ± 10 years] were included. All reconnected veins were isolated using a single catheter technique with 55 min (IQR 47–67) procedure time and 75 s (IQR 50–120) fluoroscopy time. Mean LAWT of the circumferential PV line was 1.46 ± 0.22 mm. The reconnected segment was thicker than the rest of segments of the circumferential PV line (2.05 + 0.86 vs. 1.47 + 0.76, $p < .001$ for the LPVs; 1.55 + 0.57 vs. 1.27 + 0.57, $p < .001$ for the RPVs). Mean reconnection point wall thickness (WT) was at the 82nd percentile of the circumferential line in the LPVs and at the 82nd percentile in the RPVs.

Conclusion: A single catheter technique is feasible and efficient for AF-redo procedures. Integrating the 3D-LAWT map into the navigation system allows a direct periprocedural estimation of the WT at any point of the LA. Reconnection points were more frequently present in thicker segments of the PV line. The use of 3D-LAWT maps can facilitate reconnection point identification during AF-redo ablation.

KEYWORDS
atrial fibrillation, atrial wall thickness, catheter ablation, gap identification

1 | INTRODUCTION

Circumferential pulmonary vein isolation (PVI) has become a mainstay in the treatment of AF, particularly in symptomatic patients with paroxysmal AF intolerant or refractory to medical treatment.[1] Despite the significant technical improvements occurred in the last decade, including contact force sensing catheters and the use of ablation indexes, creation of durable transmural lesions in the left atrium remains a main challenge of PVI procedures. Post-ablation pulmonary vein (PV) reconnections are responsible for atrial fibrillation/tachycardia (AT) recurrences owing to incomplete non-transmural ablation lesions that translate into gaps on ablation lines at different time lapses.[2–4]

The left atrial wall is a thin structure with heterogeneous thickness, ranging from <1 to >5 mm, with an important inter- and intrapatient variability. This variability in LAWT is the result of a complex array of three-dimensional muscular strands.[5] Isolation of PVs can be limited by inability to create transmural lesions in areas with higher LAWT.[6] In consequence, LAWT was described as an independent predictor of AF recurrence and it might even be a predictor of transition from paroxysmal to chronic AF.[7]

The aim of the present study was to analyze the relationship between reconnection gaps and local LAWT by integration of LAWT maps into the navigation system during AF-redo procedures, as well as to evaluate the feasibility of a single catheter approach in this setting.

2 | METHODS

2.1 | Patient sample

Consecutive patients referred for AF-redo ablation between November 2018 and December 2019 at a single center were included. It was accepted that first ablation procedures could have been performed at any center and with any technique. In all patients a multi-detector cardiac tomography (MDCT) study was performed prior to the re-ablation procedure. MDCT-derived maps with LAWT information were then imported into the navigation system for aiding the procedure. The minority of patients in whom all the PVs were isolated at the AF-redo procedure were excluded from the analysis, since comparison of LAWT in these cases was deemed not interpretable. No patient was excluded because of poor image quality. The study complied with the Declaration of Helsinki. The local ethics committee approved the study protocol and all included participants provided written informed consent before the procedure.

2.2 | Pre-procedural MDCT and image processing

MDCT was performed with a dual source SOMATOM Definition Flash 128 slice, scanner (Siemens Healthineers, Erlangen, Germany) or a Revolution scanner (General Electric Healthcare). Images were acquired during an inspiratory breath-hold using retrospective ECG-gating technique with tube current modulation set between 50% and 100% of the cardiac cycle. Angiographic images were acquired during the injection of a 100 mL bolus of Iopromide 370 mg I/mL (Ultravist, Bayer Hispania, Barcelona, Spain) at a rate of 3 mL/s. The administered radiation dose with this method is 160 mGy × cm which accounts for 3 mSv and ≈27 mGy total dose. Data were transmitted to the workstation for post-processing and reconstructed into axial images with slice thickness of 0.625 mm.

2.3 | Image post-processing

MDCT images were analyzed with ADAS 3D software (ADAS3D Medical, Barcelona, Spain) to obtain a 3D LAWT map by applying a 3-step algorithm: (i) the endocardial layer was delineated by means of a semi-automatic segmentation based on pixel intensity thresholds; (ii) the epicardial layer was defined manually with a multi-slice approach on the long-axis projection, with a mean of 20 ± 7 epicardial delineations per patient; (iii) Finally, wall thickness (WT) was automatically computed at each point as the distance between each endocardial point and its projection to the epicardial shell (Figure 1). These three steps result in a 3D WT map that can be imported into CARTO navigation system (Biosense Webster, Diamond Bar, CA, USA) by using the CARTO-Merge tool. A color code was used to create a range of thicknesses (red < 1 mm, yellow 1–2 mm, green 2–3 mm, blue 3–4 mm, and purple >4 mm). Intra and inter observer variability of the proposed method were evaluated. For this purpose, three independent observers with different levels of experience performed twice the WT segmentation in a random sample of 10 cases.

2.4 | Ablation procedures

The majority of the first procedures were performed by the same operator, under conscious sedation, with a single catheter, contact force-guided dragging technique and an energy between 30 and 40 W. Esophageal temperature was not monitored. Energy setting, application duration, and contact force of the first procedure were not available for analysis.

Redo interventions were performed on uninterrupted oral anticoagulation and under general anesthesia with a single catheter technique using an 8F Mullins non-steerable transseptal introducer sheath (Medtronic, Minneapolis, MN, USA) and a 3.5 mm irrigated tip catheter (NaviStar ThermoCool, Biosense Webster, Diamond Bar, CA, USA). Hemodynamic monitoring was done with a radial arterial catheter. Peri-procedural anticoagulation was performed with a first 1 mg/kg IV dose of unfractionated heparin immediately before transseptal puncture and periodic activated clotting time sampling was obtained every 30 min to guide further bolus dosing with a target between 300 and 350 s. Transseptal puncture was obtained with transesophageal echocardiogram guidance. After that, a fast-anatomical map (FAM) of the entire left atrial anatomy and the PVs was acquired with the ablation catheter. This FAM was then

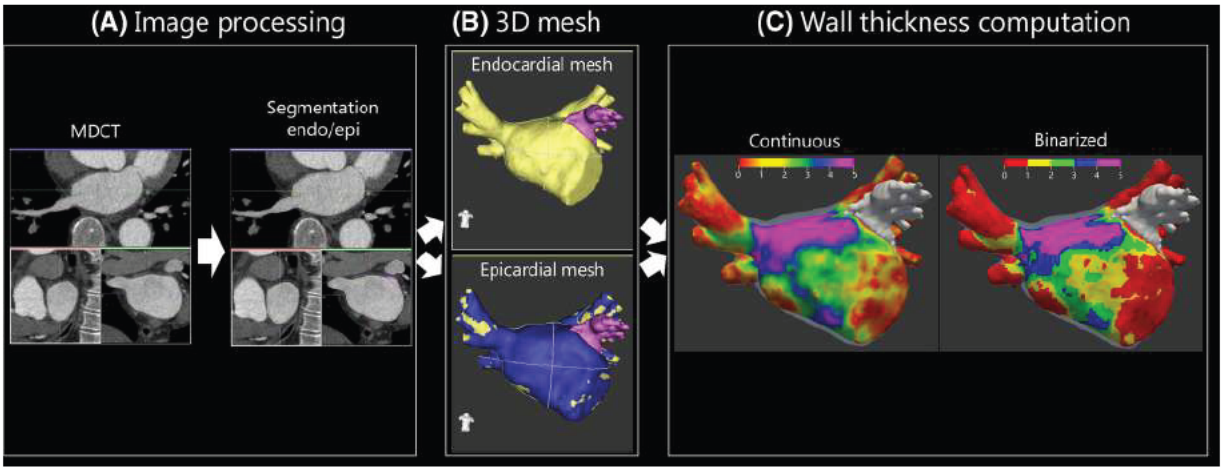

FIGURE 1 Segmentation pipeline of the 3D left atrial Wall thickness map. (A) Endocardial and epicardial layer delineation. (B) Endocardial and epicardial shells after semi-automatic segmentation in the endocardium and manual segmentation with a multi-slice approach in the epicardium. (C) Automatic computation of wall thickness as the distance between each endocardial point and its projection to the epicardial shell (color code: red < 1 mm, yellow 1–2 mm, green 2–3 mm, blue 3–4 mm, and purple > 4 mm). MDCT, multidetector computerized tomography [Color figure can be viewed at wileyonlinelibrary.com]

integrated with the LAWT map within the spatial reference coordinates of the CARTO system by means of the CARTO-Merge module.

2.5 | Reconnection site identification

Analysis of the PV reconnections was done in sinus rhythm. For patients with persistent AF, cardioversion was either scheduled days before the procedure or performed at the beginning of the procedure, once the patient was under general anesthesia. PV reconnection sites were identified by analyzing electrograms on the EP recording system (EP-TRACER, Schwarzer Cardiotek, Heilbronn, Germany), or on the CARTO navigation system, recorded with the ablation catheter according to a systematic, standardized local approach. A PV reconnection was defined as the presence of a PV potential, either a high amplitude sharp electrogram (EGM) inside the vein or a low amplitude fragmented EGM near the circumferential PV line that was identified with the ablation catheter inside the vein and/or if capture of atrial rhythm was achieved after programmed PV stimulation in any point inside the circumferential PV line.[8,9] The reconnection site was defined as the point with the earliest PV electrogram (PV-EGM) along the circumferential PV line. For this purpose, the EP recording was synchronized in a beat-to-beat manner, during stable sinus rhythm and a fixed PR interval, with a caliper in the peak of the QRS in the surface ECG marked as reference. The ablation catheter was sequentially placed on each segment of the circumferential PV line and the earliest PV potential with respect to the reference caliper is considered the reconnection site (Figure 2). If electrical activation inside the vein was still observed after ablation of the first designated reconnection point, and the local fusion between the atrial electrogram and the PV electrogram was observed at different distant points, multiple reconnection points were determined the process was repeated until all the reconnected points were identified (Figure 3). Each one of these points was considered as a reconnection and included in the analysis. RF was applied at the reconnection sites until complete isolation of all PVs was achieved. Ablation parameters were 35–50W, 45°C., with ablation time adapted to the WT with a standard pre-defined local protocol (Table 1). The procedural endpoint was PV disconnection, which was confirmed by entry block with absence of PV potentials inside the vein with the ablation catheter placed sequentially in each segment inside the circumferential PV line, and exit block by proving absence of conduction when pacing (11 mA, 2 ms) from inside the circumferential PV line sequentially at each segment.

2.6 | Wall thickness definitions and reconnection site analysis

In the first ten cases, the operator was blinded to the LAWT, since it was analyzed retrospectively. For the remaining cases the LAWT information was available during the procedure. After the procedure, LAWT maps were exported from CARTO for analysis into a Matlab customized software. The circumferential PV lines were divided following the 16-segment model (Figure 4). WT was calculated for the whole circumferential PV line and for each segment individually. During the ablation procedure, tags were generated on the 3D LAWT map for each identified reconnection site, using standard CARTO tags. The LAWT under the tag was considered the reconnection point WT. The segment where the point was located was considered a reconnected segment. Both, the reconnected point WT and the reconnected segment WT values were analyzed for each identified reconnection site. These values were compared with the WT of the non-reconnected segments of the circumferential PV line.

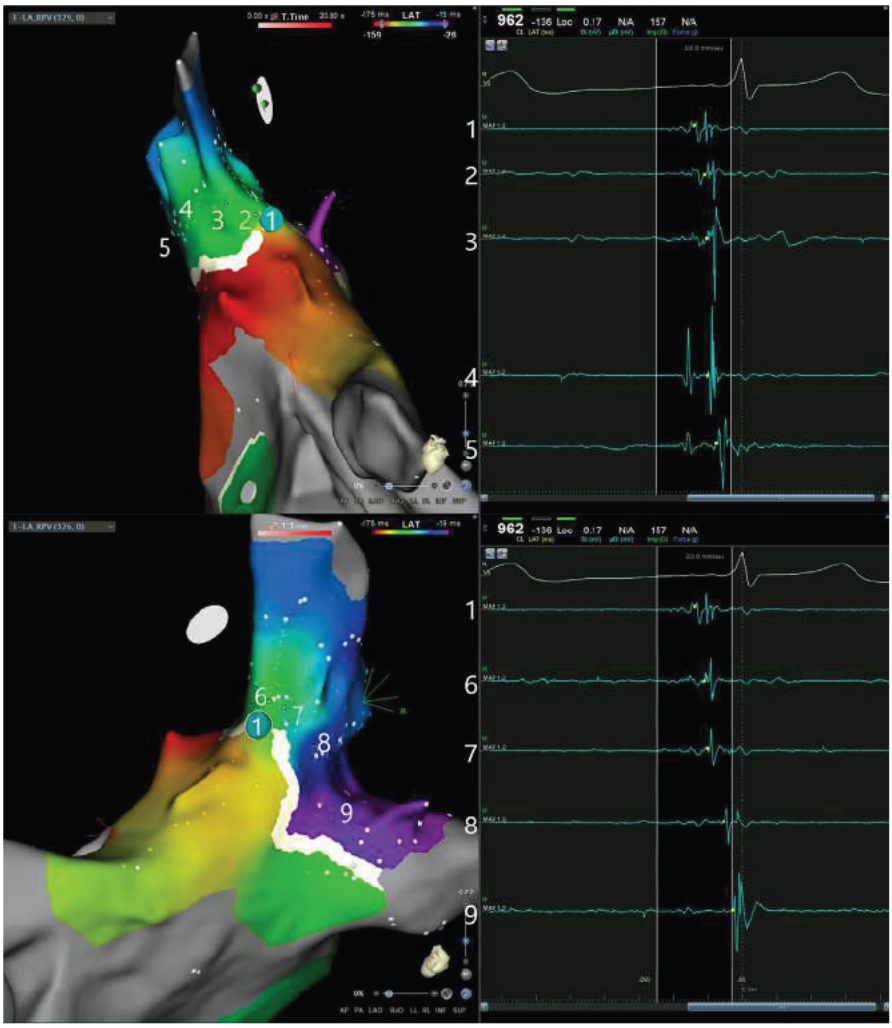

FIGURE 2 Reconnection site identification with a single catheter technique. PV reconnection sites were identified as the point with the earliest PV electrogram (PV-EGM) along the circumferential PV line. Top: Antero-superior view of the left atrium with activation map of the right superior PV. Points 1—5 represent sites where local activation was annotated and the respective local electrogram is depicted on the right-hand side. Bottom: Postero-superior view of the same case [Color figure can be viewed at wileyonlinelibrary.com]

TABLE 1 Protocol for ablation parameters adapted to left atrial wall thickness

LAWT	Color code	Ablation time (s)		RF energy (Watts)	
		Ant	Post	Ant	Post
<1 mm	Red	12	12	40	35
1–2 mm	Yellow	18	18	40	35
2–3 mm	Green	18	24	50	35
3–4 mm	Blue	30	24	50	35
>4 mm	Purple	36	30	50	35

Abbreviations: LAWT, left atrial wall thickness: RF, radiofrequency.

2.7 | Follow-up

Patients were scheduled to be followed-up at the outpatient clinic at 1, 3, 6, and 12 months. Each evaluation included an ECG and a 24-hour Holter monitoring. Recurrence was defined as any documented AF/AT episode lasting more than 30 s during this period or self-reported symptoms suggesting recurrence.

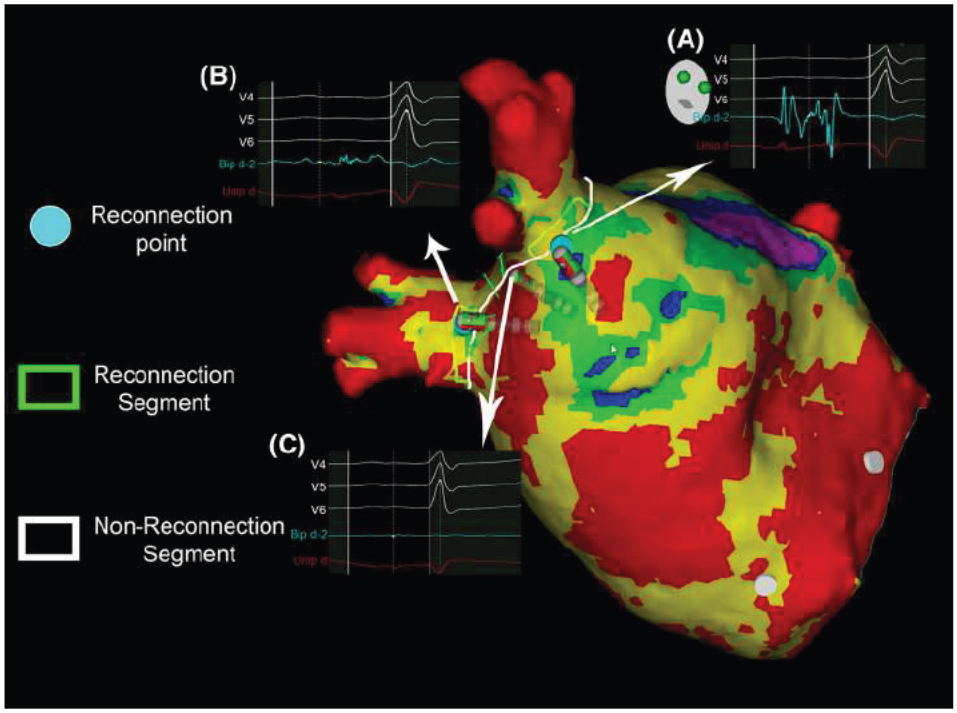

FIGURE 3 Example of a case with two pulmonary vein reconnections in the same vein pair. Low amplitude fragmented electrogram near the circumferential PV line on the antero-superior (A) and antero-inferior (B) segments of the right PVs. These reconnections were subsequently proved by capture of an atrial rhythm after pacing from the presumed reconnection site. The electrogram at the anterior carina (C) shows absence of local signal [Color figure can be viewed at wileyonlinelibrary.com]

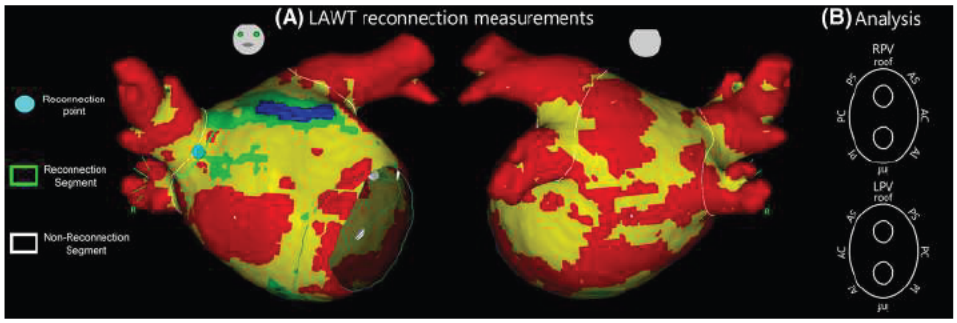

FIGURE 4 Wall thickness definitions and reconnection site analysis. **(A)** WT was calculated for the whole circumferential PV line; for each segment individually; and for the reconnection point. **(B)** 16-segment model (AS, anterosuperior; AC, anterior carina; AI, anteroinferior; Inf: inferior; PI, posteroinferior; PC, posterior carina; PS, posterosuperior; PV, pulmonary vein; WT, wall thickness) [Color figure can be viewed at wileyonlinelibrary.com]

2.8 | Statistical analysis

All applicable statistical tests are two-sided and performed using a 5% significance level. Continuous variables are presented as mean ± standard deviation or median (range or interquartile range if data are skewed) if not normally distributed. To compare means of two variables the Student's t test, Mann-Whitney U test, or ANOVA test were used, as appropriate. Categorical variables were expressed as total number (percentages) and compared between groups using Chi-square or Fisher's exact test. Statistical analysis was performed using IBM SPSS Statistics for Macintosh, version 25.0 (IBM Corp. Released 2017; Armonk, NY: IBM Corp.) and customized code for the Matlab statistics toolbox (Matlab R2010a, The Mathworks, Inc., Natick, MA, USA).

3 | RESULTS

3.1 | Patient population

Baseline characteristics are summarized in Table 2. Sixty patients were included. Mean age 61 ± 10 years, 43 (72%) male. Median time since first ablation was 19.5 months (IQR 9–55). Mean number of previous

TABLE 2 Baseline characteristics of the study population

	Total n = 60
Age, years	61 ± 10
Male, (%)	43 (72)
Hypertension n (%)	29 (48)
Dyslipemia, n (%)	14 (23.3)
Diabetes, n (%)	9 (15)
LVEF (%)	58 ± 5.8
LA diameter (mm)	41 ± 5.8
BMI (kg/m^2)	27.8 ± 8
CHADS-VASc	
0 (%)	12 (20)
1 (%)	7 (11.7)
2 (%)	3 (5)
3 (%)	11 (18.3)
4 (%)	5 (8,3)
≥5 (%)	0 (0)
Time since first ablation (months)	Median 19.4 (IQR 9–53)
Type of AF at first ablation n (%)	
• Paroxysmal	38 (63)
• Persistent	12 (37)
Type of Redo n (%)	
• AT/atypical flutter	3 (15)
• Paroxysmal	44 (73)
• Persistent	9 (15)

Abbreviations: AT, atrial tachycardia; LA, left atrium; LVEF, left ventricular ejection fraction.

ablations was 1.1 ± 0.4. Total number of previous ablations was one in 54 (90%) patients; two in five (8.3%) patients and three in 1 (1.7%) patient. All previous ablations were performed with RF ablation except for one case done with cryoablation. At first ablation, 38 out of 60 (63%) of patients presented with paroxysmal AF and 22 out of 60 (37%) with persistent AF. Three patients were excluded since all PVs were isolated at the AF-redo procedure. No patient was excluded because of impossibility to perform MDCT owing to severe kidney failure.

3.2 | Acute procedural characteristics

Median procedure time was 55 min (IQR 47—67). Merge time (FAM acquisition + MDCT merging on CARTO) was 12 min (IQR 10—15). Median fluoroscopy time was 1.25 min (IQR 0.8–2) with a Fluoroscopy dose of 1.5 mGy/m^2 (IQR 0.8–3.2).

There was a total of 113 PV reconnections, accounting for a mean of 1.89 ± 0.37 reconnected veins per patient. After analyzing the circumferential PV line, a total of 316 reconnection sites were identified with a mean of 4 ± 2 per patient. By applying radiofrequency (RF) in the identified reconnection sites, all PVs were disconnected. Median RF time was 5.8 min (IQR 2.5—8.2); 2.9 min (IQR 0.5—3.8) for the right PVs and 1.9 min (IQR 1.6—4.95) for the left PVs. There was one procedure related complication that consisted in an arterial pseudoaneurysm that did not require surgical treatment.

3.3 | Atrial wall thickness measurements and reconnection sites

Mean LAWT of the circumferential PV line was 1.46 ± 0.22 mm. The circumferential PV line was thicker in the LPVs as compared to the right pulmonary vein (RPVs) (1.56 ± 0.51 vs. 1.30 ± 0.37 mm $p = .004$, respectively). In the LPVs the antero-inferior, anterior carina and antero-superior segments were the thicker; and the posterior-carina was the thinnest. In the right PVs the thicker segments were the antero-superior, anterior-carina and the roof; and the thinnest was the inferior segment. Figure 5 shows the mean LAWT of each segment.

The reproducibility assessment showed an intra and inter observer reproducibility of the endocardial layer (automatic segmentation) for points closer than 1 mm of 99 ± 0.9% and 95 ± 5%, respectively. Intra- and interobserver reproducibility of the epicardial layer (manual segmentation) for points closer than 1 mm was 82 ± 10% and 78± 7%, respectively. This traduced on an overall mean intra-observer distance

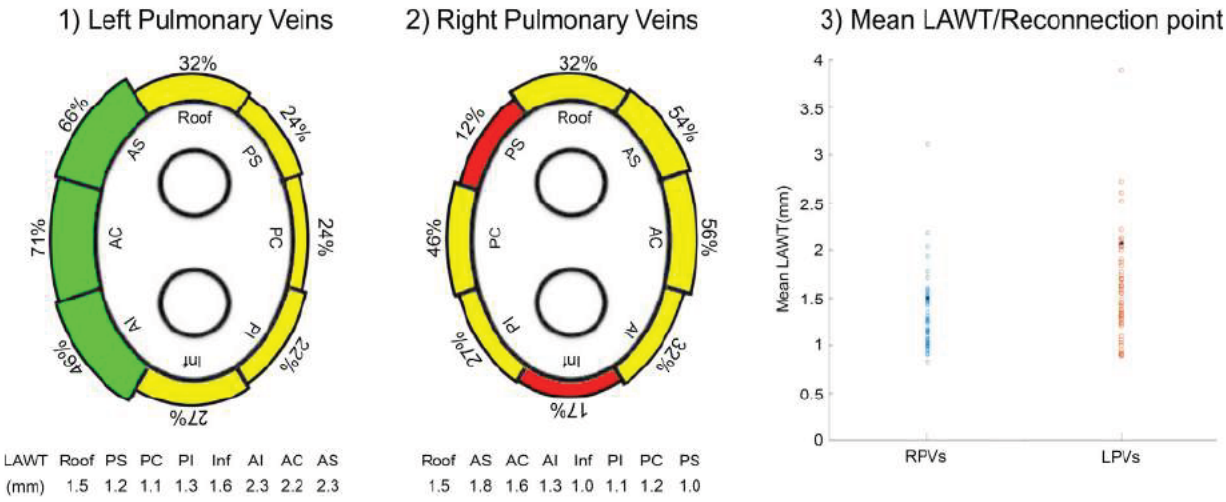

FIGURE 5 Wall thickness results at AF-redo procedure. The image depicts mean wall thickness of each PV segment and the reconnection rate of each segment (left). The mean wall thickness of the reconnected point was at the 82nd percentile (black dot) of the total circumferential PV line wall thickness at both sides (right) [Color figure can be viewed at wileyonlinelibrary.com]

between discordant points of 0.1 mm on the endocardium and 0.3 mm on the epicardium and an inter-observer mean distance of 0.2 mm on the endocardium and 0.6 mm on the epicardium.

In total, 113 PV reconnections were identified. Fifty six out of 60 (93%) patients presented reconnections in the RPVs and 57 out of 60 (95%) in the LPVs, $p = .58$. None of the 16 segments was spared from reconnections.

The most frequent location for reconnections at both sides was the anterior carina, which was reconnected on 65% of cases on the LPVs (mean WT 2.05 ± 0.86 mm) and 52% of cases on the RPVs (mean WT of 1.55 ± 0.57 mm). As compared with the rest of segments of the circumferential PV line, the reconnected segment WT was higher (2.05 ± 0.86 vs. 1.47 ± 0.76, $p < .001$ for the LVPs; 1.55 + 0.57 vs. 1.27 + 0.57, $p < .001$ for the RPVs). The reconnected point WT was also thicker as compared with the rest of the circumferential PV line [total 1.72 ± 0.86 vs. 1.46 ± 0.22, $p = .02$; LVPs 1.98 ± 1.07 vs. 1.49 ± 0.76 $p = .004$; RPVs 1.49 ± 0.58 vs. 1.27 ± 0.57 $p = .03$ s], as Figure 6 shows. Mean reconnection point WT was at the 82nd percentile of the circumferential PV line WT in the LPVs and at the 82nd percentile in the RPVs. Figure 5 shows the percentage of reconnection at each segment in the 16-segment model.

3.4 | Follow-up

Twelve out of sixty (20%) patients presented a recurrence during a mean follow-up of 7 ± 3 months (Table S1). Recurrence was more frequent in patients with persistent AF than in patients with paroxysmal AF (41% vs. 8% recurrence rate respectively, $p < .01$). Patients presenting a recurrence had a larger LA diameter (44 ± 4 mm vs. 40 ± 6 mm, $p < .01$), lower LVEF (55 ± 10 vs. 59 ± 3, $p = .01$) and presented an underlying cardiomyopathy more frequently (two hypertrophic, one ischemic, three hypertensive) [eight out of 48 (16%) patients in the non-recurrence group vs. six out of 12 (50%) in the recurrence group, $p = .05$].

4 | DISCUSSION

The present study is the first one reporting the feasibility of integrating the 3D LAWT maps into the navigation system, allowing for a direct intraprocedural estimation of the WT at any point of the LA and therefore at the reconnected points. The study shows that the mean LAWT at the identified reconnected points was thicker than the rest of the circumferential PV line. The study also proves the feasibility and usefulness of a simplified method for performing the AF-redo procedure using a single catheter technique that improves efficiency by obtaining short procedure and fluoroscopy times as compared with the literature standards.[11,12] The use of 3D LAWT maps can facilitate reconnection point identification during AF-redo ablation by permitting to focus mapping in the thicker points and segments.

4.1 | Single catheter approach

The single catheter approach has already been described for PV isolation at first ablation procedures,[9,10] showing that this method is cost-saving, and non-inferior regarding AF recurrences in the mid-term. The present study reports on a single catheter approach for performing AF-redo procedures in which the ablation line must be mapped in each and every case, with the implementation of a simplified approach for identifying the electrical breakthrough based on timing of the local PV electrogram without need of a further catheter for reference[8] (Figure 2). This as opposed to first ablations where the high rate of first pass isolation allows for avoidance of this step. The method is feasible, as all reconnected veins could be isolated by applying RF in the

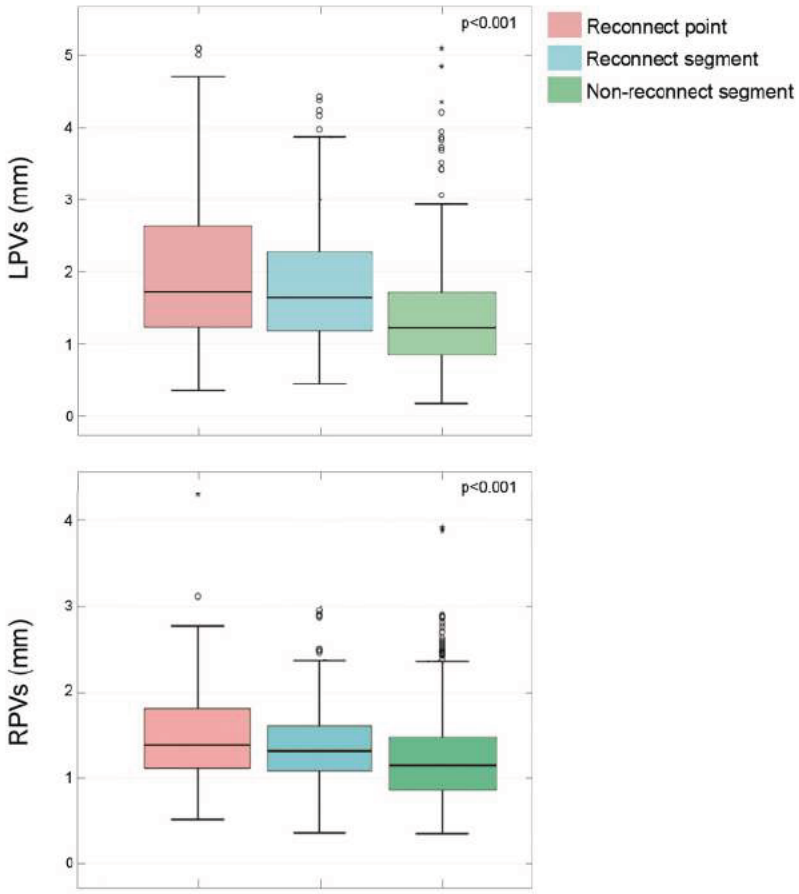

FIGURE 6 Wall thickness of the reconnected point, the reconnected segment and the rest of the circumferential PV line. *p* value for comparison between the reconnected point and the rest of the line [Color figure can be viewed at wileyonlinelibrary.com]

reconnection sites identified with this approach. The procedure workflow simplification results in high efficiency with a median procedure time under one hour and a very low fluoroscopy time and dose. Moreover, this approach had a very low complication rate (1.5%) probably related to the use of a single catheter and a single vascular and transeptal access.

4.2 | MDCT 3D LAWT maps

Imaging techniques have led to better understanding of PV anatomy and more efficient procedure planning.[13] Even though many limitations have been described on MDCT atrial wall thickness measurement for previous generations of scanners, modern machines allow for submillimetric resolution. In fact, CT atrial wall thickness measurements have been reliably validated on a porcine model,[14] and 3D LAWT maps have already been generated from contrast cardiac computed tomography images.[15] Having in mind that the spatial resolution of the MDCT is 0.4 mm, we assume that the variability of the proposed method is low and the expected clinical repercussion of this variability, is also presumably low. Although further evidence is needed to confirm this low clinical impact of the variability. Of all the determinants of lesion creation, LAWT is one key element that has been evaluated in some retrospective analysis but has never been integrated on the navigation system during the procedure. Importing the LAWT map derived from the MDCT into the navigation system allows for real-time knowledge of the atrial WT in contact with the catheter tip. This feature might be useful in different settings, as for instance in adapting energy delivery to avoid excessive application in thinned wall segments improving safety or delivering more energy in thicker regions in order to obtain more durable lesions[16]; allowing to focus mapping at the thicker points looking for reconnections in the ablation line during AF-redo procedures; and personalizing sites of RF application when drawing ablation lines to avoid thicker segments. Thus, this new imaging tool, opens the door for future diagnostic and therapeutic strategies using the integration of 3D LAWT maps into the navigation system.

4.3 | LAWT and gap identification

The result of this pilot study confirms previous observations from retrospective studies, on that atrial WT is a major determinant of lesion transmurality and that PV reconnections occur more frequently in thicker parts of the PV circumferential line. We have found that the more frequently reconnected sites are those with thicker atrial WT, in particular the right and left anterior carinas. In fact, previous histological[17] and imaging[18] studies have shown that the left atrial ridge is the thickest structure around the circumferential PV lines and that it is also where reconnection sites were more frequently found in this study. Nevertheless, despite an excellent spatial resolution which

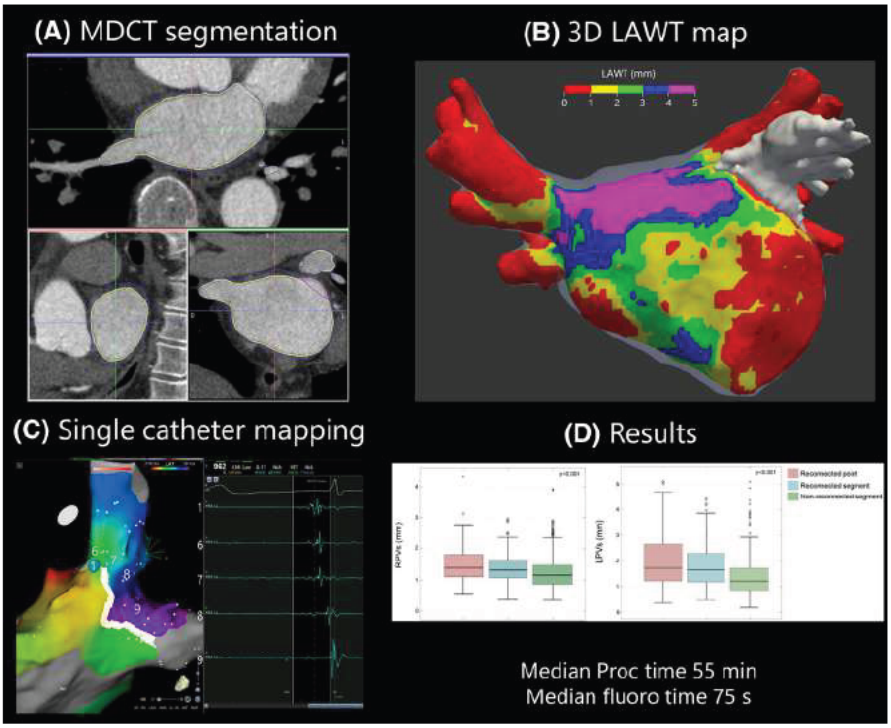

FIGURE CENTRAL FIGURE (A) Endocardial and epicardial layer delineation on MDCT. (B) 3D LAWT map categorized for thickness ranges (color code: red < 1 mm, yellow 1–2 mm, green 2–3 mm, blue 3–4 mm, and purple >4 mm). (C) Single catheter technique for identification of the reconnection site. (D) Comparison of LAWT measurements on both pairs of veins. LAWT, left atrial wall thickness; MDCT, multidetector computerized tomography [Color figure can be viewed at wileyonlinelibrary.com]

is the main robustness of CT scan, the contrast resolution of this technique is lower than that of MRI, because the difference in x-ray attenuation between different tissues is modest. In consequence, CT image cannot distinguish myocardium from other tissues especially at the very thin LA wall and therefore, it is important to bear in mind that a thick LA wall does not necessarily mean a thick myocardial sleeve.

4.4 | Follow-up

A 20% recurrence rate after AF-redo ablation was observed during follow-up and this is in line with previous observations.[10] Recurrences were more frequent in patients presenting known predictors of recurrence after a first ablation as larger atrial diameter[19]; presence of a previous structural heart disease[20]; and persistent AF at first ablation procedure.[21] The recurrence rate in patients with paroxysmal AF was as low as 8%, validating the long-term efficacy of a single catheter ablation technique for AF-redo procedures.

4.5 | Clinical implications

This study describes the clinical usefulness of MDCT derived 3D LAWT maps to allow better identification of thicker atrial wall regions which is where reconnections are more frequently located. Our results not only stress the importance of atrial WT as a determinant of long-term lesion transmurality but also set the stage for a wide use of 3D LAWT maps at first AF ablation procedures to probably increase efficacy and safety given the fact that adapting the ablation parameters to the local WT is a long-time unmet need in the AF ablation field. Besides, the use of 3D LAWT maps could allow for a shortening of the procedure time and RF delivery and fluoroscopy time since gap identification can in many cases be aided by the map. However, further prospective studies are needed to validate this hypothesis.

Furthermore, we adopted the single catheter approach for determining and ablating the reconnection site. The combination of these methods results in a very efficient and less invasive procedure with very good acute and mid-term outcomes. Once again, prospective studies are needed to compare the safety and efficacy of this approach with regard the conventional multicatheter approach.

4.6 | Limitations

The main limitation of this study is the lack of a control group for comparison. Besides, procedure characteristics of the first ablation were not available for analysis. Hence, an association between the lack of stability, the applied power settings or the presence of gaps on the circumferential PV line and the distribution of reconnection sites cannot be excluded, especially in some segments where it is difficult to ensure good catheter stability during RF application, as the left anterior carina. Furthermore, RF application at first ablation itself might

directly affect LA wall thickness through scar involution and consecutive tissue remodeling. Another limitation is that the LAWT method depends on contrast-enhanced MDCT acquisition, which is contraindicated in patients with severe kidney failure, needs special preparation in patients with contrast medium allergy, and implies radiation exposure. Nevertheless, fluoroscopic requirements for the presented method are lower than what has been reported on multicenter international registries[22] and what has been found on recent prospective trials.[23] Therefore, even though the need for a MDCT might imply additional radiation exposure, the overall radiation dose administered is still reasonable. That said, evidence is lacking, and our results warrant further research. Also, multielectrode catheters were not used to identify the reconnection sites. However, all PVs were successfully isolated, and the mid-term recurrence rate was low using a single 4-electrodes catheter. Finally, we modulated RF delivery at the redo procedure based on empiric parameters. Further studies are needed to evaluate the optimal parameters of RF application according to the LAWT.

5 | CONCLUSION

3D LAWT maps can be obtained from MDCT scan and be integrated into the navigation system. It allows for a direct periprocedural estimation of the WT at any point of the LA. Reconnection points are more frequently present in the thicker segments of the circumferential PV line and usually are the thickest point of the segment. A single catheter approach is feasible, efficient and safe during AF-redo procedures, allowing to easily identify the reconnected segment with a low recurrence rate at mid-term.

CONFLICT OF INTEREST

Dr. Berruezo is a stockholder of ADAS 3D Medical. Dr. Soto-Iglesias is an employee of Biosense Webster. The other authors have no other relevant affiliations or financial involvement with any organization or entity with a financial interest in or financial conflict with the subject matter or materials discussed in the manuscript apart from those disclosed.

FUNDING INFORMATION

Dr Teres was funded by the research fellowship grant of the Swiss Heart Rhythm Foundation.

DATA AVAILABILITY STATEMENT

Data might be available upon request.

ORCID

Antonio Berruezo MD, PhD https://orcid.org/0000-0002-5418-383X

REFERENCES

1. Calkins H, Hindricks G, Cappato R, et al. 2017 HRS/EHRA/ECAS/APHRS/SOLAECE expert consensus statement on catheter and surgical ablation of atrial fibrillation. *Europace*. 2018;20:e1-e160.
2. Ouyang F, Tilz R, Chun J, et al. Long-Term results of catheter ablation in paroxysmal lessons from a 5-Year follow-up. *Circulation*. 2010:2368-2377.
3. Cappato R, Negroni S, Pecora D, et al. Prospective assessment of late conduction recurrence across radiofrequency lesions producing electrical disconnection at the pulmonary vein ostium in patients with atrial fibrillation. *Circulation*. 2003;108:1599-1604.
4. Kuck K-H, Hoffmann BA, Ernst S, et al, Gap-AF–AFNET 1 Investigators. Impact of complete versus incomplete circumferential lines around the pulmonary veins during catheter ablation of paroxysmal atrial fibrillation: results from the gap-atrial fibrillation-german atrial fibrillation competence network 1 trial. *Circ Arrhythm Electrophysiol*. 2016;9:e003337.
5. Ho SY, Sanchez-Quintana D. The importance of atrial structure and fibers. *Clin Anat*. 2009;22:52-63.
6. Kistler PM, Ho SY, Rajappan K, et al. Electrophysiologic and anatomic characterization of sites resistant to electrical isolation during circumferential pulmonary vein ablation for atrial fibrillation: a prospective study. *J Cardiovasc Electrophysiol*. 2007;18:1282-1288.
7. Nakamura K, Funabashi N, Uehara M, et al. Left atrial wall thickness in paroxysmal atrial fibrillation by multislice-CT is initial marker of structural remodeling and predictor of transition from paroxysmal to chronic form. *Int J Cardiol*. 2011;148:139-147.
8. Arenal A, Atea L, Datino T, et al. Identification of conduction gaps in the ablation line during left atrium circumferential ablation: facilitation of pulmonary vein disconnection after endpoint modification according to electrogram characteristics. *Heart Rhythm*. 2008;5:994-1002.
9. Pambrun T, Combes S, Sousa P, et al. Contact-force guided single-catheter approach for pulmonary vein isolation: feasibility, outcomes, and cost-effectiveness. *Heart Rhythm*. 2017;14:331-338.
10. Dong J, Liu X, Long D, et al. Single-catheter technique for pulmonary vein antrum isolation: is it sufficient to identify and close the residual gaps without a circular mapping catheter?. *J Cardiovasc Electrophysiol*. 2009;20:273-279.
11. Zeljkovic I, Knecht S, Spies F, et al. Paroxysmal atrial fibrillation recurrence after redo procedure-ablation modality impact. *J Interv Card Electrophysiol*. 2020;57:77-85.
12. Johner N, Shah DC, Giannakopoulos G, Girardet A, Namdar M. Evolution of post-pulmonary vein isolation atrial fibrillation inducibility at redo ablation: electrophysiological evidence of extra-pulmonary vein substrate progression. *Heart Rhythm*. 2019;16:1160-1166.
13. Dong J, Calkins H, Solomon SB, et al. Integrated electroanatomic mapping with three-dimensional computed tomographic images for real-time guided ablations. *Circulation*. 2006;113:186-194.
14. Sun JY, Yun CH, Mok GSP, et al. Left atrium wall-mapping application for wall thickness visualisation. *Sci Rep*. 2018;8:4169.
15. Bishop M, Rajani R, Plank G, et al. Three-dimensional atrial wall thickness maps to inform catheter ablation procedures for atrial fibrillation. *Europace*. 2016;18:376-383.
16. Soor N, Morgan R, Varela M, Aslanidi O V. Towards patient-specific modelling of lesion formation during radiofrequency catheter ablation for atrial fibrillation. *Eng Med Biol Soc*. 2016;2016:489-492.
17. Cabrera JA, Ho SY, Climent V, Sanchez-Quintana D. The architecture of the left lateral atrial wall: a particular anatomic region with implications for ablation of atrial fibrillation. *Eur Heart J*. 2008;29:356-362.
18. Mansour M, Refaat M, Heist EK, et al. Three-dimensional anatomy of the left atrium by magnetic resonance angiography: implications for catheter ablation for atrial fibrillation. *J Cardiovasc Electrophysiol*. 2006;17:719-723.
19. Berruezo A, Tamborero D, Mont L, et al. Pre-procedural predictors of atrial fibrillation recurrence after circumferential pulmonary vein ablation. *Eur Heart J*. 2007;28:836-841.

20. Lee SH, Tai CT, Hsieh MH, et al. Predictors of early and late recurrence of atrial fibrillation after catheter ablation of paroxysmal atrial fibrillation. *J Interv Card Electrophysiol*. 2004;10:221-226.
21. Themistoclakis S, Schweikert RA, Saliba WI, et al. Clinical predictors and relationship between early and late atrial tachyarrhythmias after pulmonary vein antrum isolation. *Heart Rhythm*. 2008;5:679-685.
22. Sciahbasi A, Ferrante G, Fischetti D, et al. Radiation dose among different cardiac and vascular invasive procedures: the RODEO study. *Int J Cardiol*. 2017;240:92-96.
23. Quinto L, Cozzari J, Benito E, et al. Magnetic resonance-guided re-ablation for atrial fibrillation is associated with a lower recurrence rate: a case-control study. *Europace*. 2020;22:1805-1811.

SUPPORTING INFORMATION

Additional supporting information may be found online in the Supporting Information section at the end of the article.

How to cite this article: Teres C, Soto-Iglesias D, Penela D, et al. Left atrial wall thickness of the pulmonary vein reconnection sites during atrial fibrillation redo procedures. *Pacing Clin Electrophysiol*. 2021;1—11.

Artículo 2

Ablación personalizada de la fibrilación auricular paroxística adaptando el índice de ablación al grosor de la pared auricular izquierda: el estudio unicéntrico 'Ablate ByLAW'

Este estudio piloto investigó un enfoque personalizado para la ablación de fibrilación auricular paroxística. Al adaptar el índice de ablación al grosor de la pared de la aurícula izquierda, se optimizó el procedimiento. Los hallazgos de este estudio sugirieron que personalizar los parámetros de ablación basados en variaciones anatómicas individuales, como el grosor de la pared de la aurícula izquierda, puede mejorar potencialmente la eficacia y seguridad del procedimiento. Si bien los resultados son prometedores, la naturaleza piloto del estudio indica la necesidad de realizar más investigaciones a gran escala para validar estos hallazgos y determinar sus implicaciones clínicas.

ESC European Society of Cardiology
Europace (2021) **00**, 1–10
doi:10.1093/europace/euab216

CLINICAL RESEARCH

Personalized paroxysmal atrial fibrillation ablation by tailoring ablation index to the left atrial wall thickness: the 'Ablate by-LAW' single-centre study—a pilot study

Cheryl Teres, David Soto-Iglesias, Diego Penela, Beatriz Jáuregui, Augusto Ordoñez, Alfredo Chauca, Jose Miguel Carreño, Claudia Scherer, Rodolfo San Antonio, Marina Huguet, Albert Roque , Carlos Ramírez, Guillermo Oller, Agustí Jornet, Jordi Palet, David Santana, Alejandro Panaro, Giuliana Maldonado, Gustavo de Leon, Gustavo Jiménez, Arturo Evangelista, Julio Carballo, José-Tomás Ortíz-Pérez, and Antonio Berruezo *

Heart Institute, Teknon Medical Center, C/Vilana, 12, 08022 Barcelona, Spain

Received 17 December 2020; editorial decision 21 July 2021

Aims To determine if adapting the ablation index (AI) to the left atrial wall thickness (LAWT), which is a determinant of lesion transmurality, is feasible, effective, and safe during paroxysmal atrial fibrillation (PAF) ablation.

Methods and results Consecutive patients referred for PAF first ablation. Left atrial wall thickness three-dimensional maps were obtained from multidetector computed tomography and integrated into the CARTO navigation system. Left atrial wall thickness was categorized into 1 mm layers and AI was titrated to the LAWT. The ablation line was personalized to avoid thicker regions. Primary endpoints were acute efficacy and safety, and freedom from atrial fibrillation (AF) recurrences. Follow-up (FU) was scheduled at 1, 3, 6, and every 6 months thereafter. Ninety patients [60 (67%) male, age 58 ± 13 years] were included. Mean LAWT was 1.25 ± 0.62 mm. Mean AI was 366 ± 26 on the right pulmonary veins with a first-pass isolation in 84 (93%) patients and 380 ± 42 on the left pulmonary veins with first-pass in 87 (97%). Procedure time was 59 min (49–66); radiofrequency (RF) time 14 min (12.5–16); and fluoroscopy time 0.7 min (0.5–1.4). No major complication occurred. Eighty-four out of 90 (93.3%) patients were free of recurrence after a mean FU of 16 ± 4 months.

Conclusion Personalized AF ablation, adapting the AI to LAWT allowed pulmonary vein isolation with low RF delivery, fluoroscopy, and procedure time while obtaining a high rate of first-pass isolation, in this patient population. Freedom from AF recurrences was as high as in more demanding ablation protocols. A multicentre trial is ongoing to evaluate reproducibility of these results.

*Corresponding author. Tel: +34 932906251. *E mail address*: antonio.berruezo@quironsalud.es

Graphical Abstract

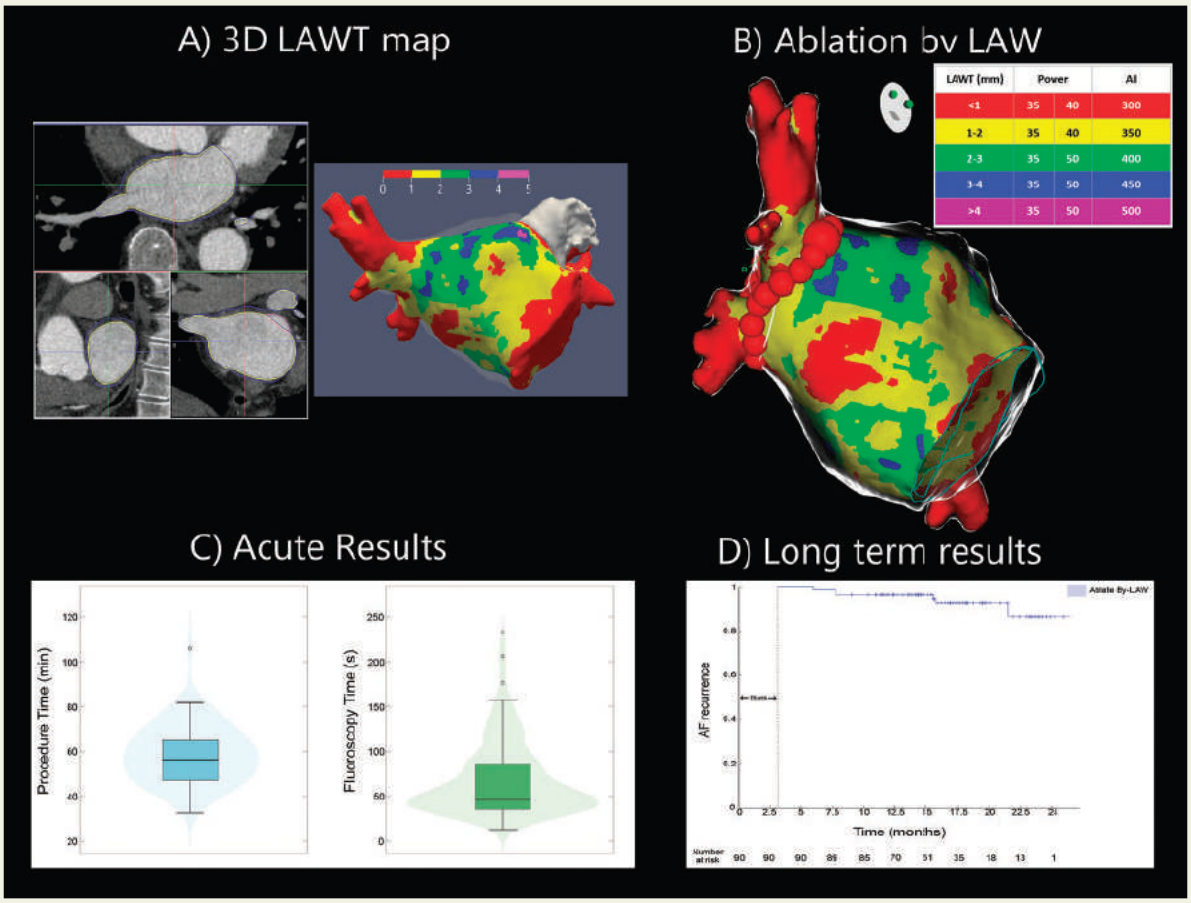

Keywords Ablation index • Atrial fibrillation • Atrial wall thickness • Catheter ablation

What's new?

- The present study constitutes the first report about feasibility of incorporating three-dimensional left atrial wall thickness (LAWT) maps into the navigation system, allowing a direct estimation of the wall thickness (WT) at any point of the left atrium during the procedure.
- This tailoring of the delivered radiofrequency (RF) energy and ablation line design depending on the WT during atrial fibrillation (AF) ablations, can increase efficiency and safety.
- Personalized AF ablation with the Ablate-By-LAW protocol using a single catheter technique and adapting the ablation index to LAWT allowed decreasing RF delivery, fluoroscopy, and procedure time while obtaining a high rate of first-pass isolation.

Introduction

Pulmonary vein isolation (PVI) has become widely available and is the foundation for paroxysmal atrial fibrillation (PAF) treatment, especially in symptomatic patients resistant to medical treatment.[1] Post-atrial fibrillation (AF) ablation pulmonary vein (PV) reconnection is the main cause of AF recurrences[2,3] and results after either insufficient radiofrequency (RF) delivery[4] or because of non-transmural or non-contiguous lesions in the PV ablation line.[5,6] In recent years, advances have been made in the ablation technique with the introduction of contact force catheters and the development of complex weighed formulas as the ablation index (AI) that allows for a more efficient lesion creation and durable PV isolation.[7]

The left atrial (LA) wall is a thin structure with heterogeneous thickness ranging from <1 mm to >5 mm.[8] Durability of PVI can be limited by the inability to create transmural lesions in certain anatomical sites where left atrial wall thickness (LAWT) is higher.[9] In fact,

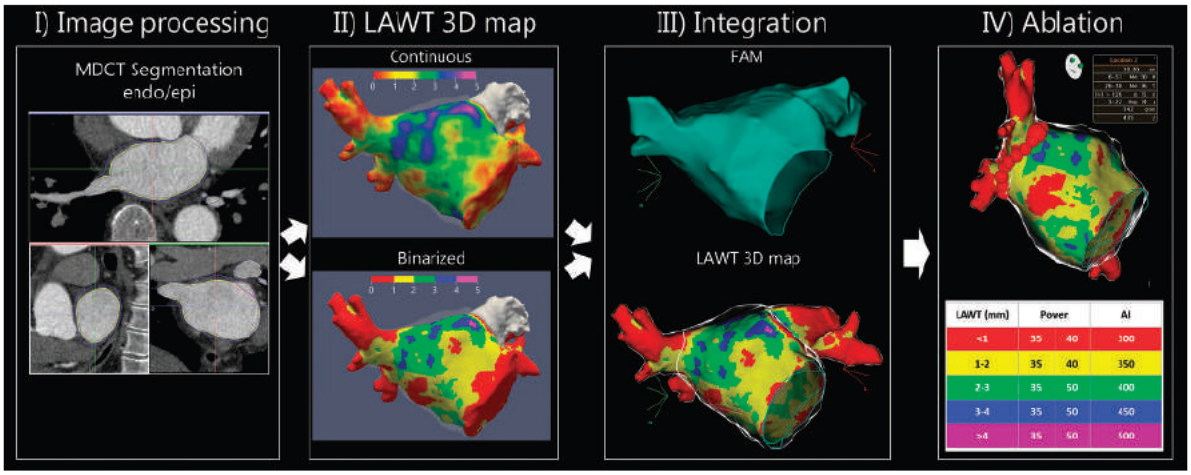

Figure 1 Segmentation pipeline of the 3D left atrial wall thickness map. (*A*) Endocardial and epicardial layer delineation on the MDCT. (*B*) Automatic computation of LAWT as the distance between each endocardial point and its projection to the epicardial shell (colour code: red <1 mm, yellow 1–2 mm, green 2–3 mm, blue 3–4 mm and purple >4 mm). (*C*) Image integration of the fast anatomical map with the LAWT using CARTO-Merge. (*D*) Ablation parameters according to the LAWT. FAM, fast anatomical map; LAWT, left atrial wall thickness; MDCT, multidetector computed tomography.

LAWT is an independent predictor of reconnection[10] and AF recurrence after 12 months of follow-up (FU).[11] The aforementioned variability in LAWT raises safety and efficacy concerns since underdosing of AI hinders lesion transmurality and overdosing of AI leads to potential complications.[12] Multidetector computed tomography (MDCT)-derived LAWT measurements have been reliably validated on a porcine model[13] and three-dimensional (3D) LAWT maps have already been generated from contrast-enhanced MDCT images.[14] However, integration of LAWT information on a 3D electroanatomical mapping system for guiding first AF ablations has not been yet described.

The aim of the present study is to describe feasibility, effectiveness, and safety of adapting the AI to the LAWT in a consecutive population of patients with PAF.

Methods

Patient sample

The present study reports the results of a prospective single-centre proof-of-concept study. Consecutive patients, aged 18 years or older, referred to Teknon Medical Center (Barcelona, Spain) for first PAF ablation were included. As per current guidelines, PAF was defined as AF that terminates spontaneously or with intervention within 7 days of onset.[1] In all patients, an MDCT study was performed prior to the ablation procedure. Multidetector computed tomography-derived maps with LAWT information were then imported into the navigation system for tailoring of the delivered energy based on AI. Exclusion criteria were impossibility to perform a cardiac MDCT and contraindication to perform high-frequency low-volume ventilation (HFLVV). The study complied with the Declaration of Helsinki, and the local ethics committee approved the study protocol. All participants included in the study provided informed written consent.

Pre-procedural multidetector computed tomography

A preprocedural MDCT was performed with a Revolution™ CT scanner (General Electric Healthcare). The images were acquired during an inspiratory breath-hold using retrospective electrocardiogram (ECG)-gating technique with tube current modulation set between 50% and 100% of the cardiac cycle. Angiographic images were acquired during the injection of a 70 mL bolus of Iopromide 370 mg I/mL (Ultravist, Bayer Hispania, Barcelona, Spain) at a rate of 3 mL/s. Data were transmitted to the workstation for post-processing and reconstructed into axial images with slice thickness of 0.625 mm.

Image post-processing

Multidetector computed tomography images were analysed with ADAS 3D™ software (ADAS3D Medical, Barcelona, Spain) to obtain a 3D atrial wall thickness map. To compute the atrial wall thickness, a three-step algorithm was applied: the endocardial layer was delineated by means of a semi-automatic segmentation based on pixel intensity thresholds. The threshold was manually defined by the operator and the rest of the endocardial segmentation was automatic; the epicardial layer was defined manually by delineation of the epicardial aspect in a mean of 20 ± 7 layers with automatic interpolation of the remaining epicardium followed by manual adjustment of the automatically interpolated epicardial layer. Finally, the wall thickness was automatically computed at each point as the distance between each endocardial point and its projection to the epicardial shell (Supplementary material online, *Figure S1*). These three steps result in a 3D wall thickness map that was then categorized into 1 mm ranges to facilitate operator's choice of the applied AI (*Figure 1*). The overall dedicated mean time to process the images by an experienced operator was 15 ± 2 min.

Data on reproducibility of the segmentation method has previously been reported[15] with an intra- and inter-observer reproducibility of the endocardial layer (automatic segmentation) for points closer than 1 mm of 99 ± 0.9% and 95 ± 5%, respectively. Intra- and inter-observer

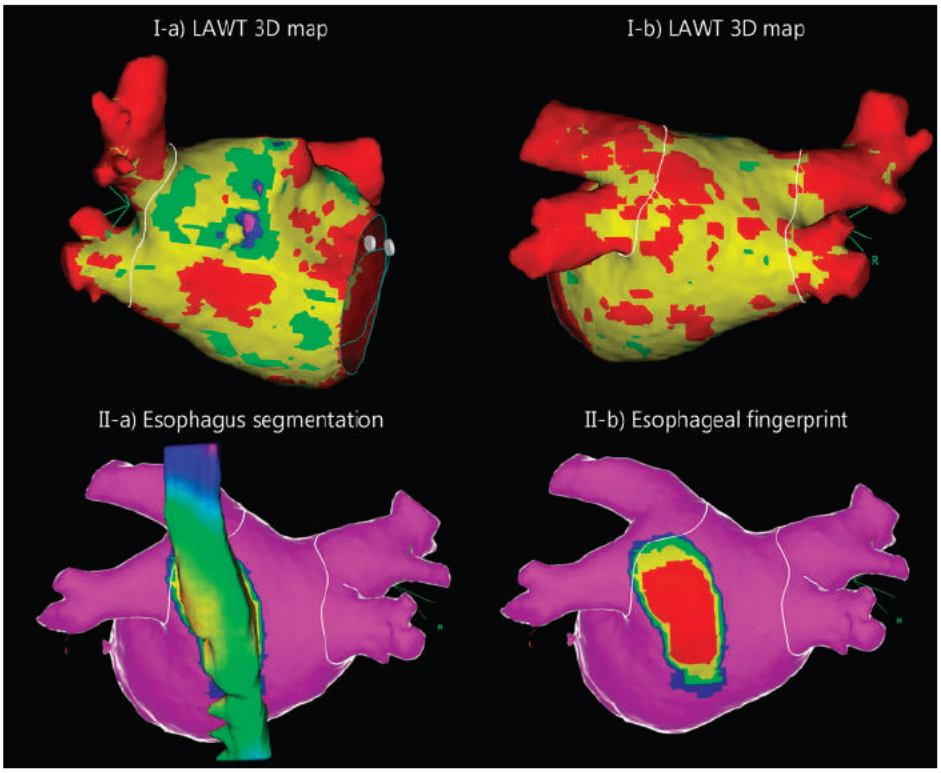

Figure 2 (*A*) The ablation lines are designed through the thinner circumferential PV regions aiming to avoid thicker regions. Example (*A-a*) shows the anterior aspect of the right pulmonary veins and example (*A-b*) the posterior aspect of both vein pairs. (*B*) Protocol for segmentation of the oesophagus and fingerprint in the posterior left atrial epicardial wall. (*B-a*) Oesophagus posterior view. (*B-b*) The isodistance fingerprint uses a colour scale to depict a range of distance between the oesophageal anterior wall and the left atrial posterior wall; red being the closest distance <1 mm, yellow 1–2 mm; green 2–3 mm; blue 3–4 mm; and purple >4 mm being the most distant. RF application in the vicinity of the oesophagus is performed as far as possible from the red fingerprinted zone. LAWT, left atrial wall thickness; PV, pulmonary vein.

reproducibility of the epicardial layer (manual segmentation) for points closer than 1 mm of 82 ± 10% and 78 ± 7%, respectively. This traduces on an overall mean intra-observer distance between discordant points of 0.1 mm on the endocardium and 0.5 mm on the epicardium and an inter-observer mean distance of 0.3 mm on the endocardium and 0.7 mm on the epicardium (Supplementary material online, *Figure S2*).

The rendered LAWT map was imported into CARTO navigation system (Biosense Webster, Diamond Bar, CA, USA) by using the Carto Merge tool. As *Figure 1* shows, a colour code was used to depict a thickness map (red <1 mm, yellow 1–2 mm, green 2–3 mm, blue 3–4 mm, and purple >4 mm). Previously to the procedure, the ablation line was manually traced on CARTO to complete an RF circle around the PV ostia (nephroid shape) on the 3D geometry. In case of a common ipsilateral vein ostium, the line was drawn around the trunk. A carina line was mandatory for the right pulmonary veins (RPVs), since there is anatomical[16] and electrophysiological evidence[17 19] for the presence of interconnections of the ipsilateral veins in up to two-thirds of the patients referred for AF ablation.[20] In case of a right common ostium this requirement was omitted. Ablation lines were designed through the thinner circumferential PV regions to avoid, as far as possible, thicker regions (*Figure 2*). Besides, the LA ablation protocol in our institution includes segmentation of the oesophagus. The distance between the LA posterior wall and the oesophagus is computed at each epicardial point, allowing to create an oesophageal print on top of the epicardial atrial layer. An isodistance colour map (oesophageal fingerprint) is created with a colour scale to depict a range of distances. This information is then used to personalize the ablation line and avoid, as far as possible, RF application on the posterior atrial wall region closest to the oesophagus (*Figure 2*).

Catheter ablation

Catheter ablation was performed by four operators (A.B., B.J., C.T., and D.P.), under general anaesthesia with HFLVV. Oral anticoagulation was uninterrupted and peri-procedural anticoagulation was performed to achieve an activated clotting time >300 s. All procedures were performed with a single venous femoral access, which is the usual local protocol. Transseptal puncture was guided by transoesophageal echocardiography. After that, a fast-anatomical map (FAM) of the entire LA anatomy and the PVs was acquired with the ablation catheter and merged with the LAWT map within the spatial reference coordinates of the CARTO system.

Pulmonary vein isolation was performed point-by-point, using a non-steerable sheath and a Thermocool SmartTouch 3.5-mm irrigated tip contact force-sensing RF ablation catheter (Biosense Webster, Inc. Diamond Bar, CA, USA). Maximal interlesion distance was 6 mm. VisiTag settings were catheter position stability minimum time 3 s, maximum range 3 mm; force over-time 25%, minimum force 3 g; lesion tag size: 3 mm. The irrigation flow rate was set to 2 mL/min during mapping and 26 mL/min during ablation. *Table 1* resumes the AI targets by local LAWT on the thickness colour map: thickness <1 mm (red): 300; 1–2 mm

(yellow): 350; 2–3 mm (green): 400; 3–4 mm (blue): 450; and >4 mm (purple): 500. To reach these AI values, the power output was set at 35 W for the posterior wall. For the anterior wall, power was set at 40 W for LAWT between <1 and 2 mm; and at 50 W wherever LAWT was >3 mm (green, blue, and purple on the thickness map). If the targeted AI value was not reached, another lesion reaching the target was applied. *Figure 3* shows examples of tailored AI applications.

Acute PVI was confirmed after first pass with the standard local single catheter method demonstrating entry block with the absence of PV potentials inside the vein with the ablation catheter placed sequentially in each segment inside the circumferential PV line, and exit block by proving absence of conduction to the left atrium when pacing from inside the circumferential PV line, at each segment sequentially.[15,21,22] Additional ablation was performed at connected sites until PVI was achieved. At the end of the procedure, a third expert not participating in the case should guarantee that there were no remaining gaps in the PVI lines; no ablation points with a lower than expected AI to LAWT target; and that the right carina line was performed. After that, the procedure was finished. There was no prespecified waiting time after PVI and adenosine challenge was not performed to detect underlying dormant PV conduction in any of the cases. Documented procedure time is the skin-to-skin time.

Table 1 Protocol for ablation parameters adapted to left atrial wall thickness

LAWT	Colour code	Ablation index		RF energy (W)	
		Anterior	Posterior	Anterior	Posterior
<1 mm	Red	300	300	40	35
1 2 mm	Yellow	350	350	40	35
2 3 mm	Green	400	400	50	35
3 4 mm	Blue	450	450	50	35
>4 mm	Purple	500	500	50	35

LAWT, left atrial wall thickness; RF, radiofrequency.

Wall thickness analysis

After the procedure, LAWT maps were exported from CARTO for analysis into a Matlab customized software. The circumferential PV lines were divided following the 16-segment model (*Figure 4*). Left atrial wall thickness was calculated for the whole LA; the circumferential PV line; the anterior and posterior walls, and each individual segment, respectively. The anterior wall was defined as the PV line continuity formed by the roof, anterosuperior (AS), anterior carina (AC), and anteroinferior segments (AI). The posterior wall was defined as the PV line continuity formed by the posterosuperior (PS), posterior carina (PC), posteroinferior (PI), and inferior (Inf) segments.

Follow-up

Patients were scheduled for FU at the outpatient clinic at 1, 3, 6, and every 6 months thereafter, or in case of symptoms. Each evaluation included an ECG and a 24-h Holter monitoring. Recurrences were considered as any documented arrhythmia (i.e. AF, atrial flutter, and atrial tachycardia) lasting longer than 30 s off anti-arrhythmic medication or symptoms suggesting clear recurrence as identified by the patient (symptoms that had been associated to a documented arrhythmia episode before the ablation procedure). All antiarrhythmic drugs (AADs) were stopped at ablation unless non-sustained AT/frequent atrial ectopic beats during in-hospital ECG monitoring. In that case, AAD were stopped at the end of the blanking period (3 months of FU).

Statistical analysis

All applicable statistical tests are two-sided and performed using a 5% significance level. Continuous variables are presented as mean ± standard deviation or median [range or interquartile range (IQR) if data are skewed] if not normally distributed. To compare means of two variables the Student's *t*-test, Mann–Whitney *U* test, or analysis of variance test were used, as appropriate. Categorical variables were expressed as total number (percentages) and compared between groups using Chi-square test. Statistical analysis was performed using IBM SPSS Statistics for Macintosh, version 25.0 (IBM Corp. Released 2017; Armonk, NY, USA: IBM Corp.) and customized code for the Matlab statistics toolbox

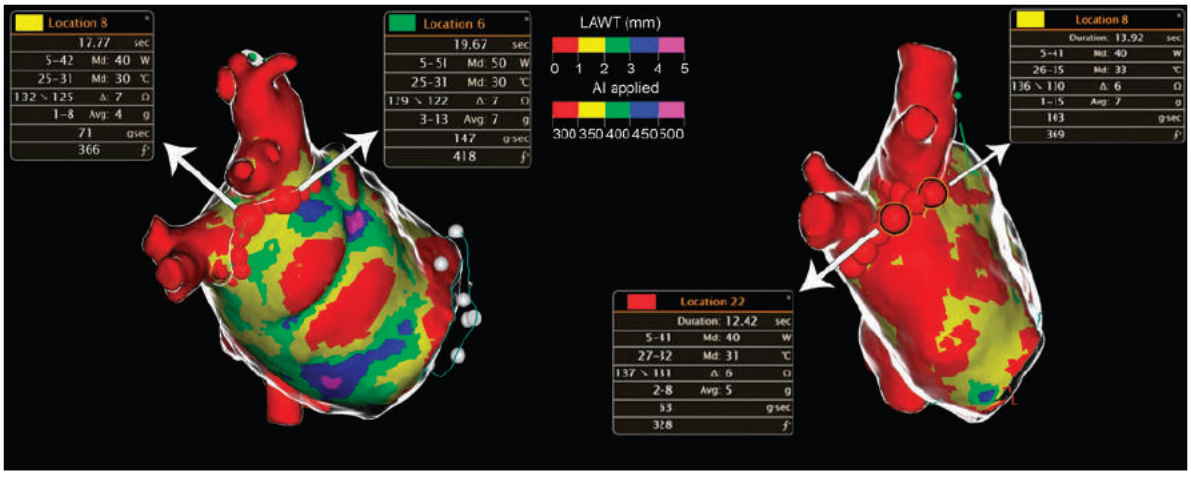

Figure 3 Left atrial wall thickness maps with different examples of tailored AI. Wall thickness maps with colour code and ablation index applied to each thickness range. AI, ablation index; LAWT, left atrial wall thickness.

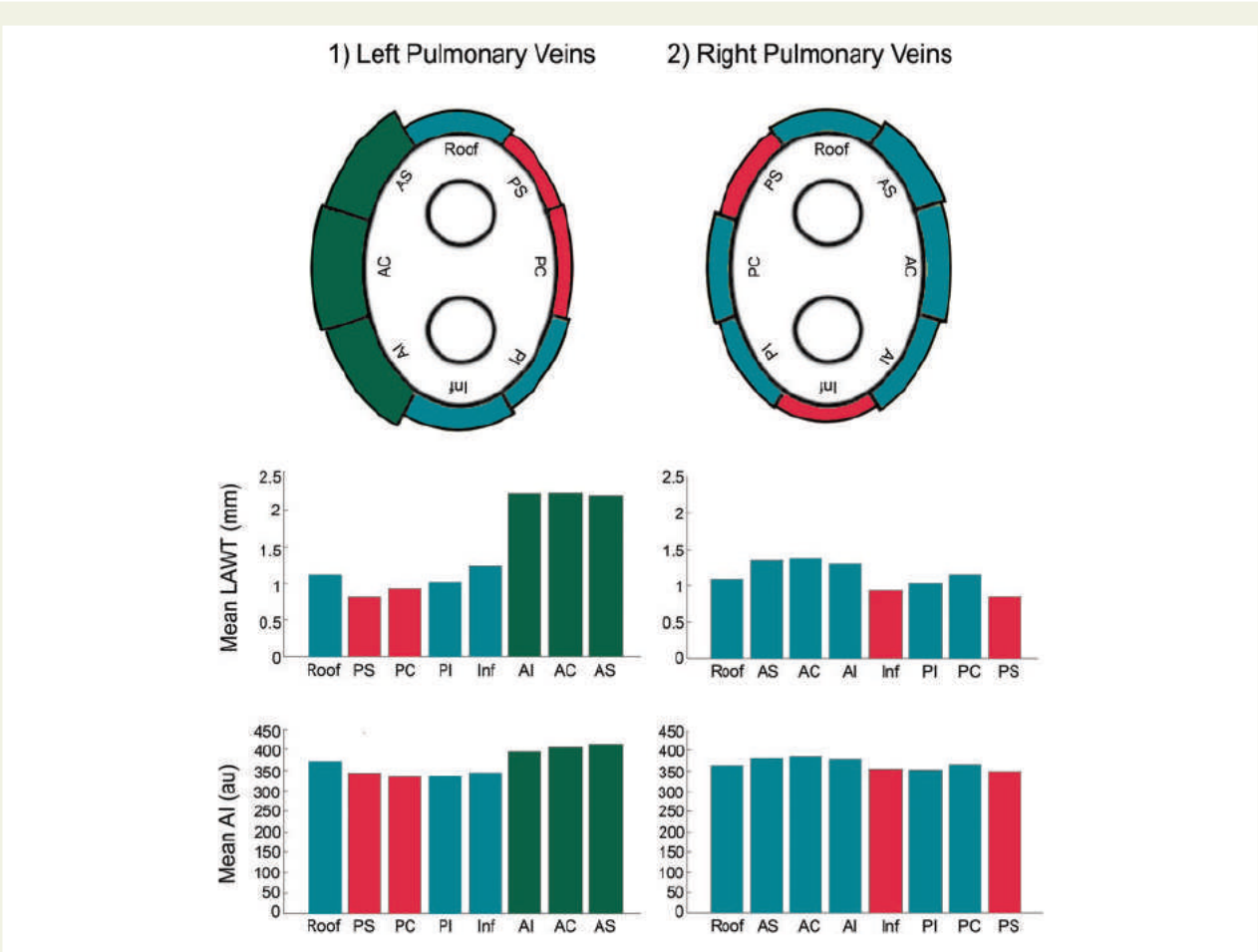

Figure 4 Ladybug plots of the pulmonary veins with left atrial wall thickness profile values for all the segments and histogram of left atrial wall thickness comparison between segments (top). Mean ablation index for each segment (bottom). AC, anterior carina; AI, anteroinferior; AS, anterosuperior; Inf, inferior; PC, posterior carina; PI, posteroinferior; PS, posterosuperior; PV, pulmonary vein; WT, wall thickness.

(Matlab R2010a, The Mathworks, Inc., Natick, MA, USA). A Kaplan–Meier survival analysis was performed for the analysis of survival free from atrial arrhythmia.

Results

Patient population

Ninety consecutive patients referred for a first PAF ablation were included from April 2019 to April 2020. Baseline clinical characteristics are summarized in *Table 2*. Resembling previously described PAF ablation populations,[7] mean age was 58 ± 13 years with 60 (67%) men with a relatively low comorbidity rate. Mean LA diameter was 38 ± 8 mm and mean left ventricular ejection fraction was 61 ± 15%. Fifteen out of 90 (16%) of the patients presented an underlying cardiomyopathy: six patients with hypertensive cardiomyopathy, four ischaemic cardiomyopathy, two tachycardiomyopathy, one valvular disease, one *cor triatriatum*, and one non-ischaemic dilated cardiomyopathy. Three patients were excluded because of impossibility to perform HFLVV (one had chronic obstructive pulmonary disease, one had severe heart failure, and one because an anaesthetist not familiar with the workflow was assigned to the lab); one patient was excluded because impossibility to obtain cardiac computed tomography (CT) scan.

Acute procedural characteristics

Procedural characteristics are summarized in *Table 3*. Ventilation rate was 50 ventilations per minute (IQR 45–60) with a tidal volume of 250 mL (220–280). Median total procedure skin-to-skin time was 59 min (IQR 49–67), including a merge time (FAM acquisition + MDCT merging on CARTO) of 12 min (IQR 11–14) and a transseptal time of 2 min (IQR 1–3). The number of RF points was 28 ± 8 for the left PVs and 31 ± 7 for the right PVs with a mean RF time of 6.5 ± 2 min on the left PVs and 8.3 ± 2 min on the right PVs (*Figure 5*). First pass PVI was obtained in 84 out of 90 (93%) of the RPVs and 87 (97%) of the left pulmonary veins (LPVs). On the RPVs absence of first pass PVI was observed in six patients and was attributable to the presence of epicardial connections in four of them. Of the two remaining patients, one had AI underdosing on the right inferior PV because of oesophageal position in the close vicinity of the PI

Table 2 Baseline characteristics of the study population

	Total ($n = 90$)
Age (years)	58 ± 13
Male	60 (67)
Arterial hypertension	24 (27)
Dyslipidaemia	10 (11)
Diabetes	5 (6)
BMI (kg/m^2)	27 ± 4
LVEF	61 ± 15
LA diameter (mm)	38 ± 8
CHADS-VASc	
0	30 (33)
1	27 (30)
2	17 (19)
3	13 (14)
4	3 (3)
Underlying heart disease	
None	76 (85)
Ischaemic	3 (3)
Hypertrophic	1 (1)
Valvular	1 (1)
Hypertensive	6 (7)
Other	3 (3)

Values are presented as *n* (%).
BMI, body mass index; LA, left atrium; LVEF, left ventricular ejection fraction.

Table 3 Acute procedural results

Procedure time (skin-to-skin) (min)	59 (49–66)
Radiofrequency time (min)	14 (12.5 16)
Fluoroscopy time (min)	0.75 (0.5 1.4)
Fluoroscopy dose area product (mGy/m^2)	1 (0.5 1.9)
Right pulmonary veins	
Perimeter (mm)	114 ± 10
RF time (min)	8.3 ± 2
Total VisiTags	31 ± 7
Mean VisiTag time (s)	14.4 ± 3.3
Mean anterior AI	376 ± 26
Mean posterior AI	355 ± 21
First pass isolation	84 (93%)
Mean anterior wall WT (mm)	1.28 ± 0.41
Mean posterior wall WT (mm)	0.99 ± 0.30
Left pulmonary veins	
Perimeter (mm)	101 ± 12
RF time (min)	6.5 ± 1.7
Total VisiTags	28 ± 8
Mean VisiTag time (s)	14.44 ± 3.32
Mean anterior AI	403 ± 41
Mean posterior AI	346 ± 28
First pass isolation	87 (97%)
Mean anterior wall WT (mm)	1.92 ± 0.72
Mean posterior wall WT (mm)	0.95 ± 0.34

Values are presented as mean ± standard deviation, median (interquartile range), or *n* (%).
AI, ablation index; RF, radiofrequency.

segment and the other patient had a failed first-pass isolation on the AC segment, in spite of correct AI dosing according to binarized LAWT map. On the LPVs absence of first pass PVI was observed in three patients because of epicardial connections in all of them (Supplementary material online, *Table S1*). Acute reconnection was observed in 1 out of 90 patients (1%) for the right superior pulmonary vein and 1 out of 90 patients (1%) for the right inferior pulmonary vein. No acute reconnections were observed in the LPVs. At the end of the procedure, PVI was obtained in all cases. No case was excluded because of third expert disapproval of the lesion set.

Ablation index was modified due to the oesophageal position in 30/90 (30%) patients. The mean number of ablation points affected by the oesophageal position was 4 ± 2. Even though AI was decreased owing to oesophageal position, 29/30 patients (97%) presented first pass isolation. Only in one case an additional RF application was necessary to obtain PVI.

No major complication occurred. There was a non-complicated haematoma owing to bleeding from a secondary branch of the superficial femoral artery without the need for surgical treatment or blood transfusion. No other procedure-related complications were documented.

Left atrial wall thickness and ablation index measurements

Mean LAWT was 1.2 ± 0.6 mm for the whole LA and 1.2 ± 0.4 mm for the circumferential PV line. The circumferential PV line was thicker in the LPVs as compared to the RPVs (1.4 ± 0.6 mm vs. 1.1 ± 0.1 mm, $P < 0.001$). The anterior segments (Roof, AS, AC, and AI) were significantly thicker than the posterior ones (PS, PC, PI, and inf) (1.2 ± 0.3 mm vs. 0.9 ± 0.3 mm, $P < 0.001$). However, substantial variability was observed on the LAWT within each of these areas (posterior/anterior) with a LAWT range of 0.3–4.5 mm on the anterior wall and 0.3–2.3 mm on the posterior wall.

Figure 4 shows the mean wall thickness of each segment. In the LPVs, AC and AS segments were the thicker (2.2 ± 0.6 and 2.1 ± 0.6, respectively); and the PS was the thinnest (0.7 ± 0.3). In the RPVs the thicker segments were the AS and AC (1.3 ± 0.4 and 1.3 ± 0.4, respectively); and the PS segment was the thinnest (0.8 ± 0.2). The mean applied AI was 385 ± 36 for the anterior and 350 ± 25 for the posterior wall; and the mean AI by vein pair was 366 ± 26 on the RPVs and 380 ± 42 on the LPVs. There was a significant correlation between LAWT and the applied AI ($P < 0.001$).

Follow-up

In-hospital stay was 24 h for all patients except for the one presenting a femoral haematoma who stayed for 72 h because of the need for imaging control. Arrhythmia recurrences have been observed in 6 out of 90 (6.6%) patients during a mean FU of 16 ± 4 months. Four patients presented clinical episodes of palpitations that required

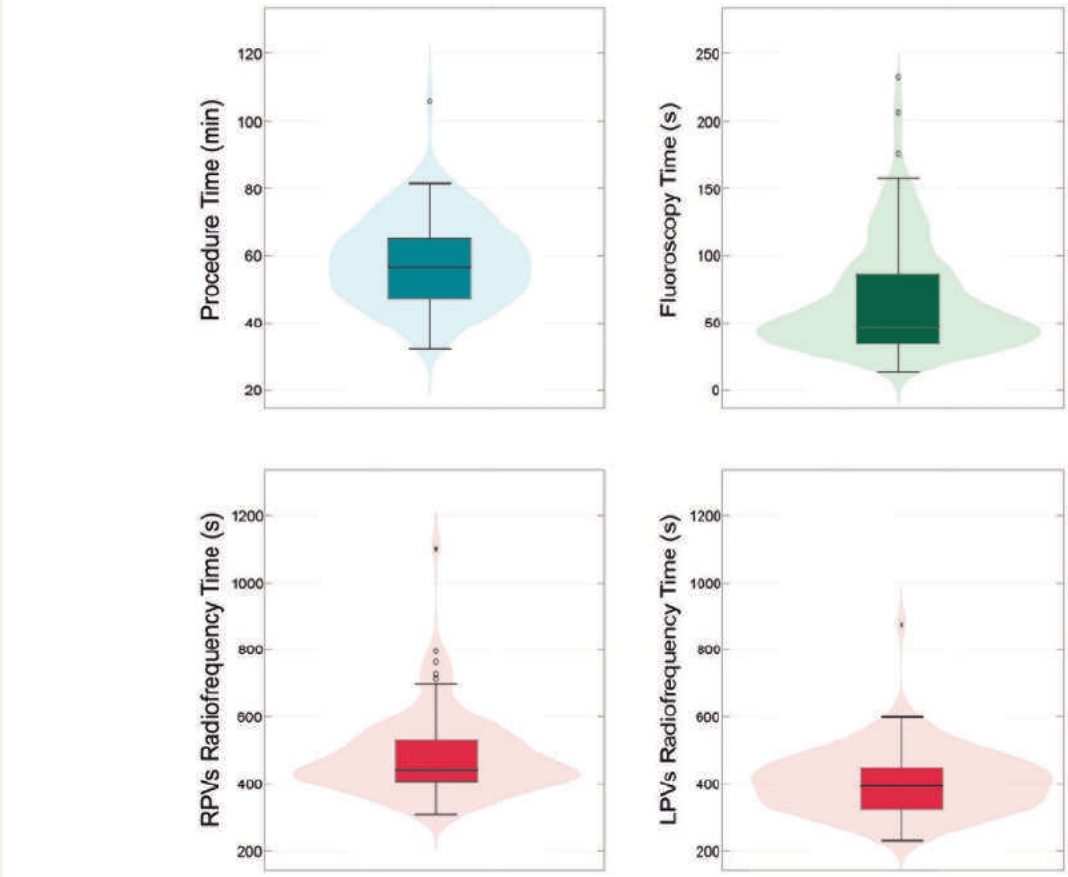

Figure 5 Graphic representation of acute procedural data. Violin plots representing procedure time (top left); fluoroscopy time (top right); right pulmonary veins radiofrequency application time; and left pulmonary veins radiofrequency application time. LPVs, left pulmonary veins; RF, radiofrequency; RPVs, right pulmonary veins.

medical care with documented AF on the ECG. In the two remaining patients, recurrence diagnosis was made based on self-reported episodes of palpitations but without documentation of AF on ECG or Holter monitoring. Only eight (9%) patients were on AADs at discharge, due to presence of non-sustained AT/frequent atrial ectopic beats during in-hospital ECG monitoring. This treatment was stopped at the 3-month FU, except for one patient who was still on AAD at 6 months FU because of patient choice and presented with a recurrence at 8 months. *Figure 6* shows the Kaplan–Meier curve for AF recurrence.

Discussion

This is the first study that describes the feasibility of integrating the LAWT maps into the navigation system in patients undergoing a first PVI procedure. Ablation index was tailored to LAWT information, a major determinant of lesion transmurality. This personalized approach adapted RF delivery by increasing AI in the thicker segments of the PV line and avoiding unnecessary high amounts of RF energy delivery in the thinnest ones, which could negatively impact procedure safety. Moreover, this study describes a single catheter approach that simplifies the ablation setting. This comprehensive approach results in a short procedure (skin-to-skin), fluoroscopy, and RF times while providing efficacy outcomes that could be comparable to those of more demanding ablation protocols,[7,23] although this hypothesis needs to be proven in further trials.

Personalized radiofrequency delivery by tailoring ablation index to the left atrial wall thickness

Three-dimensional LAWT maps have previously been obtained[14] but the present study reports a prospective application of this tool that allows for real-time evaluation of the LAWT at any location within the LA. Previous studies with MDCT have also reported that the posterior wall is significantly thinner than the anterior wall.[11,12] Having this anatomical concept in mind, current AI-guided PVI protocols target a lower AI value (in general 400) at the posterior wall near the oesophagus. Nevertheless, not all centres use oesophageal position or temperature monitoring as a standard of care. The results of the present study, in line with these previous observations, found

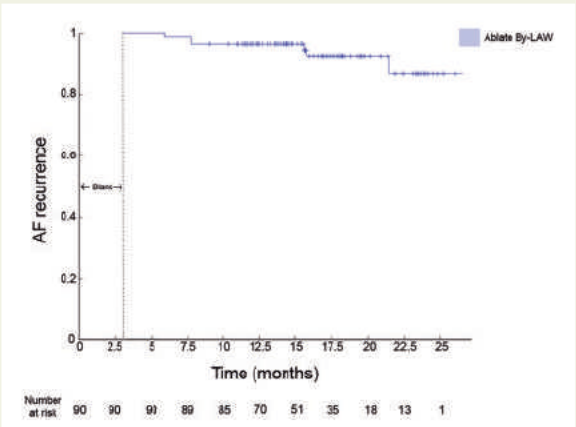

Figure 6 Survival plot for freedom of atrial fibrillation/atrial tachycardia after paroxysmal atrial fibrillation ablation with By-LAW protocol.

that the posterior wall is significantly thinner than the anterior wall. However, different ranges of wall thickness were observed regardless of the anterior/posterior aspect, with a LAWT ranging from 0.3 to 2.4 mm in the posterior wall and from 0.4 to 4.5 mm in the anterior wall. These data suggest that the strategy of dichotomizing into anterior/posterior for RF delivery is an oversimplification that does not take in consideration the complex anatomical reality of the LA.

Moreover, the proposed approach results in a very high rate of first past isolation despite delivering a low amount of RF. Recently, Taghji *et al.* described an ablation protocol (CLOSE) respecting strict criteria for lesion depth and contiguity using predefined AI cut-offs of 400 at posterior wall and 550 at anterior wall. This strategy resulted in a high rate of acute PV isolation with a low recurrence rate. The results of the present study are comparable in terms of acute and durable PV isolation. However, RF requirements to achieve these results are significantly lower by adapting AI to LAWT. In the present study mean AI values in the posterior and anterior wall were 350 ± 25 and 385 ± 36, respectively, compared with the mean AI of 456 (449–469) used in the close study. Mean RF time was 8.3 ± 2 and 6.5 ± 2 min (for right and left PV respectively) compared with 16 ± 4 and 18 ± 6 min in the CLOSE study. The low values of RF needed to isolate the PVs are probably due to the efficiency of the proposed methods (applying more RF only in the thicker segments and saving RF application in the thinner part of the circumferential line), but also to the preprocedural design of the PV ablation line aiming to avoid the thicker regions wherever possible. The value of LAWT is to deliver the proper amount of energy at any given point without doing it randomly. Importantly, MDCT has long been used in our group (as in many centres) before every AF catheter ablation to characterize PV anatomy, as has been the Carto Merge module. Therefore, the LAWT method only adds in many cases one step, which is Dicom image segmentation. At the present time, this represents image processing of 15 ± 2 min by an experienced operator. Moreover, the process is still being optimized and with the use of artificial intelligence will be even faster once it is made available.

Safety of the Ablate by-LAW protocol

The present study reports a low complication rate by adapting AI to the LAWT. In the ablate by-LAW protocol, RF power was higher than usually reported with other AI protocols, reaching 50 W in thicker regions of the anterior wall and right carina line, without raising any safety issue in this patient population. Apart from a femoral haematoma treated conservatively, no other complication was observed, namely no steam pop or cardiac tamponade. In terms of potential safety increase, the value of LAWT is to deliver the proper amount of energy at any given point without doing it randomly.

Circumferential PVI unavoidably implies RF application on the posterior wall where the distance from the atrial epicardium to the oesophagus can be less than 1 mm. This article describes the oesophageal fingerprint, a new tool for avoiding RF application in these areas of the posterior wall where the distance between the epicardial surface of the LA and the oesophagus is very low. Using this tool, circumferential PV lines were drawn in a personalized fashion previously to the procedure to improve safety of the applications in the posterior wall.

Single catheter venous access

The single catheter approach was previously described in first AF ablations by Pambrun *et al.*,[21] demonstrating that antral exit block validated with a CF-sensing ablation catheter successfully predicts PVI. When first pass PVI was not achieved, the electrical breakthrough could be identified based on timing of the local PV electrogram without the need of a further catheter for reference.[22] The present study reports on a single catheter approach in the ablate by-LAW setting. The method is feasible and efficient, as reflected in the low recurrence rate observed during the FU. Thus, the procedure workflow simplification results in high efficiency with a median procedure time under 1 h (skin-to-skin) and a very low fluoroscopy time and dose. Moreover, this approach had a very low complication rate (only one vascular complication) probably also in relation with the use of a single vascular access.

Limitations

This is a feasibility and hypothesis generating study. The main limitation is the lack of a control group for comparison. Consequently, we cannot demonstrate a superiority of the presented method as compared to an AI-guided PVI group. Also important, it was performed at a single centre. Besides, included patients were relatively healthy (CHA_2DS_2-VASc-Score = 0 in 33% of patients, mean LA diameter 38 ± 8 mm). Thus, this cohort might not represent the 'typical' all-comer population undergoing catheter ablation and extrapolation of reported results could be limited since in clinical practice, patients usually are older, have a higher cardiovascular burden, and have a more complex arrhythmogenic substrate. A multicentre study is ongoing to overcome some of these limitations. Besides, AI targets for each LAWT range were based on empiric parameters. Further research is needed to evaluate the optimal parameters of AI application according to the LAWT. We are reporting only a mean FU of 16 ± 4 months. In consequence, the benefits are indicated by this observational study and not proven and longer-term results of the proposed approach remain still unknown. In addition, given the spatial

resolution of the CT scan of 0.4 mm with a 3.5 mm catheter tip, it could be that the chosen roadmap for personalizing PVI differs because of inaccuracy of the integration. Also, asymptomatic arrhythmia episodes may have been missed due to the relatively low intensity of the ECG/Holter monitoring-based FU. Finally, oesophageal temperature was not systematically measured during ablation. Thus, we cannot evaluate the impact that modifying the circumferential PV line based on the oesophageal fingerprint has on oesophageal temperature; a randomized trial is underway (the AWESOME trial) to evaluate this issue.

Conclusion

Personalized AF ablation with the Ablate-By-LAW protocol using a single catheter technique and adapting the AI to LAWT is feasible, effective, and safe while obtaining a high rate of first-pass isolation in this patient population. Freedom from AF recurrences observed with the presented method may be as high as in more demanding ablation protocols. Nevertheless, this was an observational study and further randomized trials are needed to prove this hypothesis.

Supplementary material

Supplementary material is available at *Europace* online.

Funding

C.T. was funded by the research fellowship of the Swiss Heart Rhythm Foundation. J.M.C. was funded by a Scholarship from Sociedad Española de Cardiología (SEC).

Conflict of interest: A.B. is stockholder of ADAS 3D Medical. D.S.-I. is an employee of Biosense Webster. All remaining authors have no other relevant affiliations or financial involvement with any organization or entity with a financial interest in or financial conflict with the subject matter or materials discussed in the manuscript apart from those disclosed.

Data availability

Data are available upon request to the corresponding author.

References

1. Hindricks G, Potpara T, Dagres N, Arbelo E, Bax JJ, Blomström-Lundqvist C *et al.*; ESC Scientific Document Group. 2020 ESC Guidelines for the diagnosis and management of atrial fibrillation. *Eur Heart J* 2021;**42**:373–498.
2. Cappato R, Negroni S, Pecora D, Bentivegna S, Lupo PP, Carolei A *et al.* Prospective assessment of late conduction recurrence across radiofrequency lesions producing electrical disconnection at the pulmonary vein ostium in patients with atrial fibrillation. *Circulation* 2003;**108**:1599–604.
3. Nanthakumar K, Plumb VJ, Epstein AE, Veenhuyzen GD, Link D, Kay GN. Resumption of electrical conduction in previously isolated pulmonary veins: rationale for a different strategy? *Circulation* 2004;**109**:1226–9.
4. Das M, Loveday JJ, Wynn GJ, Gomes S, Saeed Y, Bonnett LJ *et al.* Ablation index, a novel marker of ablation lesion quality: prediction of pulmonary vein reconnection at repeat electrophysiology study and regional differences in target values. *Europace* 2017;**19**:775–83.
5. El Haddad M, Taghji P, Phlips T, Wolf M, Demolder A, Choudhury R *et al.* Determinants of acute and late pulmonary vein reconnection in contact force-guided pulmonary vein isolation: identifying the weakest link in the ablation chain. *Circ Arrhythm Electrophysiol* 2017;**10**:e004867.
6. Miller MA, d'Avila A, Dukkipati SR, Koruth JS, Viles-Gonzalez J, Napolitano C *et al.* Acute electrical isolation is a necessary but insufficient endpoint for achieving durable PV isolation: the importance of closing the visual gap. *Europace* 2012;**14**:653–60.
7. Taghji P, El Haddad M, Phlips T, Wolf M, Knecht S, Vandekerckhove Y *et al.* Evaluation of a strategy aiming to enclose the pulmonary veins with contiguous and optimized radiofrequency lesions in paroxysmal atrial fibrillation: a pilot study. *JACC Clin Electrophysiol* 2018;**4**:99–108.
8. Ho SY, Sanchez-Quintana D. The importance of atrial structure and fibers. *Clin Anat* 2009;**22**:52–63.
9. Kistler PM, Ho SY, Rajappan K, Morper M, Harris S, Abrams D *et al.* Electrophysiologic and anatomic characterization of sites resistant to electrical isolation during circumferential pulmonary vein ablation for atrial fibrillation: a prospective study. *J Cardiovasc Electrophysiol* 2007;**18**:1282–8.
10. Inoue J, Skanes AC, Gula LJ, Drangova M. Effect of left atrial wall thickness on radiofrequency ablation success. *J Cardiovasc Electrophysiol* 2016;**27**:1298–303.
11. Suenari K, Nakano Y, Hirai Y, Ogi H, Oda N, Makita Y *et al.* Left atrial thickness under the catheter ablation lines in patients with paroxysmal atrial fibrillation: insights from 64-slice multidetector computed tomography. *Heart Vessels* 2013;**28**:360–8.
12. Soor N, Morgan R, Varela M, Aslanidi OV. Towards patient-specific modelling of lesion formation during radiofrequency catheter ablation for atrial fibrillation. *Conf Proc IEEE Eng Med Biol Soc* 2016;**2016**:489–92.
13. Sun J-Y, Yun C-H, Mok GSP, Liu YH, Hung CL, Wu TH *et al.* Left atrium wall-mapping application for wall thickness visualisation. *Sci Rep* 2018;**8**:4169.
14. Bishop M, Rajani R, Plank G, Gaddum N, Carr-White G, Wright M *et al.* Three-dimensional atrial wall thickness maps to inform catheter ablation procedures for atrial fibrillation. *Europace* 2016;**18**:376–83.
15. Teres C, Soto-Iglesias D, Penela D, Jáuregui B, Ordoñez A, Chauca A *et al.* Left atrial wall thickness of the pulmonary vein reconnection sites during atrial fibrillation redo procedures. *Pacing Clin Electrophysiol* 2021;**44**:824–34.
16. Cabrera JA, Ho SY, Climent V, Fuertes B, Murillo M, Sánchez-Quintana D. Morphological evidence of muscular connections between contiguous pulmonary venous orifices: relevance of the interpulmonary isthmus for catheter ablation in atrial fibrillation. *Heart Rhythm* 2009;**6**:1192–8.
17. Valles E, Fan R, Roux JF, Liu CF, Harding JD, Dhruvakumar S *et al.* Localization of atrial fibrillation triggers in patients undergoing pulmonary vein isolation: importance of the carina region. *J Am Coll Cardiol* 2008;**52**:1413–20.
18. Udyavar AR, Chang S-L, Tai C-T, Lin YJ, Lo LW, Tuan TC *et al.* The important role of pulmonary vein carina ablation as an adjunct to circumferential pulmonary vein isolation. *J Cardiovasc Electrophysiol* 2008;**19**:593–8.
19. Lin YJ, Tsao HM, Chang SL, Lo LW, Tuan TC, Hu YF *et al.* The distance between the vein and lesions predicts the requirement of carina ablation in circumferential pulmonary vein isolation. *Europace* 2011;**13**:376–82.
20. Squara F, Liuba I, Chik W, Santangeli P, Maeda S, Zado ES *et al.* Electrical connection between ipsilateral pulmonary veins: prevalence and implications for ablation and adenosine testing. *Heart Rhythm* 2015;**12**:275–82.
21. Pambrun T, Combes S, Sousa P, Bloa ML, El Bouazzaoui R, Grand-Larrieu D *et al.* Contact-force guided single-catheter approach for pulmonary vein isolation: feasibility, outcomes, and cost-effectiveness. *Heart Rhythm* 2017;**14**:331–8.
22. Arenal A, Atea L, Datino T, González-Torrecilla E, Atienza F, Almendral J *et al.* Identification of conduction gaps in the ablation line during left atrium circumferential ablation: facilitation of pulmonary vein disconnection after endpoint modification according to electrogram characteristics. *Heart Rhythm* 2008;**5**:994–1002.
23. Hussein A, Das M, Chaturvedi V, Asfour IK, Daryanani N, Morgan M *et al.* Prospective use of ablation index targets improves clinical outcomes following ablation for atrial fibrillation. *J Cardiovasc Electrophysiol* 2017;**28**:1037–47.

Artículo 3

"Relación entre la pared auricular posterior y el esófago: posición esofágica durante la ablación de la fibrilación auricular"

Este estudio buscó comprender la relación anatómica entre la pared auricular posterior y el esófago durante los procedimientos de ablación de FA. Esta relación es fundamental debido al riesgo de lesión esofágica durante la ablación de la FA. Los hallazgos resaltaron la variabilidad en la posición del esófago en relación con la pared auricular posterior entre diferentes individuos. Sin embargo, se observó que la posición esofágica en cada paciente es poco variable. El conocimiento de la posición esofágica es crucial para mejorar la seguridad del procedimiento de ablación de FA. Al comprender la posición exacta del esófago en relación con la pared auricular, pueden realizarse adaptaciones a las técnicas de ablación para minimizar el daño potencial al esófago. Los conocimientos de este estudio subrayan la importancia de los enfoques individualizados y las evaluaciones de imágenes disponibles durante los procedimientos de ablación de FA.

Relationship between the posterior atrial wall and the esophagus: Esophageal position during atrial fibrillation ablation

Cheryl Teres, MD,*† David Soto-Iglesias, MSc, PhD,* Diego Penela, MD, PhD,* Beatriz Jáuregui, MD, MSc,* Augusto Ordoñez, MD, PhD,* Alfredo Chauca, MD,* Jose Miguel Carreño, MD,* Claudia Scherer, MD,* Marina Huguet, MD, PhD,* Carlos Ramírez, MD,* José Torres Mandujano, MD,* Giuliana Maldonado, MD,* Alejandro Panaro, MD,* Julio Carballo, MD,* Óscar Cámara, MSc, PhD,‡ Jose-Tomás Ortiz-Pérez, MD, PhD,* Antonio Berruezo, MD, PhD*

*From the *Heart Institute, Teknon Medical Center, Barcelona, Spain, †Cardiology Department, Lausanne University Hospital, Lausanne, Switzerland, and ‡PhySense group, BCN-MedTech, Department of Information and Communication Technologies, Universitat Pompeu Fabra, Barcelona, Spain.*

BACKGROUND Atrial fibrillation ablation implies a risk of esophageal thermal injury. Esophageal position can be analyzed with imaging techniques, but evidence for esophageal mobility is inconsistent.

OBJECTIVES The purpose of this study was to analyze esophageal position stability from one procedure to another and during a single procedure.

METHODS Esophageal position was compared in 2 patient groups. First, preprocedural multidetector computerized tomography (MDCT) of first pulmonary vein isolation and redo intervention (redo group) was segmented with ADAS 3D™ to compare the stability of the atrioesophageal isodistance prints. Second, 3 imaging modalities were compared for the same procedure (multimodality group): (1) preprocedural MDCT; (2) intraprocedural fluoroscopy obtained with the transesophageal echocardiographic probe in place with CARTOUNIVU™; and (3) esophageal fast anatomic map (FAM) at the end of the procedure. Esophageal position correlation between different imaging techniques was computed in MATLAB using semiautomatic segmentation analysis.

RESULTS Thirty-five redo patients were analyzed and showed a mean atrioesophageal distance of 1.2 ± 0.6 mm and a correlation between first and redo procedure esophageal fingerprint of 91% ± 5%. Only 3 patients (8%) had a clearly different position. The multi-imaging group was composed of 100 patients. Esophageal position correlation between MDCT and CARTOUNIVU was 82% ± 10%; between MDCT and esophageal FAM was 80% ± 12%; and between esophageal FAM and CARTOUNIVU was 83% ± 15%.

CONCLUSION There is high stability of esophageal position between procedures and from the beginning to the end of a procedure. Further research is undergoing to test the clinical utility of the esophageal fingerprinted isodistance map to the posterior atrial wall.

KEYWORDS Atrial fibrillation; Atrial wall thickness; Atrioesophageal fistula; Catheter ablation; Esophageal position

Introduction

Pulmonary vein isolation (PVI) can now be considered first-line rhythm control therapy for patients with symptomatic paroxysmal atrial fibrillation (AF) episodes or persistent AF without major risk factors for AF recurrence as an alternative to antiarrhythmic drugs.[1] A PVI approach implies unavoidable ablation lesions on the posterior atrial wall. The left atrial (LA) wall is a thin structure with heterogeneous thickness (range <1 mm to >5 mm), with important inter- and intrapatient variability.[2] The esophagus is closely related to the LA posterior wall. This anatomic relationship depends mainly on aortic arch anatomy and location and its influence on esophageal position.[3] Due to the proximity between these structures, posterior wall ablation may result in several complications, ranging from asymptomatic esophageal lesions to perforation with atrioesophageal fistula (AEF), which might be lethal.[4] Other possible complications include damage to periesophageal nervous plexi, which can result in postablation gastrointestinal complications such as gastroparesis, pyloric spasm, and gastroesophageal reflux.[5] Therefore, a widespread practice is to routinely modify energy delivery settings when ablating on the posterior wall. In addition,

Address reprint requests and correspondence: Dr Antonio Berruezo, Heart Institute, Teknon Medical Center, C/ Vilana, 12, 08022 Barcelona, Spain. E-mail address: antonio.berruezo@quironsalud.es.

2666-5018/

https://doi.org/10.1016/j.hroo.2022.02.007

KEY FINDINGS

- There is high stability of the atrioesophageal relationship between procedures even 6 months apart and of the esophageal position from the beginning to the end of an atrial fibrillation ablation procedure.
- The multidetector computerized tomography (MDCT)–derived esophageal fingerprinted isodistance map is a new way of depicting the complex relationship between the esophagus and the left atrial posterior wall.
- The fingerprinted map allows for better understanding of the atrioesophageal relationship, which is fundamental for improving procedural safety.

several techniques, such as endoesophageal temperature monitoring probes, have been developed to lower the risk of complications, although randomized data argue against the usefulness of this method to prevent esophageal thermal lesions[6] and even point to a potential harm.[7]

Contemporary imaging techniques allow for esophageal position identification, potentially offering new methods to prevent esophageal thermal injury. Nevertheless, it has been reported that atrioesophageal interaction could be dynamic due to esophageal mobility, with diverging evidence available to date.

The aims of the present study were (1) to analyze the stability of esophageal position inside the mediastinum, hypothesizing that it does not differ significantly on multidetector computerized tomography (MDCT) from one procedure to another; and (2) to evaluate the correlation in esophageal position with multimodality imaging performed before, during, and after a single LA ablation procedure. This information could help develop safer ablation strategies by avoiding ablation at the sites closest to the esophagus.

Methods

Patient sample

Two patient populations were analyzed: (1) a group of consecutive patients referred for AF redo ablation procedure from November 2018 to November 2019 for whom the esophageal position on MDCT was compared between the first ablation and the redo procedure (Group 1: MDCT); and (2) a group of consecutive patients referred for any AF ablation procedure from March 2020 to November 2020 in whom the esophageal position was obtained by 3 different imaging methods (MDCT, CARTOUNIVU™ module [Biosense Webster, Diamond Bar, CA], and esophageal fast anatomic map [FAM]) and compared between one another (Group 2: Multimodality). Figure 1 shows the study design. Age <18 years, pregnancy, presence of concomitant investigation treatments, patient's refusal to participate in the study, unavailability of preprocedural MDCT, and contraindication or inability to obtain esophageal FAM were exclusion criteria. Patient populations were different for both groups. The study complied with the Declaration of Helsinki, and the study protocol was approved by the local ethics committee. All participants included in the study provided written informed consent.

Preprocedural MDCT and image processing

In all patients, an MDCT study was performed before the procedure. MDCT was performed using a dual-source SOMATOM™ Definition Flash 128-slice scanner (Siemens Healthineers, Erlangen, Germany) or a Revolution™ scanner (General Electric Healthcare, Milwaukee, WI). Images were acquired during an inspiratory breathhold using retrospective electrocardiography-gating technique with tube current modulation set between 50% and 100% of the cardiac cycle. Angiographic images were acquired during injection of a 100-mL bolus of iopromide 370 mg I/mL (Ultravist, Bayer Hispania, Barcelona, Spain) at a rate of 3 mL/s. Data were transmitted to the workstation for postprocessing and reconstructed into axial images with slice thickness of 0.625 mm.

MDCT image postprocessing

MDCT digital imaging and communications in medicine (DICOM) images were analyzed using ADAS 3D™ software (ADAS3D Medical, Barcelona, Spain) to segment the esophageal anatomy and the atrioesophageal fingerprinted isodistance map. The endocardial and epicardial LA wall layers were segmented according to a previously described method.[8] The esophageal surface layer was defined by manual delineation into 7 ± 3 slices, followed by an interpolation in the missing slices. Then, esophageal position and the distance between the esophagus and the epicardial LA posterior wall and pulmonary veins (PVs) were automatically measured and projected onto the endocardial shell as a color-coded isodistance fingerprinted map, in which red depicts the closest area with an atrioesophageal distance <1 mm, yellow 1.1–2 mm, green 2.1–3 mm, blue 3.1–4 mm, and purple >4 mm. Figure 2 shows the pipeline of the segmentation method resulting in a 3-dimensional (3D) map of the atrioesophageal relationship, which can be projected to the atrial endocardial mesh and imported into the CARTO navigation system (Biosense Webster, Diamond Bar, CA). The esophageal trajectory as related to the atrial posterior wall was classified into 5 categories (left, central, right, left-central, and right-central).

Esophageal visualization with CARTOUNIVU image integration module

At the beginning of the procedure, the fluoroscopic image is centered within the coordinates of the CARTO navigation system by means of a reference ring located underneath the table at the lower part of the chest/upper abdomen. Then, fluoroscopic images with the transesophageal echocardiographic (TEE) probe positioned in the esophagus are

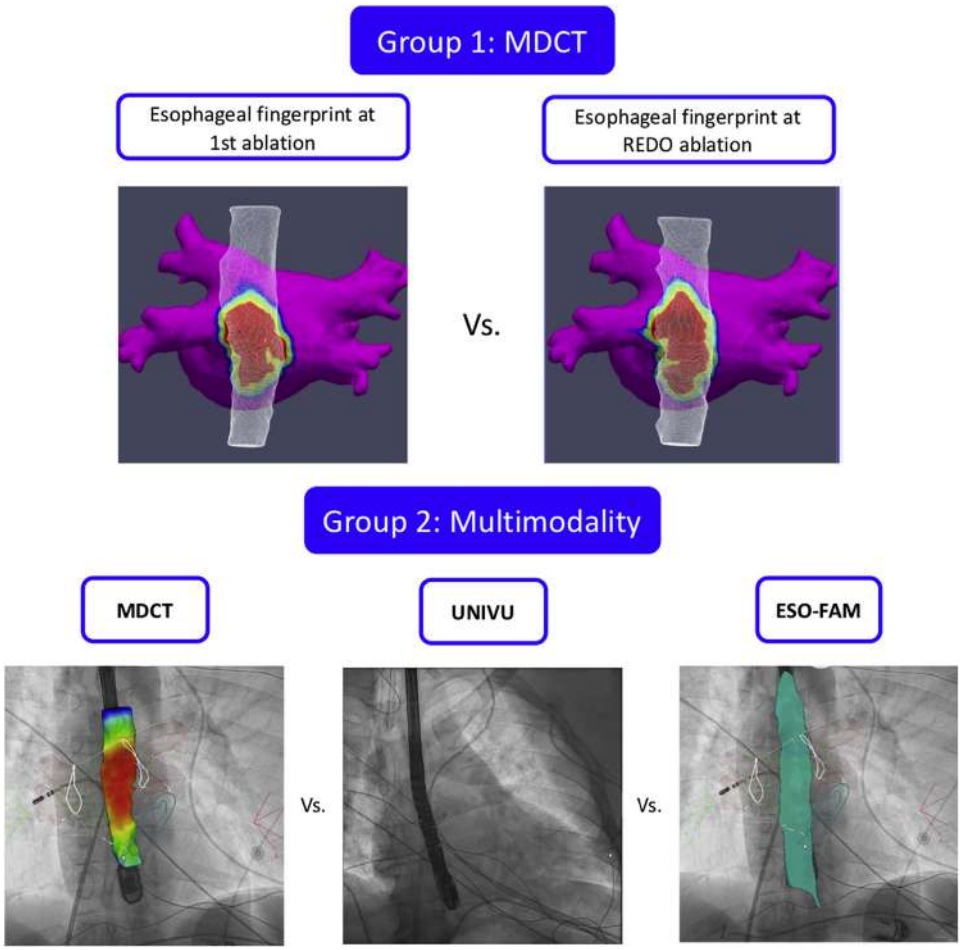

Figure 1 Study group design. **Top:** Group 1 redo: Comparison of atrioesophageal relationship as seen by the esophageal isodistance fingerprinted map, between preprocedural MDCT at first and redo ablations. **Bottom:** Group 2 multimodality: Comparison of 3 different imaging methods for the same procedure. **Left:** Anteroposterior fluoroscopic view with superposed esophageal anatomy segmented from the MDCT and atrial anatomy in glass mode. **Center:** Anteroposterior fluoroscopic view with the transesophageal echocardiographic probe inserted in the esophagus. **Right:** Anteroposterior fluoroscopic view with superposed esophageal fast anatomic map (ESO-FAM) obtained with the ablation catheter. MDCT = multidetector computerized tomography.

recorded in anteroposterior, right anterior oblique 30°, and left anterior oblique 30° fluoroscopic projections. For image acquisition, the TEE operator was asked to advance the probe in a neutral position to a location further than the fluoroscopic position of the LA. The CARTOUNIVU module provides transfer of fixed fluoroscopic images or cine loops to the CARTO3 system, allowing for real-time visualization of intracardiac catheters in the 3D mapping environment on a background of stored fluoroscopic images (Figure 3, section 1). Every capture automatically enters the original and its 180° invert orientation (as a mirror image for a virtual biplane view). Once the fluoroscopic images were acquired, the TEE probe was removed as soon as possible and at the latest before radiofrequency (RF) application.

Catheter ablation

Catheter ablation was performed by the By-LAW method,[9] with patients under general anesthesia with high-frequency, low-volume ventilation. Oral anticoagulation was uninterrupted, and periprocedural anticoagulation was performed to achieve an activated clotting time >300 seconds. All procedures were performed with a single venous femoral access and a near-zero fluoroscopy protocol,[10] which is the usual local protocol except for atypical atrial flutters requiring a reference catheter (right atrial quadripolar; St Jude Medical, Inc., St. Paul, MN). Transseptal puncture was guided by TEE. Then, FAM of the entire LA anatomy and the PVs was acquired with the ablation catheter to integrate it with the LA wall thickness map within the spatial reference coordinates of the CARTO system.

Acute PVI was confirmed after first pass with the standard local single catheter method demonstrating entry block with the absence of PV potentials inside the vein with the ablation catheter placed sequentially in each segment inside the circumferential PV line, and exit block by proving absence of conduction when pacing from inside the circumferential PV line, at each segment sequentially.[8]

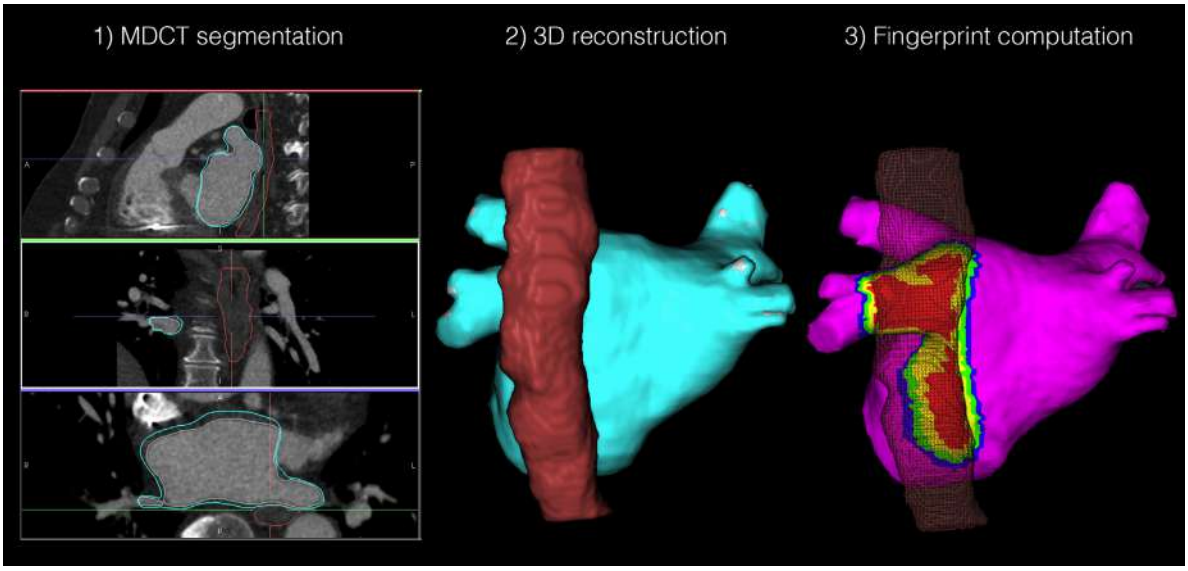

Figure 2 Segmentation pipeline of the fingerprinted atrioesophageal isodistance map. **1:** Raw MDCT DICOM images were imported into ADAS 3D for segmentation. **2:** Complete 3-dimensional (3D) reconstruction of the esophageal and atrial anatomy was obtained. **3:** The atrioesophageal fingerprinted isodistance map was projected onto the atrial endocardial surface (atrioesophageal distance: *red* <1 mm; *yellow* 1–2 mm; *green* 2.1–3 mm; *blue* 3.1–4 mm; *purple* >4.1 mm). MDCT = multidetector computerized tomography.

Esophageal FAM acquisition

Esophageal geometry was acquired at the end of the procedure with the ablation catheter (ThermoCool SmartTouch or Navistar ThermoCool, Biosense Webster). The operator introduced the catheter into the esophagus with the aid of the anesthetist. The catheter was set to a neutral curve position and gently advanced into the esophagus as far as the lower margin of the LA as seen in the CARTO matrix. Esophageal anatomy was reconstructed by slightly curving the catheter tip with rotational movements (Figure 3, section 1).

Statistical analysis and esophageal position comparison

All applicable statistical tests are 2-sided and performed using a 5% significance level. Continuous variables are given as mean ± SD or median (range or interquartile range [IQR] if data were skewed) if not normally distributed. To compare means of 2 variables, the Student *t* test, Mann-Whitney *U* test, or analysis of variance was used, as appropriate. Categorical variables are given as total number (percentage) and were compared between groups using the χ^2 or Fisher exact test. Statistical analysis was performed using IBM SPSS Statistics for Macintosh, Version 25.0 (Released 2017, IBM Corp., Armonk, NY) and customized code for the MATLAB statistics toolbox (MATLAB R2010a, The MathWorks, Inc., Natick, MA). For group 1 (redo), spatial correlation between the 2 MDCT-derived esophageal isodistance fingerprinted maps was calculated using MATLAB. The esophageal fingerprint was calculated over the LA anatomy of the first procedure. Both esophageal fingerprinted isodistance maps were projected over the same LA anatomy for computing the correlation value. Correlation was calculated between the whole fingerprinted surfaces (Figure 4). For group 2 (multimodality), image correlation between fluoroscopy, FAM, and MDCT was computed in MATLAB using semiautomatic segmentation analysis. Each image technique was either imported and merged (CT) or acquired (UNIVU and FAM) within the spatial reference coordinates of the CARTO system (Figure 3, section 3). After the procedure, the CARTO reference matrix was exported to MATLAB, and the positions as observed by the 3 methods were compared to one another with specifically developed code. A correlation between each pair was obtained in the coronal plane (anteroposterior view). This correlation was expressed as a percentage. Global image correlation was computed as the mean correlation between methods. In addition, the mean distance between the 3 modalities was computed.

Results

Patient population

Baseline characteristics of the 2 groups are summarized in Table 1. The MDCT group was composed of 39 patients: mean age 61 ± 10 years; 26 (67%) male; mean left ventricular ejection fraction 59% ± 6%; mean LA diameter 44 ± 4 mm; mean body mass index 29 ± 6 kg/m^2; and median time since first ablation (and therefore between MDCT acquisitions) 6 months (IQR 3–9).

Group 2 was composed of 100 patients: mean age 61 ± 10 years; 17 (65%) male; mean left ventricular ejection fraction 56% ± 7%; mean LA diameter 39 ± 6 mm; and mean body mass index 27 ± 5 kg/m^2. No patient was excluded because of inability to perform CT; 1 patient was excluded from group 2 because of an esophageal diverticulum that contraindicated

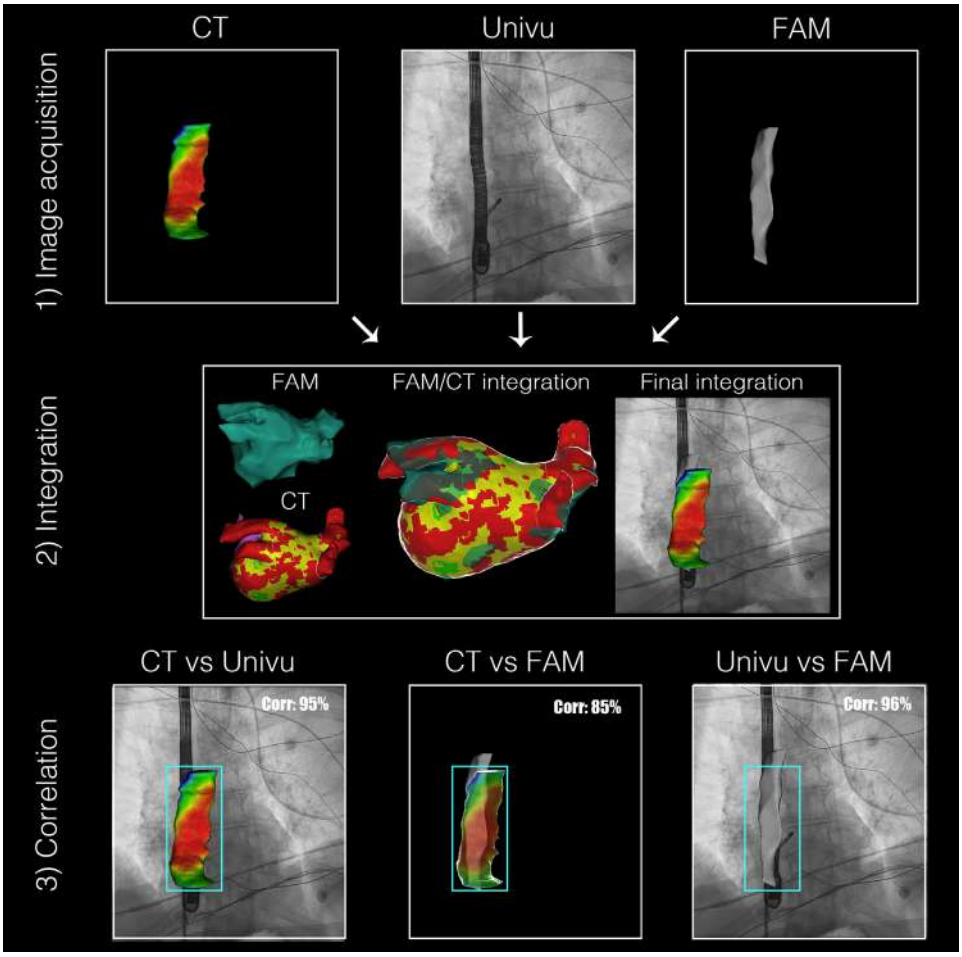

Figure 3 Esophageal position acquisition methods. **1: Left:** Three-dimensional MDCT-derived esophageal anatomy with color-coded atrioesophageal distance gradient (*red* <1mm; *yellow* 1–2 mm; *green* 2.1–3 mm; *blue* 3.1–4 mm; *purple* >4.1 mm). **Center:** UNIVU anteroposterior acquisition with the transesophageal echocardiographic probe in place. **Right:** Esophageal fast anatomic map (FAM) obtained with the ablation catheter. **2:** Image integration into the navigator. Merging of the atrial FAM with the MDCT-derived left atrial wall thickness map using the CARTOMERGE module. **3:** Mean image correlation between methods. MDCT = multidetector computerized tomography.

esophageal FAM. MDCT was performed within 48 hours preceding the intervention. Image segmentation included not only the esophageal anatomy and the atrioesophageal fingerprint but also LA wall thickness information.[8] Time for UNIVU acquisition was 1.5 ± 1 minutes and for esophageal FAM acquisition was 3 ± 1.5 minutes.

Atrioesophageal distance and position measurements in the MDCT group

Mean atrioesophageal distance was 1.2 ± 0.6 mm. Total fingerprinted area (up to 4-mm distance) was 13.2 ± 5.2 cm^2 before first ablation and 13.5 ± 5.0 cm^2 before the redo procedure. The closest fingerprinted area (red <1-mm distance to the LA epicardial wall) was 8.1 ± 2.3 cm^2 before the first ablation and 8.3 ± 2.5 cm^2 before the redo procedure (P = .34). The esophageal transversal width at the level of the PVs was 27.2 ± 4.3 mm before first ablation and 27.4 ± 4.4 mm before the redo procedure (P = .37). The esophageal position as related to the atrial posterior wall was left for 20 patients (56%); central for 6 patients (18%); right for 3 patients (9%); left-central for 4 patients (11%); and right-central for 2 patients(3%). There was a 91% ± 5% correlation on the esophageal fingerprint position between the first procedure and the redo procedure MDCT. In 3 cases (8%), the position was clearly different, with a correlation of only 40% ± 22% (Figure 4).

Atrioesophageal distance and position measurements on the multimodality group

Procedural time was 55 (IQR 50–61) minutes. Mean atrioesophageal fingerprinted distance was 1.3 ± 0.5 mm. Esophageal position as related to the atrial posterior wall was left for 55 patients(55%), central for 23 patients(23%), right for 9 patients (9%), left-central for 8 patients (8%), and right-central for 5 patients (5%). The correlation between MDCT and CARTOUNIVU was 82% ± 10%; between MDCT and esophageal FAM was 80% ± 12%; and between

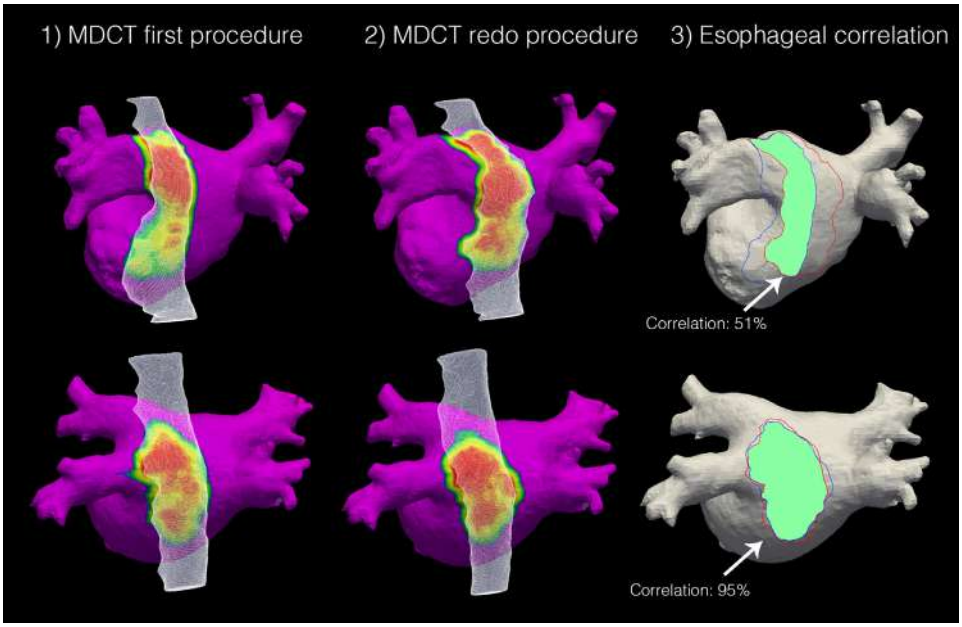

Figure 4 Group 1 (MDCT) results of esophageal fingerprinted isodistance map correlation. **Top:** Case with low correlation. Note the esophageal fingerprint contour in *blue* for the first ablation and in *red* for the redo procedure. **Bottom:** Case with high correlation of esophageal fingerprint between first and redo procedures (95% image correlation). MDCT = multidetector computerized tomography.

esophageal FAM and CARTOUNIVU 83% ± 15%. The results are shown in Figure 5.

There was an important discordance between periprocedural esophageal position in 8 patients (8%), with mean MDCT to CARTOUNIVU correlation of 52% ± 8%.

Discussion

Main findings

The main findings of the present study are as follows (1) The esophageal fingerprint is a novel 3D method of depicting the relationship between the esophagus and the LA posterior wall derived from the MDCT. (2) There is high temporal stability of the esophageal position between procedures separated by several months. (3) Multiple imaging techniques are available periprocedurally and can be used to evaluate esophageal position. (4) These imaging techniques show high stability of the esophageal position during the procedure in patients under general anesthesia.

Esophageal fingerprint

The esophageal fingerprinted isodistance map is a new way of depicting the complex relationship between the esophagus and the LA posterior wall. This anatomic information is obtained from the MDCT, which provides submillimetric spatial resolution resulting in high precision. It offers 3D information and allows for accurate representation of the atrioesophageal contact surface, not only in the sagittal and coronal planes but also in the axial plane. Given that the image is projected in a 2-dimensional manner on the LA endocardial mesh, the isodistance map provides information regarding the proximity between both structures. The observed interindividual variability of the atrioesophageal relationship and of the esophageal trajectory within the mediastinum endorses the need to develop easy-to-implement strategies that enable use of this information during catheter ablation on the posterior LA wall, particularly as different energy delivery ablation protocols are put into practice.

Stability of esophageal position between procedures

High stability of the esophageal position was observed between procedures that were 6 (IQR 3 ± 9) months apart. No position shift was observed in 91% of patients, and only subtle changes were observed between the 2 interventions. This 3D observation not only confirms earlier reports on the stability of the esophagus within the mediastinum having a so-called "lying position"[11] but also the relative stability of the atrioesophageal relationship as analyzed by the esophageal fingerprint. This was further confirmed by the closest fingerprinted esophageal area (distance to LA posterior wall <1 mm), as no significant change was observed in the contact surface. In fact, the mediastinum being filled with multiple anatomic structures within the thoracic cage provides space for passage, but important mobility within it seems unlikely in the absence of deglutition or mechanical forces.

Stability of esophageal position during the same procedure

Conflicting evidence on the stability of esophageal position during a procedure has been reported. Piorkowski et al[12]

Table 1 Baseline characteristics of the study populations

	Group 1*: MDCT (n = 39)	Group 2: Multimodality (n = 100)
Age (y)	60 ± 10	61 ± 11
Male	26 (67)	64 (64)
Hypertension	23 (60)	39 (39)
Dyslipidemia	10 (26)	17 (17)
Diabetes	2 (5)	6 (6)
LVEF	59 ± 6	56 ± 7
LA diameter (mm)	44 ± 4	39 ± 6
BMI (kg/m^2)	29 ± 6	27 ± 4
CHADS-VASc score		
0	9 (23)	30 (30)
1	16 (41)	23 (23)
2	5 (13)	23 (23)
3	8 (20)	18 (18)
4	1 (3)	3 (3)
5	—	2 (2)
6	—	1 (1)
Time between MDCT examinations (mo)	Median 6 (IQR 3–9)	N/A
Ablation type		
First ablation	0	78 (78)
Redo ablation	39 (100)	22 (22)
AF type		
Paroxysmal	25 (64)	69 (69)
Persistent	12 (31)	26 (26)
Longstanding persistent	0 (0)	1 (1)
Atrial tachycardia/flutter	2 (5)	4 (4)

Values are given as mean ± SD or n (%) unless otherwise indicated.

BMI = body mass index; IQR = interquartile range; LA = left atrium; LVEF = left ventricular ejection fraction; MDCT = multidetector computed tomography; N/A = not applicable.

*For group 1, characteristics at redo.

showed the concordance of esophageal position between the preprocedural MDCT and the electroanatomic map. Sherzer et al[13] found stability of esophageal position relative to the spine by means of an ablation catheter in the esophagus during the whole procedure in patients under general anesthesia. Another study found that esophageal position was relatively stable before and after ablation using 3D rotational angiography for the PVs and visualization of the esophagus via peroral administration of a contrast agent.[14] However, whether esophageal movement is stimulated by the swallowing of barium and whether general anesthesia has any influence on esophageal motility with a postulated hypothesis that the esophagus has a resting position are unknown. Real-time observation of the esophageal position is feasible with intracardiac echocardiography, but this costly option is not widely available.

We have also come to understand that the esophagus is a wide structure (mean width 28.1 ± 4.1 mm). This explains why previous publications described a discordant position between esophageal FAM and MDCT-derived esophageal position as observed by means of a gastric tube placed on 2 consecutive occasions,[15] as the positioning of a tube within the esophageal width is random and can differ greatly in the coronal plane.

The present study found good stability of esophageal position between pre- and periprocedural multimodality imaging. In only 8 of 100 patients (8%) was a discordance between at least 2 of the imaging techniques observed. One patient was not sufficiently sedated and coughed on the tube during the procedure. Another patient had a superior vena cava circumferential ablation that motivated local stimulation to check for phrenic nerve anatomy, which presumably could have modified the esophageal position through diaphragmatic contraction (Figure 5). In 1 patient, the transesophageal probe was inadvertently left in place during the ablation procedure. Finally, one patient had an electrical cardioversion during the procedure. Overall, 16 patients (16%) were cardioverted, and in only 1 case did the position differ. There was no apparent cause for discordance in the 5 remaining cases.

Clinical implications

This study describes MDCT-derived 3D isodistance maps to allow better understanding of the atrioesophageal relationship, which is fundamental for improving procedural safety. Our results emphasize the importance of multimodality imaging to integrate the complexity of the anatomic relationships and allow safer energy delivery without compromising the efficacy of ablation lesions in the LA posterior wall. The esophageal fingerprinted isodistance map image is a novel tool that could be used to modulate energy delivery and modify the course of RF ablation lines, cryoballoon placement, and laser application with the aim of improving safety. However, this application is merely hypothetical, and further prospective studies are underway to prove this utility (AWESOME-AF randomized trial; ClinicalTrials.gov Identifier: NCT04394923).

Study limitations

The main limitation of this study is the lack of a control group for comparison (eg, patients under conscious sedation). The study was observational and was not designed to allow for sufficient power to find predictors of significant esophageal position modification between 2 procedures or during the same procedure. In the multimodality group, a limitation is the intrinsic discordances between these techniques. The most accurate is CT because it delineates the actual anatomy as acquired (mean esophageal width 27.2 ± 4.3 mm). The other techniques are approximative, and all have limitations. The esophageal image rendered by UNIVU with the TEE probe in place is unavoidably thinner because it relies on the probe width (15 mm). For the esophageal FAM, a limitation is that esophageal anatomy can be deformed if significant force is applied to the catheter. Thus, it would have been more accurate to compare esophageal position before, during, and after the procedure using the same technique (eg, esophageal FAM), yet this was not plausible in the clinical

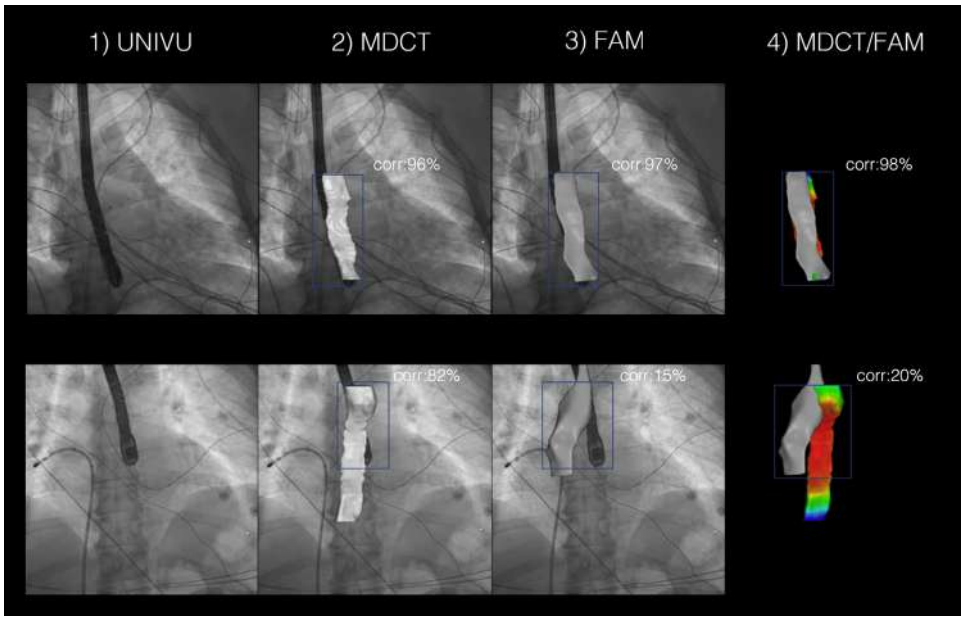

Figure 5 Group 2 (multimodality) results. **Top:** High image correlation. **Bottom:** Low image correlation). **1:** Anteroposterior UNIVU acquisition with transesophageal echocardiographic probe in place. **2:** Correlation between MDCT and CARTOUNIVU. **3:** Correlation between MDCT and esophageal FAM. **4:** Correlation between MDCT and esophageal FAM. FAM = fast anatomic mapping; MDCT = multidetector computerized tomography.

setting of the present study. Nevertheless, the presented results challenge the common belief that the esophagus undergoes significant movement. As a matter of fact, such movements are infrequent and subtle. Furthermore, these results might not be extrapolated to patients undergoing ablation under conscious sedation (as opposed to general anesthesia) or with more time-consuming ablation protocols, as the median procedural time was under 1 hour. Moreover, MDCT data of the index procedure were not available for redo patients in the multimodality group. Ultimately, the question of esophageal position needs to be evaluated by a constant intraoperative monitoring technique such as intracardiac echocardiography (ICE). However, the technique is not widespread, and data regarding real-time esophageal position with ICE are not yet available. Research is underway to test the clinical utility of the esophageal fingerprinted isodistance map in the modulation of RF delivery and design of PV ablation lines (AWESOME-AF; ClinicalTrials.gov Identifier: NCT04394923).

Conclusion

There is high stability of esophageal position between procedures and from the beginning to the end of an AF ablation procedure. The 3D fingerprinted isodistance atrioesophageal map can be obtained from MDCT scan and integrated into the navigation system. It allows for direct periprocedural estimation of the distance between the esophagus and the LA posterior wall.

Funding Sources: This research did not receive any specific grant from funding agencies in the public, commercial, or not-for-profit sectors.

Disclosures: Dr Soto-Iglesias is an employee of Biosense Webster, Inc. Dr Berruezo is a stockholder of ADAS 3D Medical. The other authors have no other relevant affiliations or financial involvement with any organization or entity with a financial interest in or financial conflict with the subject matter or materials discussed in the manuscript apart from those disclosed.

Authorship: All authors attest they meet the current ICMJE criteria for authorship.

Patient Consent: All participants included in the study provided written informed consent.

Ethics Statement: The study complied with the Declaration of Helsinki, and the local ethics committee approved the study protocol.

References

1. Hindricks G, Potpara T, Dagres N, et al; ESC Scientific Document Group. 2020 ESC guidelines for the diagnosis and management of atrial fibrillation developed in collaboration with the European Association of Cardio-Thoracic Surgery (EACTS): the Task Force for the diagnosis and management of atrial fibrillation of the European Society of Cardiology (ESC) Developed with the special contribution of the European Heart Rhythm Association (EHRA) of the ESC. Eur Heart J 2021;42:373 498.
2. Suenari K, Nakano Y, Hirai Y, et al. Left atrial thickness under the catheter ablation lines in patients with paroxysmal atrial fibrillation: insights from 64-slice multidetector computed tomography. Heart Vessels 2013;28:360 368.
3. Sanchez-Quintana D, Cabrera JA, Climent V, Farre J, de Mendonca MC, Ho SY. Anatomic relations between the esophagus and left atrium and relevance for ablation of atrial fibrillation. Circulation 2005;112:1400 1405.
4. Halbfass P, Pavlov B, Muller P, et al. Progression from esophageal thermal asymptomatic lesion to perforation complicating atrial fibrillation ablation: a single-center registry. Circ Arrhythm Electrophysiol 2017; 10:e005233.

5. Lakkireddy D, Reddy YM, Atkins D, et al. Effect of atrial fibrillation ablation on gastric motility: the atrial fibrillation gut study. Circ Arrhythm Electrophysiol 2015;8:531–536.
6. Schoene K, Arya A, Grashoff F, et al. Oesophageal Probe Evaluation in Radiofrequency Ablation of Atrial Fibrillation (OPERA): results from a prospective randomized trial. Europace 2020;22:1487–1494.
7. Grosse Meininghaus D, Blembel K, Waniek C, et al. Temperature monitoring and temperature-driven irrigated radiofrequency energy titration do not prevent thermally induced esophageal lesions in pulmonary vein isolation: a randomized study controlled by esophagoscopy before and after catheter ablation. Heart Rhythm 2021;18:926–934.
8. Teres C, Soto-Iglesias D, Penela D, et al. Left atrial wall thickness of the pulmonary vein reconnection sites during atrial fibrillation redo procedures. Pacing Clin Electrophysiol 2021;44:824–834.
9. Teres C, Soto-Iglesias D, Penela D, et al. Personalized paroxysmal atrial fibrillation ablation by tailoring ablation index to the left atrial wall thickness: the "Ablate by-LAW" single-centre study-a pilot study. Europace 2021 Sep 4;euab216. https://doi.org/10.1093/europace/euab216.
10. Falasconi G, Penela D, Soto-Iglesias D, et al. Standardized stepwise zero-fluoroscopy approach with transesophageal echocardiography guidance for atrial fibrillation ablation. J Interv Card Electrophysiol 2021 Nov 10; https://doi.org/10.1007/s10840-021-01086-9.
11. Kennedy R, Good E, Oral H, et al. Temporal stability of the location of the esophagus in patients undergoing a repeat left atrial ablation procedure for atrial fibrillation or flutter. J Cardiovasc Electrophysiol 2008; 19:351–355.
12. Piorkowski C, Hindricks G, Schreiber D, et al. Electroanatomic reconstruction of the left atrium, pulmonary veins, and esophagus compared with the "true anatomy" on multislice computed tomography in patients undergoing catheter ablation of atrial fibrillation. Heart Rhythm 2006;3:317–327.
13. Sherzer AI, Feigenblum DY, Kulkarini S, et al. Continuous nonfluoroscopic localization of the esophagus during radiofrequency catheter ablation of atrial fibrillation. J Cardiovasc Electrophysiol 2007;18:157–160.
14. Starek Z, Lehar F, Jez J, et al. Esophageal positions relative to the left atrium; data from 293 patients before catheter ablation of atrial fibrillation. Indian Heart J 2018;70:37–44.
15. Kobza R, Schoenenberger AW, Erne P. Esophagus imaging for catheter ablation of atrial fibrillation: comparison of two methods with showing of esophageal movement. J Interv Card Electrophysiol 2009;26:159–164.

Artículo 4

"Relación entre la pared auricular posterior y el esófago: posición esofágica y medición de temperatura durante la ablación de la fibrilación auricular (AWESOME-AF)"

Este estudio clínico controlado aleatorizado tuvo como objetivo principal determinar si la adaptación de la línea de ablación en la pared posterior próxima al esófago podría influir en el aumento de la temperatura detectada por una sonda posicionada en el esófago. Los hallazgos del estudio subrayaron la utilidad de una nueva herramienta derivada del angioTAC para conocer la posición esofágica (esophageal fingerprint) permitiendo una identificación confiable de la posición esofágica y su uso para el despliegue de la línea PVI dió como resultado aumentos de temperatura esofágicos menos frecuentes en comparación con el enfoque estándar. Los conocimientos del ensayo AWESOME-AF resaltan la necesidad de enfoques individualizados para la ablación de la FA basados en las relaciones anatómicas únicas de cada paciente y muestra que el desarrollo de nuevas herramientas derivadas de imágenes podría, en última instancia, mejorar la seguridad del paciente.

Journal of Interventional Cardiac Electrophysiology (2022) 65:651–661
https://doi.org/10.1007/s10840-022-01302-0

Relationship between the posterior atrial wall and the esophagus: esophageal position and temperature measurement during atrial fibrillation ablation (AWESOME-AF). A randomized controlled trial

Cheryl Teres[1,2] · David Soto-Iglesias[1] · Diego Penela[1] · Giulio Falasconi[1] · Daniel Viveros[1] · Julia Meca-Santamaria[1] · Aldo Bellido[1] · Jose Alderete[1] · Alfredo Chauca[1] · Augusto Ordoñez[1] · Julio Martí-Almor[1] · Claudia Scherer[1] · Alejandro Panaro[1] · Julio Carballo[1] · Óscar Cámara[3] · Jose-Tomás Ortiz-Pérez[1] · Antonio Berruezo[1]

Received: 25 May 2022 / Accepted: 7 July 2022 / Published online: 21 July 2022

Abstract

Background Pulmonary vein isolation (PVI) implies unavoidable ablation lesions to the left atrial posterior wall, which is closely related to the esophagus, leading to several potential complications. This study evaluates the usefulness of the esophageal fingerprint in avoiding temperature rises during paroxysmal atrial fibrillation (PAF) ablation.

Methods Isodistance maps of the atrio-esophageal relationship (esophageal fingerprint) were derived from the preprocedural computerized tomography. Patients were randomized (1:1) into two groups: (1) PRINT group, the PVI line was modified according to the esophageal fingerprint; (2) CONTROL group, standard PVI with operator blinded to the fingerprint. The primary endpoint was temperature rise detected by intraluminal esophageal temperature probe monitoring. Ablation settings were as specified on the *Ablate BY-LAW* study protocol.

Results Sixty consecutive patients referred for paroxysmal AF ablation were randomized (42 (70%) men, mean age 60 ± 11 years). Temperature rise (> 39.1 °C) occurred in 5 (16%) patients in the PRINT group vs. 17 (56%) in the CONTROL group ($p < 0.01$). Three AF recurrences were documented at a mean follow-up of 12 ± 3 months (one (3%) in the PRINT group and 2 (6.6%) in the CONTROL group, $p = 0.4$).

Conclusion The esophageal fingerprint allows for a reliable identification of the esophageal position and its use for PVI line deployment results in less frequent esophageal temperature rises when compared to the standard approach. Further studies are needed to evaluate the impact of PVI line modification to avoid esophageal heating on long-term outcomes. The development of new imaging-derived tools could ultimately improve patient safety (NCT04394923).

Keywords Atrial fibrillation · Esophageal position · Atrioesophageal fistula · Atrial wall thickness · Catheter ablation

Abbreviations

AAD	Antiarrhythmic drugs
AEF	Atrio-esophageal fistula
AF	Atrial fibrillation
FAM	Fast anatomical map
LA	Left atrium
LAWT	Left atrial wall thickness
LET	Luminal esophageal temperature
MDCT	Multidetector computerized tomography
PAF	Paroxysmal atrial fibrillation
PVI	Pulmonary vein isolation
RF	Radiofrequency
TOE	Transesophageal echocardiography

✉ Antonio Berruezo
antonio.berruezo@quironsalud.es

[1] Heart Institute, Teknon Medical Center, C/Vilana, 12; 08022 Barcelona, Spain

[2] Lausanne University Hospital, Lausanne, Switzerland

[3] Department of Information and Communication Technologies, BCN-MedTech, Universitat Pompeu Fabra, PhySense group, Barcelona, Spain

1 Introduction

A growing body of evidence supports an early rhythm control strategy for patients with atrial fibrillation (AF) [1–3]. Circumferential pulmonary vein isolation (PVI) is the mainstay of catheter ablation and the best alternative to antiarrhythmic drugs (AAD) [4]. However, this strategy results

in unavoidable ablation lesions to the posterior atrial wall, leading to several potential complications ranging from asymptomatic esophageal lesions to perforation with atrio-esophageal fistula (AEF), which can be lethal [5, 6].

Currently, luminal esophageal temperature (LET) monitoring via an endoluminal probe is a standard of care in many centers and esophageal temperature rise above 40.5 °C is an independent predictor of esophageal lesions [5]. There are various probe models differing in material, number of thermal sensors, and measurement method. Although several studies have tried to elucidate the utility of LET in reducing esophageal thermal injury, equivocal results have been obtained until now [7–10]. Other strategies to avoid thermal esophageal injuries have been formulated such as refraining from RF application adjacent to the esophagus by modifying the ablation lines [11], underdosing RF or lowering the contact force [12], modifying the esophageal position [13], or cooling [14] it with various devices. Nevertheless, a multimodal strategy integrating esophageal visualization with non-invasive imaging techniques and simultaneous temperature monitoring is lacking in routine contemporary practice.

The aim of the present study is to evaluate the impact of adapting PVI ablation lines on the posterior wall according to the esophageal position as depicted with a recently developed tool called the esophageal fingerprint [15, 16] (Fig. 1) to avoid local esophageal temperature rises caused by radiofrequency (RF) application during paroxysmal AF ablation. This tool could help develop safer ablation strategies by avoiding esophageal heating.

2 Methods

2.1 Study design and patient population

This study was a single-center, prospective, randomized trial. Figure 2 depicts the study design. Consecutive patients referred for paroxysmal AF ablation were included from June 2020 to March 2021. Age < 18 years, pregnancy, presence of concomitant investigation treatments, patient's refusal to participate in the study, unavailability of preprocedural MDCT, and any esophageal anatomical variation (diverticulum, achalasia, hiatus hernia, etc.) were exclusion criteria. Patients were randomized at the beginning of the procedure into two groups on a 1:1 basis. As shown in Fig. 3, the intervention "PRINT" group had a modified PVI line based on the esophageal fingerprint aiming to avoid RF delivery to the LA posterior wall closest to the esophagus, whenever possible. The CONTROL group underwent standard PVI, and the operator was blinded to the fingerprint. The study was registered on ClinicalTrials.gov (NCT04394923) and complied with the Declaration of Helsinki, and the local ethics committee approved the study protocol. All participants included in the study provided written informed consent.

2.2 Pre-procedural multi-detector cardiac tomography and image processing

A MDCT study was performed prior to the procedure. MDCT dicom images were analyzed with ADAS 3D™ software (ADAS3D Medical, Barcelona, Spain) to

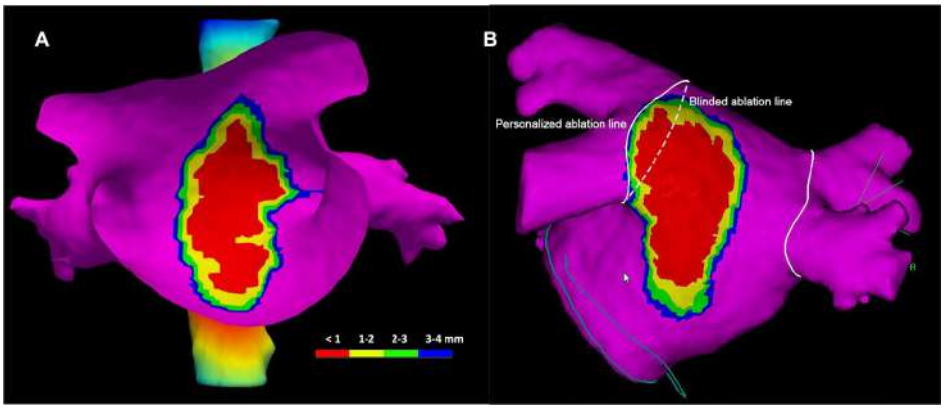

Fig. 1 **A** Endocardial antero-posterior view of the esophageal fingerprint. The distance between the LA posterior wall and the esophagus is computed at each epicardial point, allowing to create an esophageal print on top of the endocardial atrial layer. An isodistance color map (esophageal fingerprint) is created with a color scale to depict a range of distances. Red color depicts the closest area with an atrio-esophageal distance < 1 mm, yellow 1.1–2 mm, green 2.1–3 mm, blue 3.1–4 mm, and purple > 4 mm. **B** Ablation line tailoring method on a posterior view of the endocardial shell. Patients were randomized on a 1:1 basis in two groups. The intervention "PRINT" group had a modified PVI line based on the esophageal fingerprint aiming to avoid RF application on the LA posterior wall closest to the esophagus (red area), whenever possible. The CONTROL group underwent standard PVI, the line was designed as for standard PVI, and the operator was blinded to the fingerprint; PVI, pulmonary vein isolation

Journal of Interventional Cardiac Electrophysiology (2022) 65:651–661

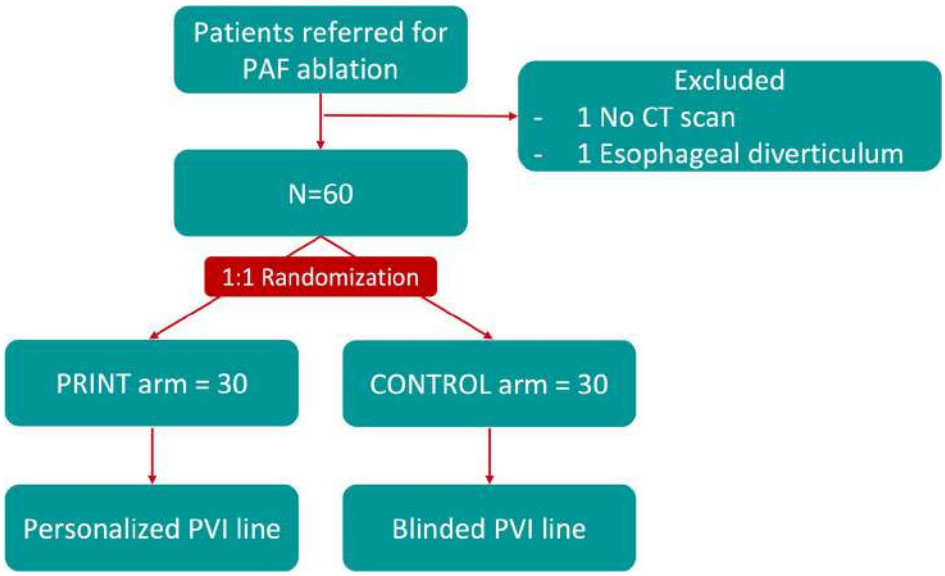

Fig. 2 Study design; CT computerized tomography, PAF paroxysmal atrial fibrillation, PVI pulmonary vein isolation

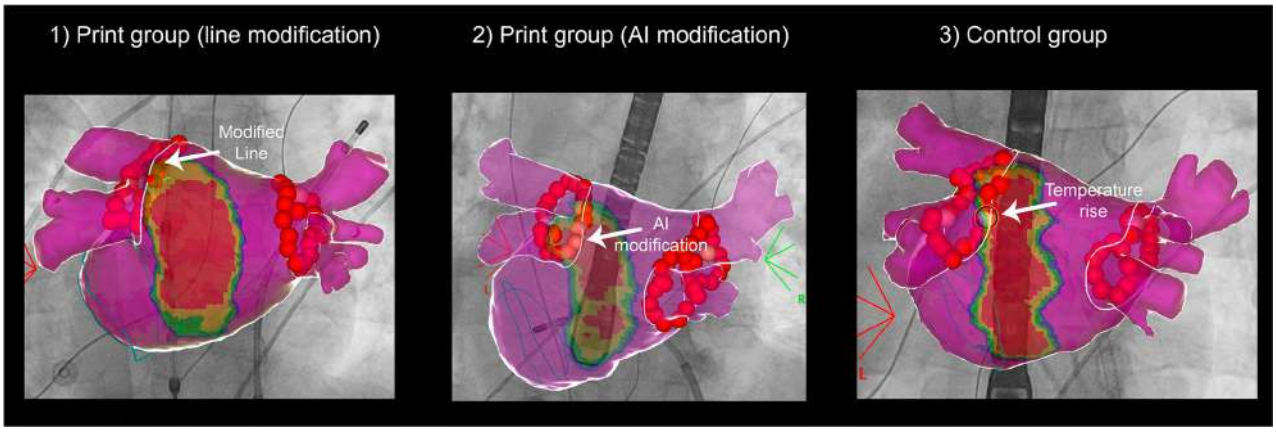

Fig. 3 Ablation index modification on the posterior wall. For the PRINT group, in cases where ablation through the red area was unavoidable, the delivered AI was lowered to 300 regardless of the local wall thickness. In the CONTROL group, the AI was modified if there were temperature rises. In this example, see how after unblinding the esophageal fingerprint the esophagus is underlying the lesion where AI target was lowered to 300; AI, ablation index

segment the esophageal anatomy and the atrio-esophageal fingerprinted isodistance map as shown in Fig. 1A, where red color depicts the closest area with an atrio-esophageal distance < 1 mm, yellow 1.1–2 mm, green 2.1–3 mm, blue 3.1–4 mm, and purple > 4 mm. Figure 1 shows the result of the segmentation method resulting in a 3D map of the atrio-esophageal relationship that can be projected to the atrial endocardial mesh and imported into CARTO navigation system (Biosense Webster, Diamond Bar, CA, USA). A detailed description of the methods has already been reported [16].

2.3 Complementary esophageal imaging modalities

Two complementary imaging modalities could be used at operators' discretion. The esophageal geometry could be acquired with the ablation catheter (Thermocool SmartTouch or Navistar Thermocool, Biosense-Webster, Diamond Bar, CA) by means of an EAM following a previously described method [16]; however, as this acquisition is performed at the end of procedure, it was not used to guide PVI ablation. In addition, LET and TEE probe position could be

registered with CARTOUNIVU™ image integration module in AP, RAO 30°, and LAO 30° fluoroscopic projections allowing for real time visualization of intracardiac catheters in the 3D mapping environment on a background of stored fluoroscopic images, as shown in Fig. 4.

2.4 Catheter ablation

Catheter ablation was performed with the previously described *ablate By-LAW* method [15], with a single catheter strategy under general anesthesia with high-frequency low-volume ventilation. Oral anticoagulation was uninterrupted and intra-procedural anticoagulation was performed to achieve an activated clotting time > 300 s. All procedures were performed with a single venous femoral access, a single transeptal puncture guided by a transesophageal echocardiography, and a near-zero fluoroscopy protocol [17] which is the usual local protocol. After that, a fast anatomical map (FAM) of the entire left atrial anatomy and the pulmonary veins was acquired with the ablation catheter and merged within the spatial reference coordinates of the CARTO system with the MDCT-derived 3D map, consisting of a left atrial wall thickness (LAWT) map and the atrioesophageal isodistance map.

2.5 Pulmonary vein ablation lines regarding esophageal fingerprint

Before randomization, an investigator, blinded to the esophageal position, drew the standard PVI ablation lines around both pairs of veins. As shown in Fig. 1B, after randomization on the intervention or "PRINT" group, the previously drawn ablation line was modified depending on the esophageal fingerprint position and redrawn as distant as possible from the red area of the fingerprint, to avoid RF application where the atrio-esophageal distance is the shortest (< 1 mm). Whenever possible, the line elapsed at the closest over the blue (further) iso distance zone. If the line was modified, the maximal distance and the area between the original blinded line and the modified line were documented. As described in the *Ablate by-Law* method, ablation parameters were adapted to the LAWT (see Table 1 Complementary material). In cases where ablation through the red area was unavoidable, the delivered AI was lowered to 300 regardless of the local wall thickness (Fig. 3). Whenever the temperature rose above 39℃, ablation was immediately stopped, and a second ablation point was later delivered with a reduced target AI of 300. If the temperature rose before reaching an AI of 300, a second application was later attempted

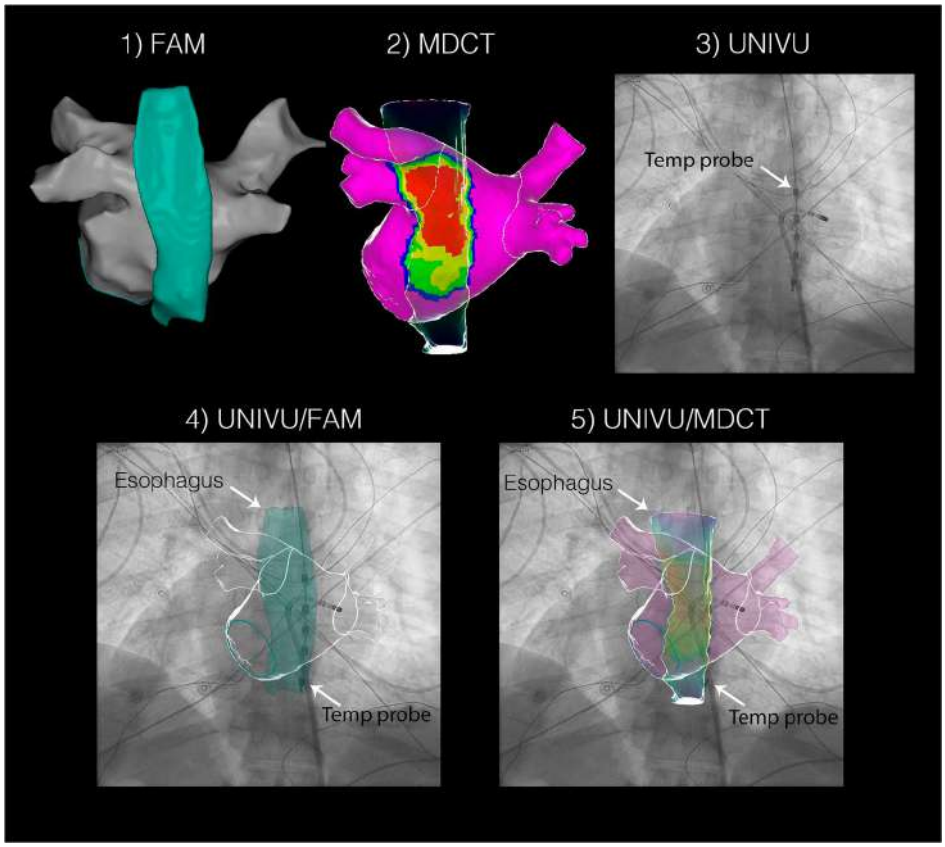

Fig. 4 Available imaging modalities to evaluate esophageal position. (1) Esophageal FAM; (2) MDCT segmentation (esophagus in transparency) with the fingerprinted esophageal position; (3) UNIVU acquisition of the esophageal temperature monitoring probe; (4) overlap of esophageal FAM and UNIVU showing the limitation of temperature probes with a random position within the esophagus; (5) matching position of the esophagus between FAM and MDCT; FAM fast anatomical map, MDCT multidetector computerized tomography

Table 1 Baseline characteristics of the study population

	Overall $n=60$	Print $n=30$	Control $n=30$	p value
Age, y	60 ± 11	60 ± 11	60 ± 12	ns
Male	42 (70)	21 (70)	21 (70)	ns
Arterial hypertension	24 (40)	9 (30)	15 (50)	ns
Dyslipemia	15 (25)	5 (16)	10 (33)	ns
Diabetes	4 (7)	3 (10)	1 (3)	ns
BMI (kg/m^2)	27 ± 4	25 ± 4	27 ± 4	ns
LVEF	58 ± 5	58 ± 4	58 ± 5	ns
LA diameter (mm)	36 ± 5	35 ± 4	36 ± 5	ns
CHADS-VASc				
0	19 (31)	10 (34)	10 (34)	ns
1	19 (31)	10 (34)	8 (27)	ns
2	10 (17)	4 (13)	6 (20)	ns
3	7 (12)	3 (10)	4 (13)	ns
4	3 (5)	1 (3)	2 (6)	ns
5	1 (2)	1 (3)	0	ns
6	1 (2)	1 (3)	0	ns
Underlying heart disease				
None	51 (88)	26 (87)	25 (84)	ns
Ischemic	2 (3)	1 (3)	1 (3)	ns
Valvular	1 (2)	1 (3)	0	ns
Hypertensive	6 (7)	2 (7)	4 (13)	ns

Values are presented as *n* (%)

BMI body mass index, *LA* left atrium, *LVEF* left ventricular ejection fraction

to reach the target. For the CONTROL group, the ablation line was not modified from the original blinded one drawn before randomization. If the temperature rose above 39℃, ablation was immediately stopped, and target AI was also reduced to a minimum of 300. Besides, after a temperature rise, the operator was allowed to perform a skipping technique to avoid application of consecutive lesions in close anatomical proximity at the posterior segments to prevent local "heat stacking." Acute PVI was confirmed after first pass with the standard local single catheter method, at each segment sequentially [18].

2.6 Luminal esophageal temperature monitoring

A multi-thermocouple temperature probe (SensiTherm, St. Jude Medical, Inc., St. Paul, MN, USA) was advanced via transnasal or transoral access into the esophagus once the patient was under general anesthesia. Before performing ablation on the posterior wall, the temperature probe was advanced under fluoroscopic guidance until the thermocouple sensors completely covered the pulmonary veins in the cranio-caudal direction. Esophageal temperature rises above 39 °C were documented in a categorical manner for each case and as a location tag on the navigation system.

2.7 Esophageal fingerprinted isodistance map and posterior wall AI analysis

At the end of the procedure, the esophageal position was unblinded for the CONTROL group and the CARTO reference matrix was exported for analysis into a Matlab customized software. The circumferential PVI lines were divided in anterior and posterior walls. Mean atrio-esophageal distance, total fingerprinted area, and closest fingerprinted area (atrio-esophageal distance < 1 mm) were calculated. Ablation settings were analyzed in both groups, documenting the need for AI modification as related to the esophageal position in the PRINT group or depending on temperature increase on the CONTROL group.

2.8 Follow-up

Patients were scheduled for follow-up (FU) at the outpatient clinic at 1, 3, and 6 months post-op and every 6 months thereafter, or in case of symptoms. Each

evaluation included an ECG and a 24-h Holter monitoring. Recurrences were considered as any documented arrhythmia (i.e., AF, atrial flutter, and atrial tachycardia) lasting longer than 30 s off anti-arrhythmic medication or symptoms suggesting clear recurrence as identified by the patient (symptoms that had been correlated with a documented arrhythmia episode before the ablation procedure).

2.9 Statistical analysis

All applicable statistical tests are 2-sided and performed using a 5% significance level. Continuous variables are presented as mean ± standard deviation or median (range or interquartile range if data are skewed) if not normally distributed. To compare means of two variables, the Student's *t* test, Mann–Whitney *U* test, or Anova test were used, as appropriate. Categorical variables were expressed as total number (percentages) and compared between groups using Chi-square or Fisher's exact test. Statistical analysis was performed using IB SPSS Statistics for Macintosh, version 25.0 (IBM Corp. Released 2017; Armonk, NY), analysis or customized code for the Matlab statistics toolbox (Matlab R2010a, The Mathworks, Inc., Natick, MA, USA).

3 Results

3.1 Patient population

Sixty-two patients referred for a first PAF ablation were screened. One patient was excluded because CT scan quality did not comply with the minimal quality requirements for accurate segmentation; one patient was excluded because of a Zenker diverticulum. Sixty patients underwent randomization. Baseline characteristics are summarized in Table 1. Mean age was 60 ± 11 years, 42 (70%) were male, the mean LVEF was 58 ± 5%, the mean LA diameter was 36 ± 5 mm, and the mean BMI was 27 ± 4 kg/m^2.

3.2 MDCT derived LAWT, atrio-esophageal distance, and position measurements

MDCT acquisition was performed shortly before ablation (mean time 18 ± 10 h). Mean LAWT at the posterior wall was 1.1 ± 0.5 for the PRINT group and 1.2 ± 0.6 for the CONTROL group ($p = 0.91$), and for the anterior wall, it was 2.3 ± 0.8 for the PRINT group and 2.4 ± 0.9 for the CONTROL group ($p = 0.85$).

Mean atrio-esophageal distance was 1.4 ± 0.7 mm, and total fingerprinted area (up to 4 mm atrio-esophageal distance) was 12.3 ± 4.8 cm^2. The closest fingerprinted area (red < 1 mm distance to the left atrial epicardial wall) was 7.8 ± 2.1 cm^2. The esophageal position as related to the atrial posterior wall was left for 26 (43%) patients; central for 18 (30%) patients; right for 2 (3%) patients; left-central for 10 (17%) patients; right-central for 1 (2%) patient; and left-central-right for 3 patients (5%).

3.3 Esophageal temperature measurement and probe position

Overall, 22 out of 60 (37%) patients presented the primary endpoint (esophageal temperature rise > 39 °C). As shown in Fig. 5, a temperature rise occurred in 5 (17%) patients in the PRINT group vs. 17 (57%) in the CONTROL group ($p < 0.01$).

3.4 Procedural characteristics

Acute procedural characteristics are described in Table 2. Procedure time (skin-to-skin) was 50 min (IQR 42–56), including a merge time (FAM acquisition + MDCT merging on CARTO) of 12 min (IQR 10–13) and a transseptal time of 2 min (IQR 1–3). The number of RF points was 28 ± 8 for the left PVs and 29 ± 5 for the right PVs with a mean RF time of 6.5 ± 1.7 min for the left PVs and 7.3 ± 1.4 min for the right PVs. On the RPVs, first pass PVI was obtained in 29 (96%) patients on the PRINT group and 27 (90%) patients in the CONTROL group ($p = 0.3$). On the LPVs, first pass PVI was obtained in 26 (87%) patients in the PRINT group and 28 (93%) patients on the CONTROL group ($p = 0.4$). No acute reconnections were observed. At the end of the procedure, PVI was obtained in all cases. Ventilation rate was 45 ventilations per minute (IQR 45–50) with a tidal volume of 250 ml (250–280). No major complication occurred. Two femoral access-related complications were documented (one arteriovenous fistula, one pseudoaneurism); none required surgical treatment.

3.5 Posterior wall ablation as related to esophageal position

Mean AI at the posterior wall was 345 ± 27 for the PRINT group and 352 ± 24 for the CONTROL group ($p = 0.89$), and for the anterior wall, it was 379 ± 40 for the PRINT group and 370 ± 32 for the CONTROL group ($p = 0.88$).

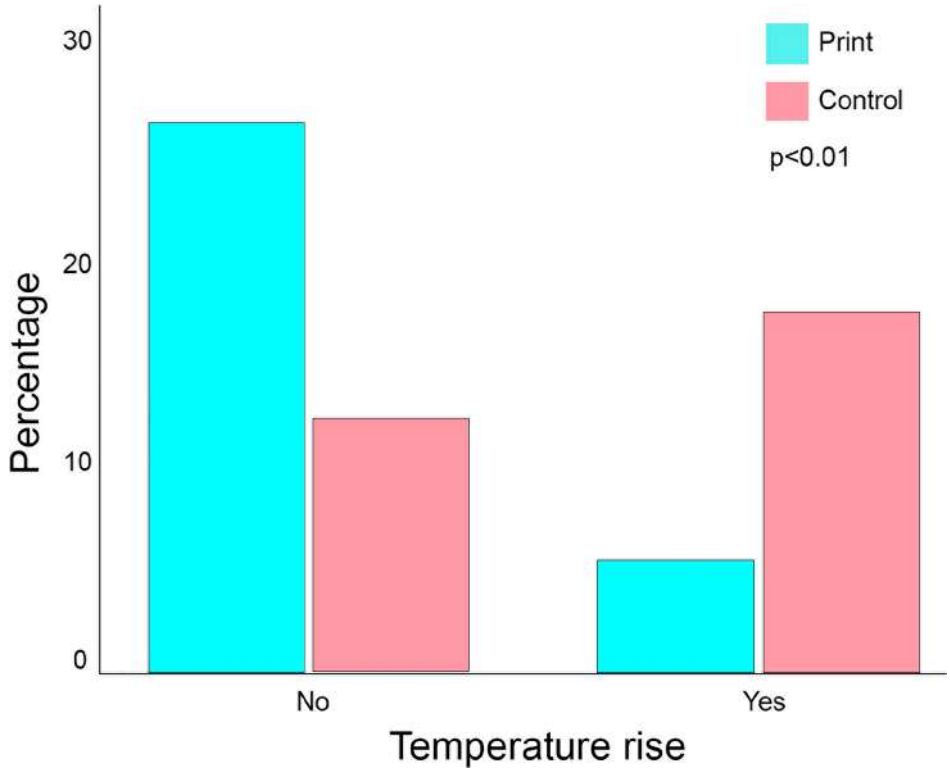

Fig. 5 Temperature rise results 22 out of 60 (37%) patients presented the primary endpoint (esophageal temperature > 39ºC), 5 (17%) patients on the PRINT group vs. 17 (57%) on the CONTROL group ($p < 0.01$)

Table 2 Acute procedural results

	Overall $n = 60$	Print $n = 30$	Control $n = 30$	p value
Procedure time (min)	50 (42–56)	48 (40–54)	51 (44–58)	ns
Radiofrequency time (min)	13.8 (12–15)	13.3 (11.2–15)	14 (13–15)	ns
Fluoroscopy time (min)	0.6 (0.2–1)	0.5 (0.2–1)	0.8 (0.2–1.1)	ns
Fluoroscopy dose area product (mGy/m^2)	0.8 (0.3–1.5)	0.7 (0.3–1.3)	1.1 (0.2–1.6)	ns
Right pulmonary veins	7.3 ± 1.4	7.1 ± 1.4	7.6 ± 1.5	ns
RF time (min)	29 ± 5	28 ± 5	29 ± 5	
Total Visitags	56 (93%)	29 (96%)	27 (90%)	
First pass isolation				
Left pulmonary veins	6.5 ± 1.7	6.1 ± 1.6	6.9 ± 1.7	ns
RF time (min)	28 ± 8	25 ± 5	27 ± 6	
Total Visitags	54 (90%)	26 (87%)	28 (93%)	
First pass isolation				

Values are presented as mean ± standard deviation, median (interquartile range), or *n* (%)

AI ablation index, *RF* radiofrequency

The AI was modified in 5 patients; 3 (10%) patients in the PRINT group due to the esophageal position, since ablation over the closest isodistance area (red) was unavoidable (Fig. 3); and 2 (6.6%) patients in the CONTROL group, since there were temperature rises. Out of these five patients, first-pass isolation was not achieved in 2 patients (40%), one patient in each group. The mean number of ablation points affected by the esophageal position was 2 ± 1 per patient. For the PRINT group, after PVI line tailoring on the posterior wall, the mean area between the standard line and the modified line was 0.5 ± 0.6 cm^2, and the mean maximum distance between both lines was 2 ± 2.4 mm.

3.6 Follow-up

In-hospital stay was 24 h for all patients except for the two patients with vascular complications. Arrhythmia

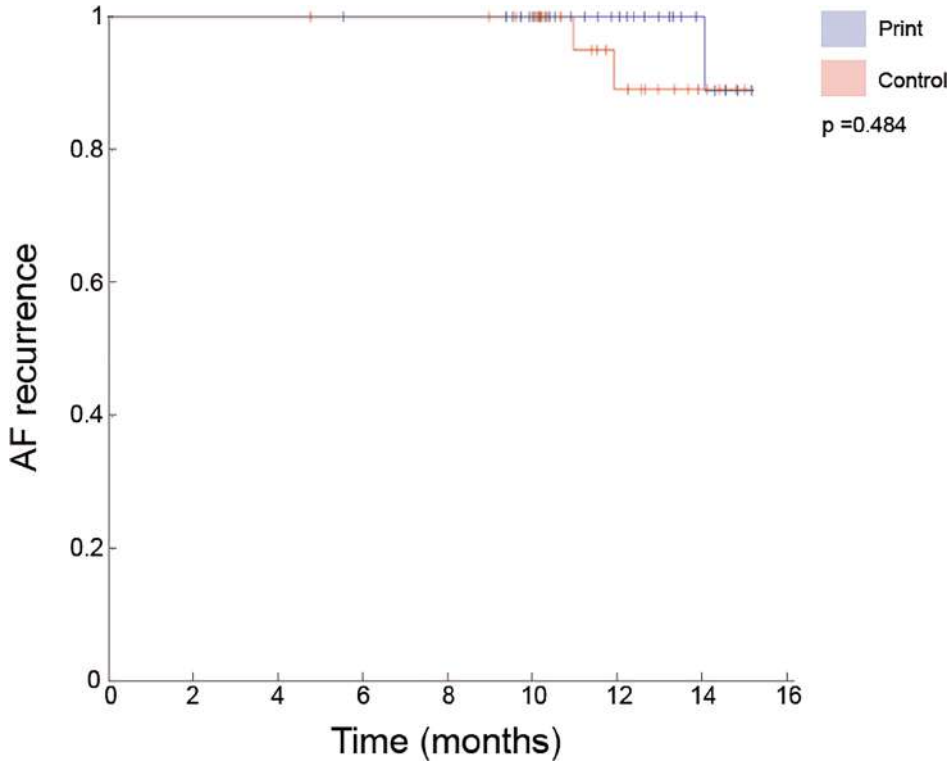

Fig. 6 Results Kaplan–Meier curve for atrial fibrillation recurrences at 12 ± 3 months

recurrences were observed in 2 (6.6%) patients in the PRINT group and in 1 (3%) in the CONTROL group during a mean FU of 12 ± 3 months. All three patients presented clinical episodes of palpitations that required medical care with documented AF on the ECG. There were no significant differences in AF recurrence between groups ($p = 0.4$). Figure 6 shows the Kaplan–Meier curve for AF recurrence. There were no long-term esophageal complications or AE fistulas.

4 Discussion

4.1 Main findings

This study describes the clinical utility of integrating the esophageal fingerprinted isodistance map into the CARTO navigation system during AF ablation. This innovative method of depicting the complex relationship between the esophagus and the left atrial posterior wall allows for a personalized approach by adapting the PVI line to the esophageal position. It results in a significant decrease in esophageal heating during RF delivery to the left atrial posterior wall, without an impact on acute outcomes or rates of AF recurrence at 1-year follow-up in this randomized study of patients referred for PAF ablation.

4.2 Esophageal fingerprint

The esophageal fingerprint offers a reliable representation of the three-dimensional atrio-esophageal relationship. This MDCT-derived tool is simple, non-invasive, and comprehensible, offering the operator valuable information on the proximity between both structures on the anteroposterior plane, which is otherwise unavailable, as opposed to previously described techniques for avoiding esophageal heating, such as soluble contrast swallowing [19], mechanical deviation of the esophagus [13, 20], or even esophageal cooling [14], which need further esophageal instrumentation.

4.3 Personalized RF delivery by tailoring the posterior aspect of the PVI lines to the esophageal fingerprint

Reliability of the esophageal fingerprint has already been validated in a preceding publication that ratified the stability of the esophageal position during AF ablations in patients under general anesthesia [16]. The association between temperature rises and esophageal thermal injury has been established in several studies [5, 10]. In addition, robust randomized evidence shows that esophageal thermal injury occurs more often in patients in whom the posterior atrial wall lesion set overlaps the esophagus with

Journal of Interventional Cardiac Electrophysiology (2022) 65:651–661

a greater risk of esophageal injury when overlap occurs [19]. The presented randomized trial demonstrates the superiority of tailoring the posterior atrial wall PVI lines to the esophageal fingerprint, as compared to a standard approach, with regard to avoiding esophageal temperature rises. This may potentially reduce both the incidence and the severity of thermal injury and improve procedure safety. In fact, a slight modification in the line location led to significant results in terms of temperature rise reduction, since the mean distance change between the blinded and the modified lines for the intervention group was only 2 ± 2.4 mm. In cases where ablation in the closest area (red zone) was unavoidable to attain PVI, the target AI was lowered to 300, thus leading to a significantly lower amount of temperature rises on the PRINT group. Furthermore, a very high rate of first past isolation was observed despite delivering a lower AI.

4.4 Esophageal temperature monitoring probe

There is conflicting evidence regarding whether the use of LET probes can help decrease the probability of developing esophageal lesions. The presented evidence confirms that, at least with the LET probe used in this study (SensiTherm, St. Jude Medical, Inc., St. Paul, MN, USA), the detection of esophageal heating is related to the proximity between RF delivery and the esophagus (as measured with the esophageal fingerprint), and even in the absence of the esophageal fingerprint, it allowed for a strategy that targeted avoiding heat stacking on the posterior wall in the CONTROL group. Nevertheless, co-registration of the esophageal FAM provided relevant insight on the limitations of the esophageal temperature probe and on why sometimes there is no temperature rise even though RF is applied in the red area (closest location to the esophagus). In fact, placement of the probe is completely random as related to the esophageal width, and as shown by this study and illustrated in Fig. 4, an esophagus overlapping the pulmonary veins can be wide enough to harbor the probe in a completely opposite margin. As a result, this creates an inaccurate sense of security. In fact, other authors have already postulated the limitation of a method that depends on probe position [21] which is why prior knowledge of esophageal contact surface, as provided by the fingerprint, is fundamental. Moreover, some studies have postulated that LET probe could even cause harm by acting as an antenna thus promoting bipolar ablation between RF catheter and probe [22, 23].

4.5 Implications of ablation line modification

The personalized posterior wall lesion set tailors the ablation line trajectory to the esophageal fingerprint and the AI settings to the left atrial wall thickness as described by the *Ablate by-LAW* protocol. Although it is widespread practice to limit the radiofrequency (RF) settings when ablating the posterior LA wall during AF ablation to avoid thermal injury to the esophagus, it is not clear whether these changes influence outcomes. Modification of the line trajectory is further a matter of concern since it can mean isolating less venous tissue; in the present study of PAF patients, this non-excluded area was as low as 0.5 ± 0.6 cm^2. Although personalization of ablation lines has already been reported [11, 24], reports on clinical outcomes of this modification are sparce with only one small (probably underpowered) randomized trial showing a neutral effect [19]. The present study reports similar results with no difference between groups in terms of recurrences at 1-year follow-up. Nevertheless, this pilot study was not powered to detect such differences and further studies are needed to clarify this aspect in a broader population of AF patients with special concern for patients with persistent AF, where ablation is usually performed including the complete PV antrum.

4.6 Limitations

First, this randomized pilot study shows that the esophageal fingerprint is useful in avoiding esophageal temperature rises. By no means does it prove a lower risk of AEF but, since this fatal outcome is rather rare; a trial with such an efficacy endpoint might not be feasible since it would require a considerably larger population. Furthermore, an esophagogastroduodenoscopy was not performed after the procedure in search for esophageal thermal lesions. Nevertheless, despite limitations of esophageal temperature monitoring, esophageal temperature rises predict esophageal thermal injury, and the presented workflow is expected to reduce the incidence and severity of thermal injury, suggesting a capacity to minimize the risk of AEF. However, the ablation settings were those of the by-law method with an energy delivery that is substantially lower than that of other protocols and these results should be further evaluated in the context of other ablation methods/settings. Nevertheless, efficacy of lowering the AI delivered to the posterior wall was analyzed in patients who underwent periprocedural LA intracardiac echocardiography (ICE) with a first-pass rate comparable to more demanding protocols [25]. Additionally, this work showed the feasibility of evaluating periprocedural esophageal position with ICE showing a stability of the esophageal position as compared to preprocedural contrast esophagography saved in Carto UNIVU™.

Second, nonthermal ablation technologies are an expanding field which has shown sparing of the esophagus, thus potentially solving this long-standing challenge. Nevertheless, thermal approaches are still the most widely used, and the presented findings remain of relevance to many centers worldwide. Finally, previous studies have shown that in rare

cases, there can be a significant shift in esophageal position from one CT scan to another [16, 25] or intraprocedurally (4–8% of cases). Having this in mind, caution should be used not to create a false sense of safety.

5 Conclusion

The esophageal fingerprint allows for a reliable identification of the esophageal 3D position. Personalized AF ablation by adapting the posterior aspect of the PVI lines is superior to the standard approach with regard to avoiding esophageal temperature rises. Further studies are needed to evaluate the impact of PVI line modification to avoid esophageal heating on AF recurrences with special concern for patients with persistent AF, where broader ablation is usually performed. The development of new imaging-derived tools could ultimately improve patient safety.

Supplementary Information The online version contains supplementary material available at https://doi.org/10.1007/s10840-022-01302-0.

Declarations

Ethical approval The local ethics committee approved the study protocol.

Informed consent All participants included in the study provided written informed consent.

Conflict of interest Dr. Berruezo is stockholder of Galgo Medical. Dr. Soto-Iglesias is an employee of Biosense Webster. All remaining authors have no other relevant affiliations or financial involvement with any organization or entity with a financial interest in or financial conflict with the subject matter or materials discussed in the manuscript apart from those disclosed.

References

1. Chew DS, Jones KA, Loring Z, et al. Diagnosis-to-ablation time predicts recurrent atrial fibrillation and rehospitalization following catheter ablation. Heart Rhythm O2. 2022;3(1):23–31. https://doi.org/10.1016/j.hroo.2021.11.012.
2. Iwasaki Y, Nishida K, Kato T, Nattel S. Atrial fibrillation pathophysiology: implications for management. Circulation. 2011;124(20):2264–74. https://doi.org/10.1161/CIRCULATIONAHA.111.019893.
3. Kirchhof P, Camm AJ, Goette A, et al. Early rhythm-control therapy in patients with atrial fibrillation. N Engl J Med. 2020;383(14):1305–16. https://doi.org/10.1056/NEJMoa2019422.
4. Hindricks G, Potpara T, Dagres N, et al. ESC Guidelines for the diagnosis and management of atrial fibrillation developed in collaboration with the European Association of Cardio-Thoracic Surgery (EACTS). Eur Heart J. August 2020. https://doi.org/10.1093/eurheartj/ehaa612
5. Halbfass P, Pavlov B, Muller P, et al. Progression from esophageal thermal asymptomatic lesion to perforation complicating atrial fibrillation ablation: a single-center registry. Circ Arrhythm Electrophysiol. 2017;10(8). https://doi.org/10.1161/CIRCEP.117.005233
6. Lakkireddy D, Reddy YM, Atkins D, et al. Effect of atrial fibrillation ablation on gastric motility: the atrial fibrillation gut study. Circ Arrhythm Electrophysiol. 2015;8(3):531–6. https://doi.org/10.1161/CIRCEP.114.002508.
7. Kadado AJ, Akar JG, Hummel JP. Luminal esophageal temperature monitoring to reduce esophageal thermal injury during catheter ablation for atrial fibrillation: a review. Trends Cardiovasc Med. 2019;29(5):264–71. https://doi.org/10.1016/j.tcm.2018.09.010.
8. Turagam MK, Miller S, Sharma SP, et al. Differences in transient thermal response of commercial esophageal temperature probes: insights from an experimental study. JACC Clin Electrophysiol. 2019;5(11):1280–8. https://doi.org/10.1016/j.jacep.2019.07.013.
9. Schoene K, Arya A, Grashoff F, et al. Oesophageal Probe Evaluation in Radiofrequency Ablation of Atrial Fibrillation (OPERA): results from a prospective randomized trial. Europace. 2020;22(10):1487–94. https://doi.org/10.1093/europace/euaa209.
10. Grosse Meininghaus D, Blembel K, Waniek C, et al. Temperature monitoring and temperature-driven irrigated radiofrequency energy titration do not prevent thermally induced esophageal lesions in pulmonary vein isolation: a randomized study controlled by esophagoscopy before and after catheter ablation. Heart Rhythm. 2021;18(6):926–34. https://doi.org/10.1016/j.hrthm.2021.02.003.
11. Kottkamp H, Piorkowski C, Tanner H, et al. Topographic variability of the esophageal left atrial relation influencing ablation lines in patients with atrial fibrillation. J Cardiovasc Electrophysiol. 2005;16(2):146–50. https://doi.org/10.1046/j.1540-8167.2005.40604.x.
12. Zhang X, Kuang X, Gao X, et al. RESCUE-AF in patients undergoing atrial fibrillation ablation: the RESCUE-AF trial. Circ Arrhythm Electrophysiol. 2019;12(5):e007044. https://doi.org/10.1161/CIRCEP.118.007044.
13. Aguinaga L, Palazzo A, Bravo A, et al. Esophageal deviation with vacuum suction and mechanical deflection during ablation of atrial fibrillation: first in man evaluation. J Cardiovasc Electrophysiol. 2021;32(1):67–70. https://doi.org/10.1111/jce.14801.
14. Leung LWM, Bajpai A, Zuberi Z, et al. Randomized comparison of oesophageal protection with a temperature control device: results of the IMPACT study. Europace. 2021;23(2):205–15. https://doi.org/10.1093/europace/euaa276.
15. Teres C, Soto-Iglesias D, Penela D, et al. Personalized paroxysmal atrial fibrillation ablation by tailoring ablation index to the left atrial wall thickness: the "Ablate by-LAW" single-centre study-a pilot study. Europace. 2022;24(3):390–9. https://doi.org/10.1093/europace/euab216.
16. Teres C, Soto-Iglesias D, Penela D, et al. Relationship between the posterior atrial wall and the esophagus: esophageal position during atrial fibrillation ablation. In Press Corrected Proof. Published online: February 13, 2022. https://doi.org/10.1016/j.hroo.2022.02.007
17. Falasconi G, Penela D, Soto-Iglesias D, et al. A standardized stepwise zero-fluoroscopy approach with transesophageal echocardiography guidance for atrial fibrillation ablation. J Interv Card Electrophysiol. 2021. https://doi.org/10.1007/s10840-021-01086-9.
18. Teres C, Soto-Iglesias D, Penela D, et al. Left atrial wall thickness of the pulmonary vein reconnection sites during atrial fibrillation redo procedures. Pacing Clin Electrophysiol. 2021;44(5):824–34. https://doi.org/10.1111/pace.14222.
19. Ye Y, Chen S-Q, Lu Y-F, et al. PV isolation guided by esophageal visualization with a tailored ablation strategy for the avoidance of esophageal thermal injury: a randomized trial. J Interv Card

Electrophysiol an Int J Arrhythm pacing. 2020;58(2):219–27. https://doi.org/10.1007/s10840-019-00572-5.
20. Parikh V, Swarup V, Hantla J, et al. Feasibility, safety, and efficacy of a novel preshaped nitinol esophageal deviator to successfully deflect the esophagus and ablate left atrium without esophageal temperature rise during atrial fibrillation ablation: the DEFLECT GUT study. Heart Rhythm. 2018;15(9):1321–7. https://doi.org/10.1016/j.hrthm.2018.04.017.
21. Leung LWM, Akhtar Z, Sheppard MN, Louis-Auguste J, Hayat J, Gallagher MM. Preventing esophageal complications from atrial fibrillation ablation: a review. Heart Rhythm O2. 2021;2(6Part A):651–64. https://doi.org/10.1016/j.hroo.2021.09.004.
22. Carroll BJ, Contreras-Valdes FM, Heist EK, et al. Multi-sensor esophageal temperature probe used during radiofrequency ablation for atrial fibrillation is associated with increased intraluminal temperature detection and increased risk of esophageal injury compared to single-sensor probe. J Cardiovasc Electrophysiol. 2013;24(9):958–64. https://doi.org/10.1111/jce.12180.
23. Müller P, Dietrich J-W, Halbfass P, et al. Higher incidence of esophageal lesions after ablation of atrial fibrillation related to the use of esophageal temperature probes. Heart Rhythm. 2015;12(7):1464–9. https://doi.org/10.1016/j.hrthm.2015.04.005.
24. Sherzer AI, Feigenblum DY, Kulkarini S, et al. Continuous non-fluoroscopic localization of the esophagus during radiofrequency catheter ablation of atrial fibrillation. J Cardiovasc Electrophysiol. 2007;18(2):157–60. https://doi.org/10.1111/j.1540-8167.2006.00674.x.
25. Hayashi K, Okumura K, Okamatsu H, Kaneko S, Negishi K, Tsurugi T, Tanaka Y, Nakao K, Sakamoto T, Koyama J. Real-time visualization of the esophagus and left atrial posterior wall by intra-left atrial echocardiography. J Interv Card Electrophysiol. 2022;63(3):629–37. https://doi.org/10.1007/s10840-021-01093-w.
26. Nakatani Y, Nuñez-Garcia M, Cheniti G, et al. Preoperative personalization of atrial fibrillation ablation strategy to prevent esophageal injury: impact of changes in esophageal position. J Cardiovasc Electrophysiol. 2022;33(5):908–16. https://doi.org/10.1111/jce.15447.

DISCUSIÓN

1. Hallazgos principales

Este trabajo de investigación se centra en el desarrollo de nuevas herramientas derivadas de estudios de imagen con la intención de personalizar las ablaciones con catéter de fibrilación auricular. Los principales hallazgos de este trabajo de investigación se pueden resumir en:

- Importar el mapa de grosor (LAWT) al sistema de navegación 3D es posible y proporciona información en tiempo real sobre el LAWT en cualquier punto de la aurícula izquierda.
- El LAWT medio en los puntos de reconexión identificados es más grueso que el LAWT del resto de la línea de aislamiento de VP en pacientes sometidos a reintervenciones.
- La viabilidad y utilidad de un método simplificado para realizar el procedimiento de reablación de FA utilizando una técnica de catéter único que mejora la eficiencia al obtener tiempos de procedimiento y fluoroscopia más cortos en comparación con los estándares de la literatura.
- La viabilidad, eficacia y seguridad de un novedoso protocolo que adapta el índice de ablación al espesor de la pared local, lo que resulta en un procedimiento, de fluoroscopia y de RF corto al tiempo que proporciona resultados de eficacia que podrían ser comparables a los de Protocolos de ablación más exigentes.
- La creación de la huella digital esofágica, un innovador método 3D para representar la relación entre el esófago y la pared posterior de la AI derivado del TAC.
- Existe una alta estabilidad temporal de la posición esofágica entre procedimientos separados por varios meses.
- Múltiples técnicas de imagen disponibles periprocedimiento permiten evaluar la posición esofágica mostrando una alta estabilidad de la posición esofágica en pacientes bajo anestesia general.

- La integración del mapa de isodistancia o huella dactilare esofágica en el sistema de navegación durante la ablación de FA para un enfoque personalizado adaptando la línea de aislamiento de las VP a la posición esofágica. Lo que resultó en una disminución significativa del calentamiento esofágico durante la administración de RF a la pared posterior de la aurícula izquierda, sin impacto en los resultados agudos o las tasas de recurrencia de FA al año de seguimiento.

2. Innovación de los mapas 3D de espesor de la pared de la aurícula izquierda.

El TAC moderno ha marcado el comienzo de una era de imágenes de alta definición. Con su resolución submilimétrica, como lo demuestran las validaciones en modelos porcinos, favorece la creación de mapas LAWT 3D precisos. Estas imágenes tan detalladas son fundamentales para que la electrofisiología avance en la medicina de precisión, permitiendo un tratamiento personalizado. Y si bien el tiempo inicial de procesamiento de imágenes de 15 ± 2 minutos podía parecer largo, ya hemos observado un avance gracias a un módulo de inteligencia artificial que permite un proceso de segmentación más rápido de los mapas 3D LAWT.

Hay un carácter pionero en la investigación presentada en este trabajo que muestra la plausibilidad de integrar por primera vez mapas 3D LAWT en los sistemas de navegación existentes. Aunque ya se habían desarrollado mapas 3D LAWT, nuestro estudio los reposiciona, no como meros estudios preparatorios o para análisis fuera de línea, sino como herramientas de evaluación en tiempo real, que generan una imagen en de la aurícula izquierda durante el procedimiento. Esta integración tiene como objetivo perfeccionar la precisión del procedimiento y equipa a los médicos con una capacidad para medir el espesor de la pared en cualquier punto de la aurícula izquierda durante el procedimiento (Figura 3). Esta técnica enriquece el ámbito de la ablación de la FA al fusionar los principios de la imagen y la modulación de energía, ofreciendo un enfoque matizado y personalizado para el tratamiento de la FA.

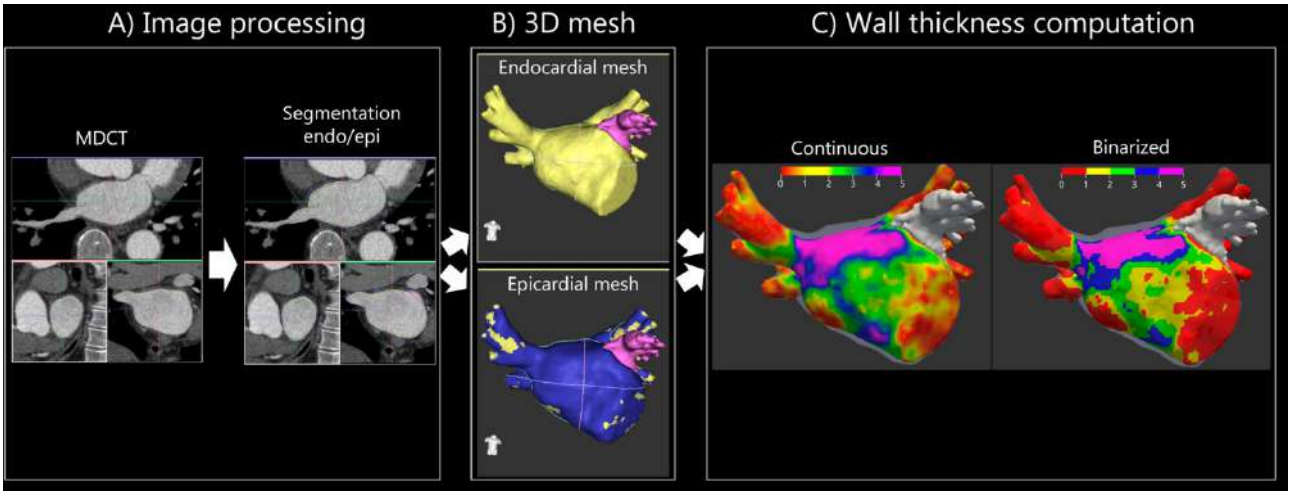

Figura 3. Procedimiento de segmentación del mapa de grosor 3D a partir de las imágenes DICOM del angioTAC cardíaco. Se segmentan una malla endocárdica y otra epicárdica y se computa el grosor en cada punto de la malla creando así un mapa con grosor contínuo que se categoriza en cpas de 1 mm de diferencia (Rojo <1 mm, Amarillo 1,1-2 mm, Verde 2,1-3 mm, Azul 3,1-4 mm, Magenta > 4 mm).

3. Reconexiones de venas pulmonares y su implicación en la recurrencia de FA post aislamiento.

La sostenibilidad del impacto terapéutico del aislamiento de venas pulmonares se ve socavada por las reconexiones que se traducen en recurrencias arrítmicas. Después del aislamiento de las VP, se reestablecen de vías eléctricas o reconexiones entre estas y la aurícula izquierda. Estas reconexiones, probablemente atribuibles a la recuperación de tejidos previamente desconectados o a un aislamiento inicial incompleto, se manifiestan como "espacios" eléctricos y sirven como conductos para los desencadenantes de la FA. Múltiples estudios han demostrado consistentemente que las reconexiones de las VP son una causa predominante para la recurrencia de FA después de su aislamiento. La esencia misma de la intervención (aislar eléctricamente los desencadenantes de la FA de las venas pulmonares) queda anulada por estas reconexiones, restableciendo así el medio arritmogénico. La compleja anatomía del sistema venoso pulmonar, con variaciones del grosor inter e intrapaciente puede plantear desafíos para garantizar una línea de aislamiento perfecta alrededor de las VP. Esta diversidad anatómica a menudo se traduce en áreas de suministro inadecuado

de energía durante el procedimiento inicial, lo que predispone a las reconexiones. La integración del mapa LAWT 3D permite la observación de estos matices anatómicos (Figura 4).

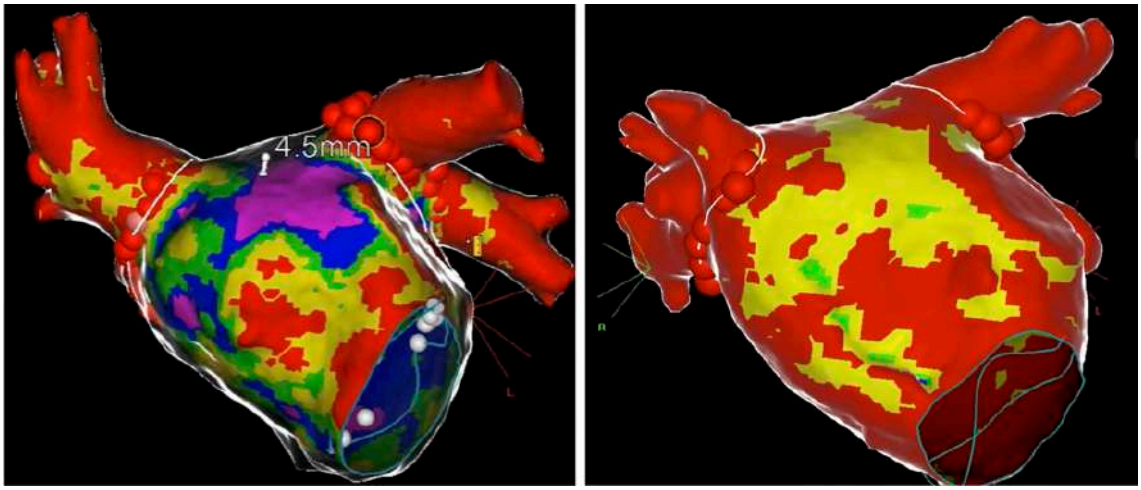

Figura 4. Comparación entre el mapa de grosor auricular de dos pacientes que ilustra la diferencia interpacientes del grosor y el potencial de personalización de las intervenciones.

Nuestro primer estudio resaltó que los puntos reconectados o brechas eléctricas se correlacionan de manera muy sólida con un grosor significativamente mayor del tejido auricular izquierdo en comparación con el resto de la línea de ablación circunferencial de las VP. Investigaciones previas ya habían descrito esta observación mediante análisis fuera de línea del grosor auricular por TAC. Sin embargo, en operaciones de reablación de fibrilación auricular, es clínicamente crucial que hayamos podido corroborar este hallazgo perprocedimiento. Este trabajo de investigación demostró que el mapa de grosor auricular tiene la capacidad de resaltar los sitios de reconexión de las venas pulmonares, lo cual constituye una ventaja única dada la evaluación en tiempo real que puede ayudar a mejorar la precisión de las intervenciones, arrojando luz sobre áreas potencialmente vulnerables a reconexiones y resaltando la importancia de una formación de lesiones transmural durante los procedimientos iniciales.

El presente trabajo también esclarece una técnica simplificada de catéter único, que implica una reducción del tiempo de procedimiento y de fluoroscopia en comparación con referentes establecidos. Históricamente empleada para el

aislamiento de VP por primera vez, la técnica de catéter único emerge como un arsenal rentable. Con métricas de recurrencia de FA comparables, tiempos de procedimiento más cortos, exposición minimizada a la fluoroscopia y una incidencia de complicaciones encomiablemente baja, este enfoque denota un cambio transformador en la estrategia de ablación de FA. Estas mejoras en los procedimientos no sólo garantizan la seguridad del paciente, sino que también economizan recursos sanitarios (figura 5).

Figura 5. Ejemplo de acceso vascular con catéter único.

4. **El espesor de la pared de la aurícula izquierda entre otros determinantes de la transmuralidad de la lesión y el avance hacia terapias personalizadas mediante la adaptación del índice de ablación.**

Corroborando hallazgos anteriores ex vivo y de TAC, nuestra investigación subraya la naturaleza más delgada de la pared posterior de la aurícula izquierda en comparación con su contraparte anterior. Pero lo que distingue a nuestra publicación es la atención a la variabilidad intrarregional, que aboga por una estrategia de administración de RF más personalizada, que trascienda la clasificación binaria anteroposterior, que es una simplificación excesiva (Figura 6).

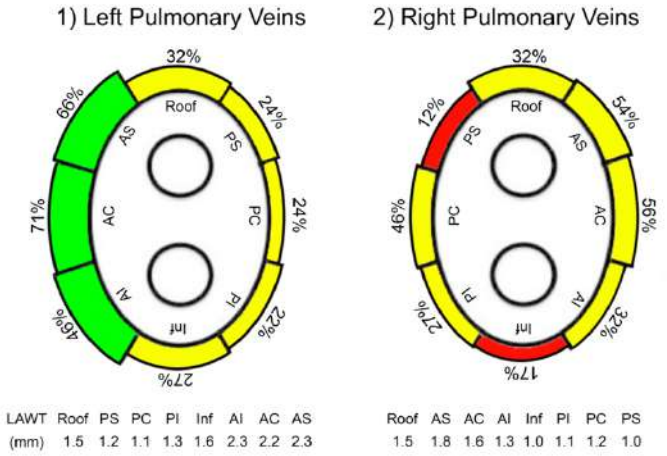

Figura 6. Grosor medio observado por segmento que ilustra un mayor grosor en la pared anterior respecto a la pared posterior así que el porcentaje de reconexiones por segmento que muestra una mayor incidencia en los segmentos con mayor grosor.

La llegada de sistemas avanzados de mapeo y navegación, junto con la innovación en la tecnología de los catéteres, ha marcado el comienzo de una mayor precisión en los procedimientos de aislamiento de VP. Sin embargo, incluso con herramientas de última generación, el espectro de las reconexiones persiste. Esto subraya los desafíos inherentes a lograr lesiones perennes que lleven a un aislamiento duradero.

La ablación por RF emplea corriente alterna (normalmente en el rango de 500 kHz) para generar calentamiento resistivo en los tejidos cardíacos. La conversión de energía eléctrica en energía térmica en la interfaz tejido-electrodo provoca un aumento de la temperatura del tejido y la consiguiente muerte celular.

La profundidad y el tamaño de las lesiones de RF dependen de varios determinantes: (1) Potencia: una potencia de RF más alta generalmente da como resultado lesiones más grandes y profundas. Sin embargo, una potencia excesiva puede provocar un calentamiento rápido y carbonización de la superficie, impidiendo una penetración más profunda en el tejido; (2) Duración: la aplicación prolongada de RF aumenta la profundidad de la lesión, pero con rendimientos decrecientes con el tiempo debido a los mecanismos de enfriamiento pasivo y la desecación del tejido; (3) Impedancia del tejido: una impedancia más baja facilita un mayor flujo de corriente y, por tanto, un mejor calentamiento. La caída de la impedancia es un marcador de la creación de lesión, pero este parámetro aumenta a medida que el tejido se seca, lo que

indica una eficacia reducida del suministro de energía; (4) Fuerza de contacto: la fuerza ejercida por la punta del catéter sobre el tejido cardíaco influye en el tamaño de la lesión. Un contacto adecuado garantiza una transferencia de energía eficaz, mientras que una fuerza excesiva puede provocar compresión del tejido, lesiones subóptimas o incluso perforación. De manera similar, el contacto uniforme entre el electrodo y el tejido garantiza un calentamiento uniforme, mientras que la inclinación del catéter o el contacto desigual pueden provocar lesiones asimétricas; (5) El flujo sanguíneo participa al enfriamiento. Las áreas con alto flujo sanguíneo pueden disipar el calor más rápidamente, lo que provoca lesiones más pequeñas o menos profundas. Por el contrario, la reducción del flujo sanguíneo (como puede ocurrir con flujo bajo o durante aplicaciones de alta potencia) puede aumentar el tamaño de la lesión, pero aumentar el riesgo de formación de carbonilla; (6) Tamaño y diseño del electrodo: los electrodos más grandes distribuyen la corriente sobre una superficie más amplia, lo que a menudo resulta en lesiones más anchas y menos profundas. Por el contrario, los electrodos más pequeños pueden crear lesiones más profundas, pero más estrechas. Los catéteres de ablación de FA modernos vienen equipados con puntas irrigadas para evitar el sobrecalentamiento y permitir aplicaciones de RF más prolongadas.

El desafío fundamental en la ablación por RF radica en optimizar estos parámetros para garantizar la transmuralidad de la lesión sin dañar estructuras adyacentes como el esófago en las ablaciones de la aurícula izquierda o el nervio frénico durante las ablaciones del lado derecho, especialmente en áreas donde la pared auricular es delgada. De la misma manera, para las primoablaciones, el grosor auricular constituye una métrica cardinal en la creación de lesiones. Sin embargo, este parámetro nunca había sido considerado como lo hemos introducido de forma totalmente personalizada en nuestro método. Recientemente, se han desarrollado índices de ablación que fusionan parámetros de ablación para estandarizar la creación de lesiones. En nuestro caso la fórmula utilizada es el índice de ablación (IA) que es una fórmula compleja que considera voltaje, tiempo y fuerza de contacto entre el catéter y el tejido. La heterogeneidad del grosor auricular en diferentes

regiones, especialmente entre las paredes anterior y posterior, tiene implicaciones para la administración de energía de RF. Garantizar la

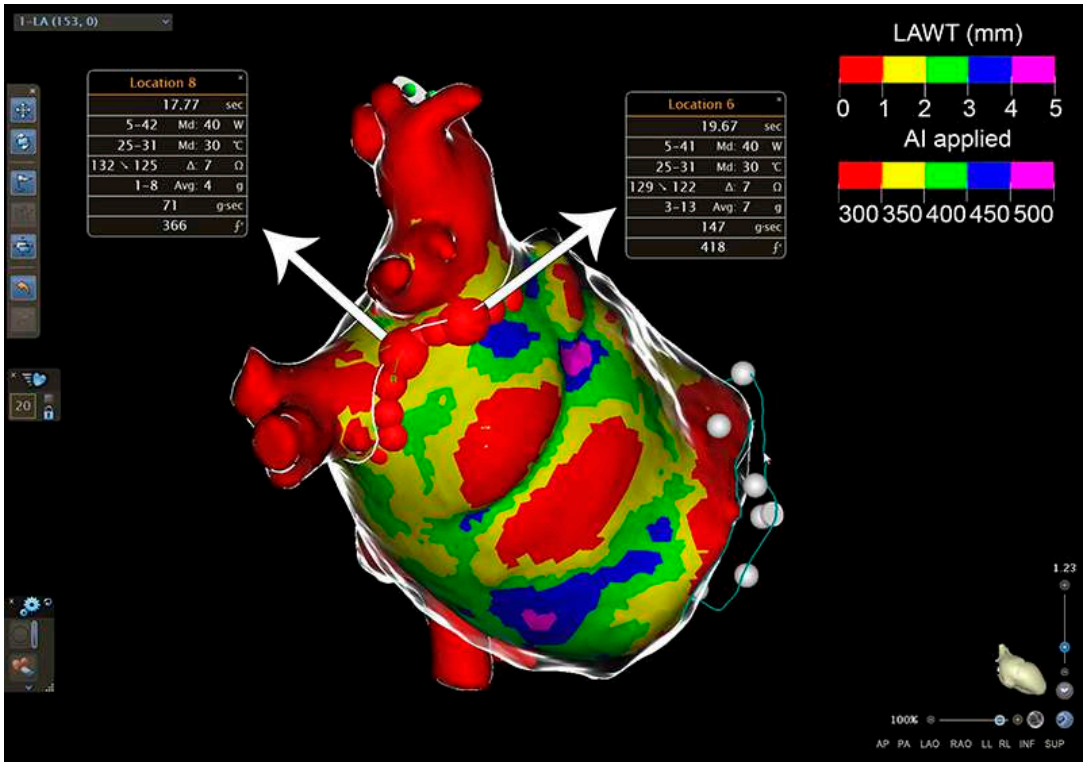

transmuralidad en regiones más gruesas podría requerir aplicaciones de RF prolongadas o de alta potencia en comparación con áreas más delgadas (Figura 7).

Figura 7. Ejemplo de la adaptación del índice de ablación al grosor de la pared auricular (en la escala de colores se aprecian las categorías de grosor aplicadas a cada color y debajo el índice de ablación aplicado en el protocolo personalizado.

La fusión de mapas LAWT con sistemas de navegación en tiempo real brinda a los médicos datos dinámicos, lo que garantiza un despliegue óptimo de energía durante los procedimientos, maximizando así las tasas de seguridad y éxito. Tradicionalmente, el índice de ablación (AI) permanecía estático y sólo cambiaba con respecto a la cara anterior/posterior. Con la novedosa idea de utilizar el grosor para adaptar el AI, abogamos por un enfoque dinámico. Reconociendo la importancia del grosor en la transmuralidad de las lesiones, nuestro método modula la administración de radiofrecuencia (RF), intensificándola en zonas más gruesas y moderándola en las más delgadas. Esta adaptabilidad promete un énfasis equilibrado en la eficacia terapéutica y la

seguridad del procedimiento. El enfoque personalizado de combinar AI con LAWT cultiva un modelo de aplicación de RF eficiente. Imitando resultados similares al protocolo del estudio CLOSE, nuestro método reduce los requisitos de RF (Tabla 2).

Procedure characteristics		
	CLOSE (N=130)	**ABLATE BY LAW (N=86)**
PV isolation, n(%)	130 (100)	86 (100)
General anesthesia, n(%)	72 (55)	86 (100)
HFLTV, n(%)		71 (82.6)
Procedure time (min)	155 ± 28	**60** (IQR 51.2-69.5)
Fluoroscopy time (min)	16.7 ± 7.1	**0.95** (IQR 0.5-1.5)
Fluoroscopy dose (mGy/cm²)	11.314 ± 8.687	**2.3** ± 4.1
Right veins		
• **RF tags**	29 ± 5	30.2 ± 5.5
• **RF time**	16 ± 4	**8.2** ± 2.2
• **First pass isolation**	130 (100%)	82 (**95.3%**)
Left veins		
• **RF tags**	27 ± 5	27 ± 6.5
• **RF time**	18 ± 6	**7** ± 1.8
• **First pass isolation**	126 (97%)	80 (**93%**)
Complication rate, %	0%	**0%**

Tabla 2. Comparación de los resultados del método By-Law con el estudio CLOSE que validó el índice de ablación para la primoablación de FA paroxística.

Atribuimos esta eficiencia a la adaptación de RF y a estrategias proactivas para navegar por la pared auricular personalizando la línea de ablación a través de las regiones más delgadas de la aurícula izquierda (Figura 8). Esto da como resultado menos requisitos de ablación y un menor riesgo de reconexión. Nuestro estudio también pone énfasis en la seguridad, informando complicaciones mínimas incluso cuando las potencias de RF se amplificaron hasta 50 W en regiones más gruesas, con una notable ausencia de complicaciones graves como estallidos de vapor o taponamiento cardíaco.

Esto prepara el escenario para avances potencialmente innovadores en el tratamiento de las arritmias y, a medida que el campo continúa evolucionando, mayores mejoras en nuestra comprensión de estas interacciones biofísicas sin duda mejorarán los resultados de los procedimientos y la seguridad del paciente.

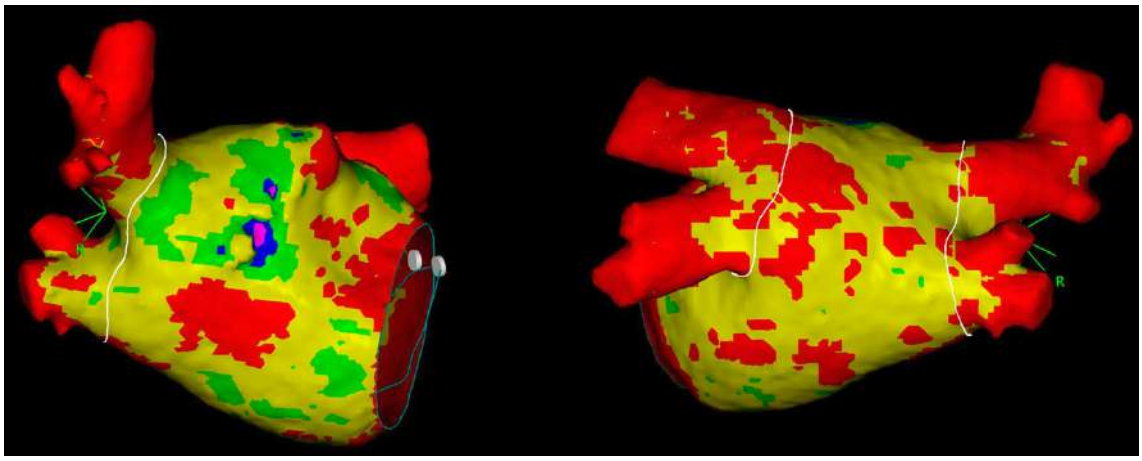

Figura 8. Ejemplo de personalización de la línea de ablación que discurre por las zonas más delgadas de la circunferencia de las venas pulmonares.

5. Importancia de la estabilidad de la posición esofágica y la monitorización de la temperatura durante la ablación de la FA

Este trabajo de investigación también profundiza en la yuxtaposición anatómica del esófago a la pared posterior de la aurícula izquierda que lo hace susceptible a la lesión térmica durante la ablación de la FA. De ahí la importancia de comprender esta relación anatómica para cualquier procedimiento en el que se realicen aplicaciones de RF en la pared posterior de la aurícula izquierda. Los estudios AWESOME introducen un concepto innovador, la huella esofágica. Este mapa de isodistancia (Figura 9) genera una imagen visual de la distancia entre la pared posterior de la aurícula izquierda y el esófago que puede integrarse en el sistema de navegación para modular los sitios y parámetros de ablación y, en última instancia, desmitifica este enigma anatómico que constituye un desafío de consideración durante la ablación con catéter en términos de seguridad.

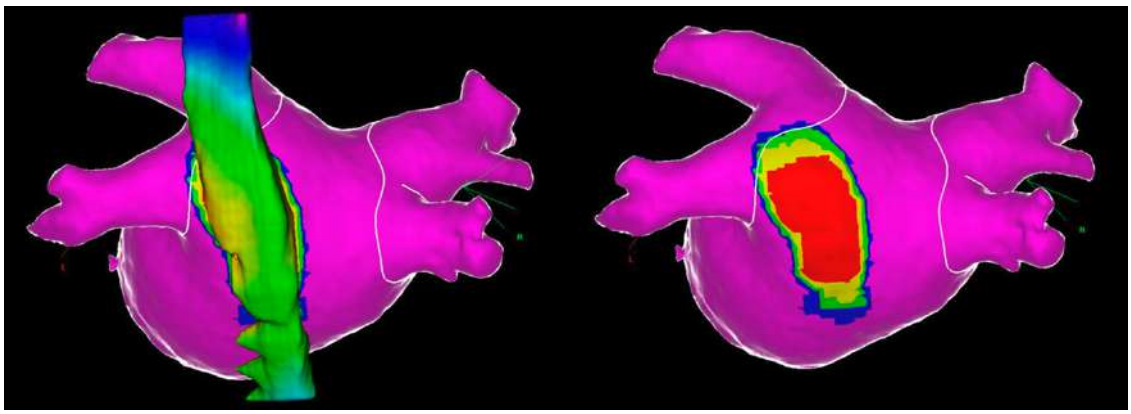

Figura 9. Ejemplo de huella esofágica. Mapa de isodistancias entre el esófago y la pared posterior de la aurícula izquierda. Rojo <1 mm, Amarillo 1,1-2 mm, Verde 2,1-3 mm, Azul 3,1-4 mm, Magenta > 4 mm).

Estudios anteriores han mostrado resultados contradictorios sobre la estabilidad de la posición esofágica durante la ablación. Nuestra investigación subraya la estabilidad temporal de la posición esofágica. El 92% de los casos que analizamos demostró una posición esofágica estable en todas las modalidades de imagen antes, durante y después del procedimiento (se analizó la posición esofágica con la huella esofágica en la primo y la reablación así como durante el mismo procedimiento con el CT, el módulo CARTOUNIVU que co-registra la fluoroscopia con el sistema de navegación en 3D y por último un mapa anatómico 3D de el esófago adquirido con el catéter de ablación al final del procedimiento). El 8% residual presentó variaciones, atribuidas a diversas causas, desde eventos como tos hasta una cardioversión eléctrica durante la ablación. Sorprendentemente, esta estabilidad persevera a lo largo de intervalos prolongados, incluso entre procedimientos secuenciales separados por varios meses (Figura 10). Esta previsibilidad aumenta la precisión y la confianza de la huella esofágica. Sin embargo, estos resultados sólo son aplicables a casos realizados bajo anestesia general.

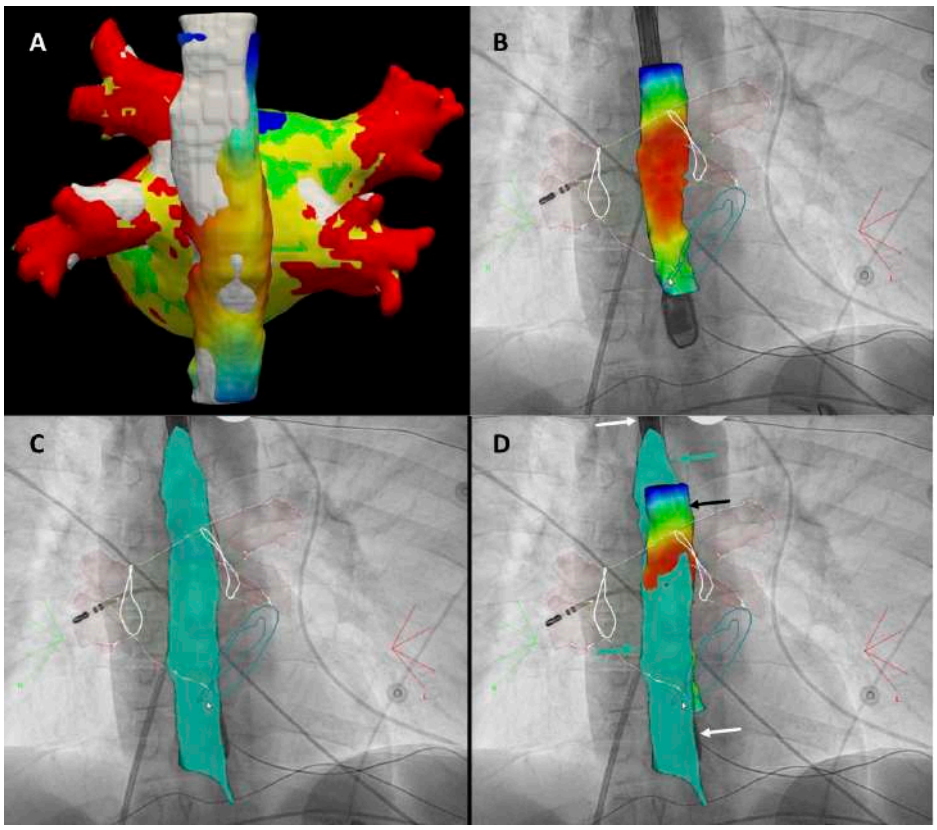

Figura 10 A) Comparación de la posición esofágica en la TAC en la primera ablación (estructura en gris) respecto a la reablación (en color), **B)** TAC vs. CARTOUNIVU™ con sonda ETE ubicada en el esófago, **C)** CARTOUNIVU™ Vs Mapa electroanatómico, **D)** Imagen superpuesta del esófago observado con las tres técnicas diferentes: 2D CARTOUNIVU™ (flecha blanca), 3D MDCT (flecha negra) y 3D FAM (flecha verde).

La monitorización de la temperatura esofágica actúa como protección y proporciona retroalimentación en tiempo real para prevenir el sobrecalentamiento del esófago y posibles complicaciones posteriores, como la fístula auriculo-esofágica. El beneficio clínico directo de la monitorización de la temperatura esofágica es la prevención de lesiones esofágicas. La detección temprana del aumento de temperatura esofágica permite una pronta intervención, generalmente lo que se hace es abstenerse de realizar la ablación en un sitio donde ha habido un aumento de temperatura hasta que se enfríe, mitigando así el riesgo de complicaciones. Otra posibilidad es que, una vez que se observa la susceptibilidad a un aumento de temperatura en una zona determinada de la aurícula, el operador realice las lesiones de una manera alternativa entre diferentes sitios de la línea para evitar el aumento general de la temperatura. Si bien el control de la temperatura es invaluable, no

es infalible. La colocación de la sonda, especialmente en relación con el sitio de ablación, puede afectar la precisión. Con un ancho medio de 28,1 ± 4,1 mm, el esófago no es sólo un tubo delgado. Tal amplitud puede generar variabilidades en su posición percibida, dependiendo de la ubicación de la sonda durante la toma de imágenes (Figura 11).

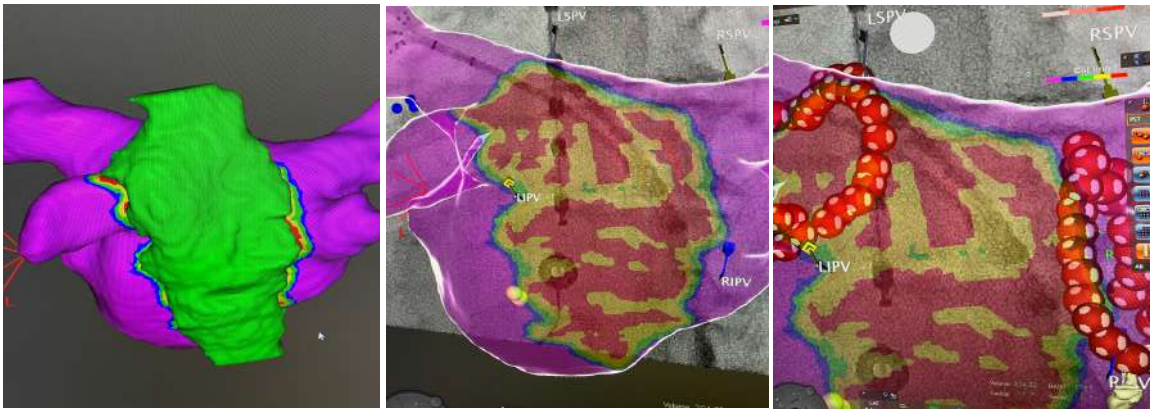

Figura 11 Ejemplo de un esófago ancho (en verde) que se sitúa posteriormente a las venas derechas e izquierdas mientras que al observar la sonda de temperatura el operador puede concluir que el esófago se sitúa únicamente detrás de las VP izquierdas.

Además, es posible que los gradientes de temperatura dentro de la pared esofágica no siempre sean uniformes, lo que lleva a posibles subestimaciones del riesgo de lesión. La monitorización de la temperatura esofágica es sólo una faceta de los mecanismos de seguridad en la ablación de la FA. Debe integrarse con otras estrategias, incluidas las imágenes para delimitar la posición del esófago, el poder de ablación y la modulación de la duración.

6. Personalización de la línea PVI en la vecindad esofágica.

Nuestro estudio aclara el papel clave de incorporar de la huella esofágica en el sistema de navegación CARTO. Esta integración permite una modificación de la línea aislamiento de las VP centrada en el paciente según la posición del esófago. La alteración de las trayectorias de ablación podría reducir inadvertidamente el aislamiento del tejido venoso. En nuestro estudio, esta exclusión fue insignificante. En particular, nuestro ensayo aleatorizado mostró una disminución notable el aumento de la temperatura esofágica durante las aplicaciones de RF en la pared posterior de la aurícula izquierda, sin poner en

peligro los resultados inmediatos o las recurrencias de FA después de un seguimiento de 1 año (Figura 12).

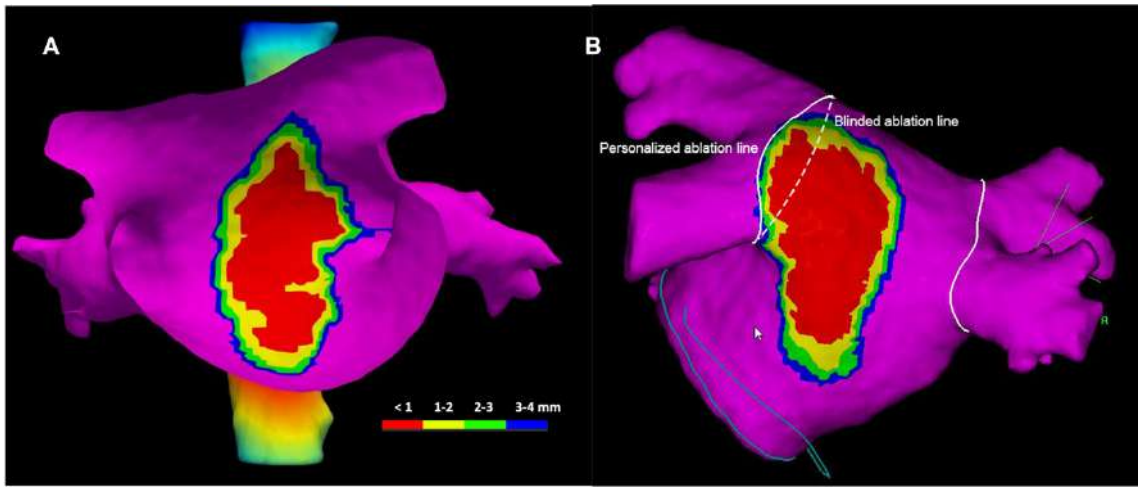

Figura 12. Ejemplo de huella esofágica y de cómo se modifica la línea de ablación posterior en el grupo intervención con el fin de limitar la ablación en zonas muy cercanas al esófago.

En resumen, la naturaleza compleja de las ablaciones de FA, las especificidades anatómicas y las posibles complicaciones requieren soluciones innovadoras para mejorar la seguridad y eficacia del procedimiento. Más allá de las ventajas procesales inmediatas, la fusión de mapas 3D LAWT con sistemas de navegación marca el comienzo de un horizonte repleto de nuevas vías de diagnóstico y terapéuticas. Esta tesis abre nuevos corredores en el tratamiento de la FA, con la integración de mapas LAWT y la modulación de RF que prometen intervenciones terapéuticas más personalizadas y seguras.

CONCLUSIÓN

Este trabajo ha contribuido a enriquecer el conocimiento actual sobre la ablación de la fibrilación auricular al proporcionar una mayor comprensión sobre la importancia del grosor de la pared de la aurícula izquierda como determinante de la creación de lesiones y proporcionar nuevas herramientas que pueden mejorar la eficiencia y seguridad del procedimiento.

En resumen, hemos demostrado que:

1. Los mapas 3D de grosor de la aurícula izquierda pueden obtenerse a partir de imágenes del CT cardíaco e integrarse en el sistema de navegación. Permiten una estimación peri-procedimiento directa del grosor de la pared en cualquier punto de la aurícula izquierda. Los puntos de reconexión están presentes con mayor frecuencia en los segmentos más gruesos de la línea de aislamiento circunferencial y generalmente son el punto más grueso del segmento. Un abordaje con un solo catéter es factible, eficiente y seguro durante los procedimientos de reablación, lo que permite identificar fácilmente el segmento reconectado con una baja tasa de recurrencia a medio plazo.

2. La ablación personalizada de la FA con el protocolo Ablate-By-LAW utilizando una técnica de catéter único y adaptando el índice de ablación al grosor de la pared auricular es factible, eficaz y segura, al mismo tiempo que se obtiene una alta tasa de aislamiento de primer paso en esta población de pacientes. La

tasa de recurrencias de FA observada con el método presentado es equivalente a protocolos de ablación más exigentes. Sin embargo, este fue un estudio observacional y se necesitan más ensayos aleatorios para probar esta hipótesis.

3. Existe una alta estabilidad de la posición esofágica entre procedimientos y desde el principio hasta el final de un procedimiento de ablación de FA. El mapa de isodistancia con huella esofágica en 3D se puede obtener mediante a partir de las imágenes del TAC e integrar en el sistema de navegación. Permite la estimación periprocedimiento directa de la distancia entre el esófago y la pared posterior de la aurícula izquierda.

4. La huella esofágica permite una identificación fiable de la posición 3D del esófago. La ablación personalizada de la fibrilación auricular (FA) mediante la adaptación del aspecto posterior de las líneas de aislamiento de las venas pulmonares es superior al enfoque estándar en lo que respecta a evitar aumentos de temperatura esofágica. Se necesitan más estudios para evaluar el impacto de la modificación de la línea de aislamiento con el fin de evitar el calentamiento esofágico en las recurrencias de FA, con especial preocupación en pacientes con FA persistente, donde generalmente se debe realizar una ablación más amplia.
5. El desarrollo de nuevas herramientas derivadas de imágenes puede, en última instancia, mejorar la eficiencia del procedimiento y la seguridad del paciente.

BIBLIOGRAFÍA

1. Virani SS, Alonso A, Benjamin EJ, Bittencourt MS, Callaway CW, Carson AP, et al. Heart disease and stroke statistics-2020 update: A report from the American Heart Association. Circulation. 2020;141(9):e139-e596.
2. Krijthe BP, Kunst A, Benjamin EJ, Lip GYH, Franco OH, Hofman A, et al. Projections on the number of individuals with atrial fibrillation in the European Union, from 2000 to 2060. Eur Heart J. 2013;34(35):2746-2751.
3. Martinez C, Katholing A, Wallenhorst C, Granziera S, Cohen AT, Freedman SB. Increasing incidence of non-valvular atrial fibrillation in the UK from 2001 to 2013. Heart. 2015;101(21):1748-1754.
4. Hindricks G, Potpara T, Dagres N, Arbelo E, Bax JJ, Blomström-Lundqvist C, et al. 2020 ESC guidelines for the diagnosis and management of atrial fibrillation developed in collaboration with the European Association of Cardio-Thoracic Surgery (EACTS). Eur Heart J. 2021 Feb 1;42(5):373-498
5. Wijffels MC, Kirchhof CJ, Dorland R, Allessie MA. Atrial fibrillation begets atrial fibrillation. A study in awake chronically instrumented goats. Circulation. 1995;92(7):1954-1968.
6. Rensma PL, Allessie MA, Lammers WJ, Bonke FI, Schalij MJ. Length of excitation wave and susceptibility to reentrant atrial arrhythmias in normal conscious dogs. Circ Res. 1988;62(2):395-410.
7. Wakili R, Voigt N, Kääb S, Dobrev D, Nattel S. Recent advances in the molecular pathophysiology of atrial fibrillation. J Clin Invest. 2011;121(8):2955-2968.
8. Coetzee WA, Opie LH. Effects of components of ischemia and metabolic inhibition on delayed afterdepolarizations in guinea pig papillary muscle. Circ Res. 1987;61(2):157-165.
9. Katra RP, Laurita KR. Cellular mechanism of calcium-mediated triggered activity in the heart. Circ Res. 2005;96(5):535-542.
10. Dobrev D, Voigt N, Wehrens XHT. The ryanodine receptor channel as a molecular motif in atrial fibrillation: Pathophysiological and therapeutic implications. Cardiovasc Res. 2011;89(4):734-743.
11. Ming Z, Nordin C, Aronson RS. Role of L-type calcium channel window current in generating current-induced early afterdepolarizations. J Cardiovasc Electrophysiol. 1994;5(4):323-334.
12. Morillo CA, Klein GJ, Jones DL, Guiraudon CM. Chronic rapid atrial pacing: Structural, functional, and electrophysiological characteristics of a new model of sustained atrial fibrillation. Circulation. 1995;91(5):1588-1595.
13. Ausma J, Wijffels M, Thoné F, Wouters L, Allessie M, Borgers M. Structural changes of atrial myocardium due to sustained atrial fibrillation in the goat. Circulation. 1997;96(9):3157-3163.
14. Aimé-Sempé C, Folliguet T, Rücker-Martin C, Krajewska M, Krajewska S, Heimburger M, et al. Myocardial cell death in fibrillating and dilated human right atria. J Am Coll Cardiol. 1999;34(5):1577-1586.

15. Hanna N, Cardin S, Leung T-K, Nattel S. Differences in atrial versus ventricular remodeling in dogs with ventricular tachypacing-induced congestive heart failure. Cardiovasc Res. 2004;63(2):236-244.
16. Cardin S, Li D, Thorin-Trescases N, Leung T-K, Thorin E, Nattel S. Evolution of the atrial fibrillation substrate in experimental congestive heart failure: Angiotensin-dependent and -independent pathways. Cardiovasc Res. 2003;60(2):315-325.
17. Kostin S, Klein G, Szalay Z, Hein S, Bauer EP, Schaper J. Structural correlate of atrial fibrillation in human patients. Cardiovasc Res. 2002;54(2):361-379.
18. Xu J, Cui G, Esmailian F, Plunkett M, Marelli D, Ardehali A, et al. Atrial extracellular matrix remodeling and the maintenance of atrial fibrillation. Circulation. 2004;109(3):363-368.
19. Verheule S, Tuyls E, Gharaviri A, Hulsmans S, van Hunnik A, Kuiper M, et al. Loss of continuity in the thin epicardial layer because of endomysial fibrosis increases the complexity of atrial fibrillatory conduction. Circ Arrhythm Electrophysiol. 2013;6(1):202-211.
20. Banerjee I, Fuseler JW, Price RL, Borg TK, Baudino TA. Determination of cell types and numbers during cardiac development in the neonatal and adult rat and mouse. Am J Physiol Heart Circ Physiol. 2007;293(3):H1883-H1891.
21. Rohr S. Arrhythmogenic implications of fibroblast-myocyte interactions. Circ Arrhythm Electrophysiol. 2012;5(2):442-452.
22. Yue L, Xie J, Nattel S. Molecular determinants of cardiac fibroblast electrical function and therapeutic implications for atrial fibrillation. Cardiovasc Res. 2011;89(4):744-753.
23. Camelliti P, Borg TK, Kohl P. Structural and functional characterisation of cardiac fibroblasts. Cardiovasc Res. 2005;65(1):40-51.
24. Burstein B, Qi X-Y, Yeh Y-H, Calderone A, Nattel S. Atrial cardiomyocyte tachycardia alters cardiac fibroblast function: a novel consideration in atrial remodeling. Cardiovasc Res. 2007;76(3):442-452.
25. Benjamin EJ, Levy D, Vaziri SM, D'Agostino RB, Belanger AJ, Wolf PA. Independent risk factors for atrial fibrillation in a population-based cohort: The Framingham Heart Study. JAMA. 1994;271(11):840-844.
26. Sanfilippo AJ, Abascal VM, Sheehan M, Oertel LB, Harrigan P, Hughes RA, et al. Atrial enlargement as a consequence of atrial fibrillation: A prospective echocardiographic study. Circulation. 1990;82(3):792-797.
27. Welikovitch L, Lafreniere G, Burggraf GW, Sanfilippo AJ. Change in atrial volume following restoration of sinus rhythm in patients with atrial fibrillation: a prospective echocardiographic study. Can J Cardiol. 1994;10(10):993-996.
28. Haemers P, Hamdi H, Guedj K, Suffee N, Farahmand P, Popovic N, et al. Atrial fibrillation is associated with the fibrotic remodelling of adipose tissue in the subepicardium of human and sheep atria. Eur Heart J. 2017;38(1):53-61.
29. Kanazawa H, Yamabe H, Enomoto K, Koyama J, Morihisa K, Hoshiyama T, et al. Importance of pericardial fat in the formation of

complex fractionated atrial electrogram region in atrial fibrillation. Int J Cardiol. 2014;174(3):557-564.
30. Mahajan R, Lau DH, Brooks AG, Shipp NJ, Manavis J, Wood JPM, et al. Electrophysiological, electroanatomical, and structural remodeling of the atria as consequences of sustained obesity. J Am Coll Cardiol. 2015;66(1):1-11.
31. Coumel P, Attuel P, Lavallée J, Flammang D, Leclercq JF, Slama R. The atrial arrhythmia syndrome of vagal origin. Arch Mal Coeur Vaiss. 1978;71(6):645-656.
32. Yu L, Scherlag BJ, Li S, Fan Y, Dyer J, Male S, et al. Low-level transcutaneous electrical stimulation of the auricular branch of the vagus nerve: A noninvasive approach to treat the initial phase of atrial fibrillation. Heart Rhythm. 2013;10(3):428-435.
33. Yu L, Scherlag BJ, Sha Y, Li S, Sharma T, Nakagawa H, et al. Interactions between atrial electrical remodeling and autonomic remodeling: How to break the vicious cycle. Heart Rhythm. 2012;9(5):804-809.
34. Zhang L, Po SS, Wang H, Scherlag BJ, Li H, Sun J, et al. Autonomic remodeling: How atrial fibrillation begets atrial fibrillation in the first 24 hours. J Cardiovasc Pharmacol. 2015;66(3):307-315.
35. Haïssaguerre M, Jaïs P, Shah DC, Takahashi A, Hocini M, Quiniou G, et al. Spontaneous initiation of atrial fibrillation by ectopic beats originating in the pulmonary veins. N Engl J Med. 1998;339(10):659-666.
36. Ho SY, Cabrera JA, Tran VH, Farre J, Anderson RH, Sanchez-Quintana D. Architecture of the pulmonary veins: Relevance to radiofrequency ablation. Heart. 2001;86(3):265-270.
37. Haïssaguerre M, Jaïs P, Shah DC, Arentz T, Kalusche D, Takahashi A, et al. Catheter ablation of chronic atrial fibrillation targeting the reinitiating triggers. J Cardiovasc Electrophysiol. 2000;11(1):2-10.
38. Chen Y-J, Chen S-A. Electrophysiology of pulmonary veins. J Cardiovasc Electrophysiol. 2006;17(2):220-224.
39. Corradi D, Callegari S, Gelsomino S, Lorusso R, Macchi E. Morphology and pathophysiology of target anatomical sites for ablation procedures in patients with atrial fibrillation. Part I: Atrial structures (atrial myocardium and coronary sinus). Int J Cardiol. 2013;168(3):1758-1768.
40. Chen SA, Hsieh MH, Tai CT, Tsai CF, Prakash VS, Yu WC, et al. Initiation of atrial fibrillation by ectopic beats originating from the pulmonary veins: Electrophysiological characteristics, pharmacological responses, and effects of radiofrequency ablation. Circulation. 1999;100(18):1879-1886.
41. Anselmino M, Ferraris F, Cerrato N, Barbero U, Scaglione M, Gaita F. Left persistent superior vena cava and paroxysmal atrial fibrillation: The role of selective radio-frequency transcatheter ablation. J Cardiovasc Med (Hagerstown). 2014;15(8):647-652.
42. Nattel S, Burstein B, Dobrev D. Atrial remodeling and atrial fibrillation: Mechanisms and implications. Circ Arrhythm Electrophysiol. 2008;1(1):62-73.

43. Zou R, Kneller J, Leon LJ, Nattel S. Substrate size as a determinant of fibrillatory activity maintenance in a mathematical model of canine atrium. Am J Physiol Heart Circ Physiol. 2005;289(3):H1002-H1012.
44. Schotten U, Verheule S, Kirchhof P, Goette A. Pathophysiological mechanisms of atrial fibrillation: A translational appraisal. Physiol Rev. 2011;91(1):265-325.
45. Allessie MA, Bonke FI, Schopman FJ. Circus movement in rabbit atrial muscle as a mechanism of tachycardia. Circ Res. 1973;33(1):54-62.
46. Comtois P, Kneller J, Nattel S. Of circles and spirals: Bridging the gap between the leading circle and spiral wave concepts of cardiac reentry. Europace. 2005;7(Suppl 2):10-20.
47. Jalife J, Berenfeld O, Mansour M. Mother rotors and fibrillatory conduction: A mechanism of atrial fibrillation. Cardiovasc Res. 2002;54(2):204-216.
48. Winfree AT. Spiral waves of chemical activity. Science. 1972;175(4022):634-636.
49. Winfree AT. Varieties of spiral wave behavior: An experimentalist's approach to the theory of excitable media. Chaos. 1991;1(3):303-334.
50. Narayan SM, Baykaner T, Clopton P, Schricker A, Lalani GG, Krummen DE, et al. Ablation of rotor and focal sources reduces late recurrence of atrial fibrillation compared with trigger ablation alone: Extended follow-up of the CONFIRM trial (Conventional Ablation for Atrial Fibrillation With or Without Focal Impulse and Rotor Modulation). J Am Coll Cardiol. 2014;63(17):1761-1768.
51. Moe GK, Rheinboldt WC, Abildskov JA. A computer model of atrial fibrillation. Am Heart J. 1964;67(2):200-220.
52. Gleason KT, Nazarian S, Dennison Himmelfarb CR. Atrial fibrillation symptoms and sex, race, and psychological distress: A literature review. J Cardiovasc Nurs. 2018;33(2):137-143.
53. Streur M, Ratcliffe SJ, Ball J, Stewart S, Riegel B. Symptom clusters in adults with chronic atrial fibrillation. J Cardiovasc Nurs. 2017;32(3):296-303.
54. McCabe PJ, Rhudy LM, DeVon HA. Patients' experiences from symptom onset to initial treatment for atrial fibrillation. J Clin Nurs. 2015;24(5-6):786-796.
55. Blum S, Muff C, Aeschbacher S, Ammann P, Erne P, Moschovitis G, et al. Prospective assessment of sex-related differences in symptom status and health perception among patients with atrial fibrillation. J Am Heart Assoc. 2017 Jun;6(7):e005641.
56. Randolph TC, Simon DN, Thomas L, Allen LA, Fonarow GC, Gersh BJ, et al. Patient factors associated with quality of life in atrial fibrillation. Am Heart J. 2016;182:135-143.
57. Steinberg BA, Holmes DN, Pieper K, Allen LA, Chan PS, Ezekowitz MD, et al. Factors associated with large improvements in health-related quality of life in patients with atrial fibrillation: Results from ORBIT-AF. Circ Arrhythm Electrophysiol. 2020;13(5):e007775.
58. Walters TE, Wick K, Tan G, Mearns M, Joseph SA, Morton JB, et al. Symptom severity and quality of life in patients with atrial fibrillation:

Psychological function outweighs clinical predictors. Int J Cardiol. 2019;279:84-89.
59. Ceornodolea AD, Bal R, Severens JL. Epidemiology and management of atrial fibrillation and stroke: Review of data from four European countries. Stroke Res Treat. 2017; 2017:8593207.
60. Lin HJ, Wolf PA, Kelly-Hayes M, Beiser AS, Kase CS, Benjamin EJ, et al. Stroke severity in atrial fibrillation: The Framingham Study. Stroke. 1996;27(10):1760-1764.
61. Frost L, Engholm G, Johnsen S, Møller H, Henneberg EW, Husted S. Incident thromboembolism in the aorta and the renal, mesenteric, pelvic, and extremity arteries after discharge from the hospital with a diagnosis of atrial fibrillation. Arch Intern Med. 2001;161(2):272-276.
62. Kotecha D, Lam CSP, Van Veldhuisen DJ, Van Gelder IC, Voors AA, Rienstra M. Heart failure with preserved ejection fraction and atrial fibrillation: Vicious twins. J Am Coll Cardiol. 2016;68(20):2217-2228.
63. Ziff OJ, Carter PR, McGowan J, Uppal H, Chandran S, Russell S, et al. The interplay between atrial fibrillation and heart failure on long-term mortality and length of stay: Insights from the United Kingdom ACALM registry. Int J Cardiol. 2018;252:117-121.
64. Steinberg BA, Kim S, Fonarow GC, Thomas L, Ansell J, Kowey PR, et al. Drivers of hospitalization for patients with atrial fibrillation: Results from the Outcomes Registry for Better Informed Treatment of Atrial Fibrillation (ORBIT-AF). Am Heart J. 2014;167(5):735-742.e2.
65. Kirchhof P, Schmalowsky J, Pittrow D, Rosin L, Kirch W, Wegscheider K, et al. Management of patients with atrial fibrillation by primary-care physicians in Germany: 1-year results of the ATRIUM registry. Clin Cardiol. 2014;37(5):277-284.
66. Meyre P, Blum S, Berger S, Aeschbacher S, Schoepfer H, Briel M, et al. Risk of hospital admissions in patients with atrial fibrillation: A systematic review and meta-analysis. Can J Cardiol. 2019;35(10):1332-1343.
67. Sepehri Shamloo A, Dagres N, Müssigbrodt A, Stauber A, Kircher S, Richter S, et al. Atrial fibrillation and cognitive impairment: New insights and future directions. Heart Lung Circ. 2020;29(1):69-85.
68. Conen D, Rodondi N, Müller A, Beer JH, Ammann P, Moschovitis G, et al. Relationships of overt and silent brain lesions with cognitive function in patients with atrial fibrillation. J Am Coll Cardiol. 2019;73(9):989-999.
69. Magnussen C, Niiranen TJ, Ojeda FM, Gianfagna F, Blankenberg S, Njølstad I, et al. Sex differences and similarities in atrial fibrillation epidemiology, risk factors, and mortality in community cohorts: Results from the BiomarCaRE Consortium (Biomarker for Cardiovascular Risk Assessment in Europe). Circulation. 2017;136(17):1588-1597.
70. König S, Ueberham L, Schuler E, Wiedemann M, Reithmann C, Seyfarth M, et al. In-hospital mortality of patients with atrial arrhythmias: Insights from the German-wide Helios hospital network of 161,502 patients and 34,025 arrhythmia-related procedures. Eur Heart J. 2018;39(44):3947-3957.
71. An Y, Ogawa H, Yamashita Y, Ishii M, Iguchi M, Masunaga N, et al.

Causes of death in Japanese patients with atrial fibrillation: The Fushimi Atrial Fibrillation Registry. Eur Heart J Qual Care Clin Outcomes. 2019;5(1):35-42.
72. Papez JW. Heart musculature of the atria. Am J Anat. 1920;27(3):255-285.
73. Ho SY, Sanchez-Quintana D, Cabrera JA, Anderson RH. Anatomy of the left atrium: Implications for radiofrequency ablation of atrial fibrillation. J Cardiovasc Electrophysiol. 1999;10(11):1525-1533.
74. Kistler PM, Ho SY, Rajappan K, Morper M, Harris S, Abrams D, et al. Electrophysiologic and anatomic characterization of sites resistant to electrical isolation during circumferential pulmonary vein ablation for atrial fibrillation: A prospective study. J Cardiovasc Electrophysiol. 2007;18(12):1282-1288.
75. Inoue J, Skanes AC, Gula LJ, Drangova M. Effect of left atrial wall thickness on radiofrequency ablation success. J Cardiovasc Electrophysiol. 2016;27(11):1298-1303.
76. Takahashi K, Okumura Y, Watanabe I, Nagashima K, Sonoda K, Sasaki N, et al. Relation between left atrial wall thickness in patients with atrial fibrillation and intracardiac electrogram characteristics and ATP-provoked dormant pulmonary vein conduction. J Cardiovasc Electrophysiol. 2015;26(6):597-605.
77. Suenari K, Nakano Y, Hirai Y, Ogi H, Oda N, Makita Y, et al. Left atrial thickness under the catheter ablation lines in patients with paroxysmal atrial fibrillation: Insights from 64-slice multidetector computed tomography. Heart Vessels. 2013;28(3):360-368.
78. Nakamura K, Funabashi N, Uehara M, Ueda M, Murayama T, Takaoka H, et al. Left atrial wall thickness in paroxysmal atrial fibrillation by multislice-CT is initial marker of structural remodeling and predictor of transition from paroxysmal to chronic form. Int J Cardiol. 2011;148(2):139-147.
79. Sun J-Y, Yun C-H, Mok GSP, Liu Y-H, Hung C-L, Wu T-H, et al. Left atrium wall-mapping application for wall thickness visualization. Sci Rep. 2018;8(1):4169.
80. Bishop M, Rajani R, Plank G, Gaddum N, Carr-White G, Wright M, et al. Three-dimensional atrial wall thickness maps to inform catheter ablation procedures for atrial fibrillation. Europace. 2016;18(3):376-383.
81. Kirchhof P, Camm AJ, Goette A, Brandes A, Eckardt L, Elvan A, et al. Early rhythm-control therapy in patients with atrial fibrillation. N Engl J Med. 2020;383(14):1305-1316.
82. Roy D, Talajic M, Dorian P, Connolly S, Eisenberg MJ, Green M, et al. Amiodarone to prevent recurrence of atrial fibrillation: Canadian trial of atrial fibrillation investigators. N Engl J Med. 2000;342(13):913-920.
83. Doyle JF, Ho KM. Benefits and risks of long-term amiodarone therapy for persistent atrial fibrillation: A meta-analysis. Mayo Clin Proc. 2009;84(3):234-242.
84. Khan AR, Khan S, Sheikh MA, Khuder S, Grubb B, Moukarbel GV. Catheter ablation and antiarrhythmic drug therapy as first- or second-line therapy in the management of atrial fibrillation: Systematic review

and meta-analysis. Circ Arrhythm Electrophysiol. 2014;7(5):853-860.
85. Poole JE, Bahnson TD, Monahan KH, Johnson G, Rostami H, Silverstein AP, et al. Recurrence of atrial fibrillation after catheter ablation or antiarrhythmic drug therapy in the CABANA trial. J Am Coll Cardiol. 2020;75(25):3105-3118.
86. Santangeli P, Di Biase L, Burkhardt DJ, Horton R, Sanchez J, Bai R, et al. Catheter ablation of atrial fibrillation: State-of-the-art techniques and future perspectives. J Cardiovasc Med. 2012;13(2):108-124.
87. Oral H, Knight BP, Tada H, Ozaydin M, Chugh A, Hassan S, et al. Pulmonary vein isolation for paroxysmal and persistent atrial fibrillation. Circulation. 2002;105(9):1077-1081.
88. Huang C, Wang J, He C, Yang K, Zhao H, Chen J, et al. The efficacy and safety of cryoballoon versus radiofrequency ablation for the treatment of atrial fibrillation: A meta-analysis of 15 international randomized trials. Cardiol Rev. 2023 Mar 28. doi: 10.1097/CRD.0000000000000531.
89. Ouyang F, Tilz R, Chun J, Schmidt B, Wissner E, Zerm T, et al. Long-term results of catheter ablation in paroxysmal atrial fibrillation: Lessons from a 5-year follow-up. Circulation. 2010;122(23):2368-2377.
90. Kuck K-H, Hoffmann BA, Ernst S, Wegscheider K, Treszl A, Metzner A, et al. Impact of complete versus incomplete circumferential lines around the pulmonary veins during catheter ablation of paroxysmal atrial fibrillation: Results from the Gap-Atrial Fibrillation-German Atrial Fibrillation Competence Network 1 Trial. Circ Arrhythm Electrophysiol. 2016 Jan;9(1):e003337.
91. Cappato R, Negroni S, Pecora D, Bentivegna S, Lupo PP, Carolei A, et al. Prospective assessment of late conduction recurrence across radiofrequency lesions producing electrical disconnection at the pulmonary vein ostium in patients with atrial fibrillation. Circulation. 2003 Sep;108(13):1599-1604.
92. Ikeda A, Nakagawa H, Lambert H, Shah DC, Fonck E, Yulzari A, et al. Relationship between catheter contact force and radiofrequency lesion size and incidence of steam pop in the beating canine heart: Electrogram amplitude, impedance, and electrode temperature are poor predictors of electrode-tissue contact force and lesion. Circ Arrhythm Electrophysiol. 2014 Dec;7(6):1174-1180.
93. Thiagalingam A, D'Avila A, Foley L, Guerrero JL, Lambert H, Leo G, et al. Importance of catheter contact force during irrigated radiofrequency ablation: Evaluation in a porcine ex vivo model using a force-sensing catheter. J Cardiovasc Electrophysiol. 2010 Jul;21(7):806-811.
94. Barkagan M, Rottmann M, Leshem E, Shen C, Buxton AE, Anter E. Effect of baseline impedance on ablation lesion dimensions. Circ Arrhythm Electrophysiol. 2018 Oct;11(10):e006690.
95. Reddy VY, Dukkipati SR, Neuzil P, Natale A, Albenque J-P, Kautzner J, et al. Randomized, controlled trial of the safety and effectiveness of a contact force-sensing irrigated catheter for ablation of paroxysmal atrial fibrillation: Results of the TactiCath Contact Force Ablation Catheter Study for Atrial Fibrillation (TOCCASTAR) Study. Circulation. 2015

Sep;132(10):907-915.
96. Shah DC, Lambert H, Nakagawa H, Langenkamp A, Aeby N, Leo G. Area under the real-time contact force curve (force-time integral) predicts radiofrequency lesion size in an in vitro contractile model. J Cardiovasc Electrophysiol. 2010 Sep;21(9):1038-1043.
97. De Potter T, Van Herendael H, Balasubramaniam R, Wright M, Agarwal SC, Sanders P, et al. Safety and long-term effectiveness of paroxysmal atrial fibrillation ablation with a contact force-sensing catheter: Real-world experience from a prospective, multicentre observational cohort registry. Europace. 2018 Nov;20(FI_3):f410-f418.
98. Das M, Loveday JJ, Wynn GJ, Gomes S, Saeed Y, Bonnett LJ, et al. Ablation index, a novel marker of ablation lesion quality: Prediction of pulmonary vein reconnection at repeat electrophysiology study and regional differences in target values. Europace. 2017 May;19(5):775-783.
99. Hussein A, Das M, Chaturvedi V, Asfour IK, Daryanani N, Morgan M, et al. Prospective use of ablation index targets improves clinical outcomes following ablation for atrial fibrillation. J Cardiovasc Electrophysiol. 2017 Sep;28(9):1037-1047.
100. Blomström-Lundqvist C, Gizurarson S, Schwieler J, Jensen SM, Bergfeldt L, Kennebäck G, et al. Effect of catheter ablation vs antiarrhythmic medication on quality of life in patients with atrial fibrillation: The CAPTAF randomized clinical trial. JAMA. 2019 Mar;321(11):1059-1068.
101. Mark DB, Anstrom KJ, Sheng S, Piccini JP, Baloch KN, Monahan KH, et al. Effect of catheter ablation vs medical therapy on quality of life among patients with atrial fibrillation: The CABANA randomized clinical trial. JAMA. 2019 Apr;321(13):1275-1285.
102. Saliba W, Schliamser JE, Lavi I, Barnett-Griness O, Gronich N, Rennert G. Catheter ablation of atrial fibrillation is associated with reduced risk of stroke and mortality: A propensity score-matched analysis. Heart Rhythm. 2017 May;14(5):635-642.
103. Friberg L, Tabrizi F, Englund A. Catheter ablation for atrial fibrillation is associated with lower incidence of stroke and death: Data from Swedish health registries. Eur Heart J. 2016 Aug;37(31):2478-2487.
104. Marrouche NF, Kheirkhahan M, Brachmann J. Catheter ablation for atrial fibrillation with heart failure. N Engl J Med. 2018;378(5):417-427.
105. Hunter RJ, Berriman TJ, Diab I, Kamdar R, Richmond L, Baker V, et al. A randomized controlled trial of catheter ablation versus medical treatment of atrial fibrillation in heart failure (the CAMTAF trial). Circ Arrhythm Electrophysiol. 2014 Feb;7(1):31-38.
106. Di Biase L, Mohanty P, Mohanty S, Santangeli P, Trivedi C, Lakkireddy D, et al. Ablation versus amiodarone for treatment of persistent atrial fibrillation in patients with congestive heart failure and an implanted device: Results from the AATAC multicenter randomized trial. Circulation. 2016 Apr;133(17):1637-1644.
107. Turagam MK, Garg J, Whang W, Sartori S, Koruth JS, Miller MA, et al. Catheter ablation of atrial fibrillation in patients with heart failure: A

meta-analysis of randomized controlled trials. Ann Intern Med. 2019 Jan;170(1):41-50.
108. Benali K, Khairy P, Hammache N, Petzl A, Da Costa A, Verma A, et al. Procedure-related complications of catheter ablation for atrial fibrillation. J Am Coll Cardiol. 2023 May;81(21):2089-2099.
109. Sanchez-Quintana D, Cabrera JA, Climent V, Farre J, Mendonca MC, Ho SY. Anatomic relations between the esophagus and left atrium and relevance for ablation of atrial fibrillation. Circulation. 2005 Sep;112(10):1400-1405.
110. Lakkireddy D, Reddy YM, Atkins D, Rajasingh J, Kanmanthareddy A, Olyaee M, et al. Effect of atrial fibrillation ablation on gastric motility: The atrial fibrillation gut study. Circ Arrhythm Electrophysiol. 2015 Jun;8(3):531-536.
111. Halbfass P, Pavlov B, Müller P, Nentwich K, Sonne K, Barth S, et al. Progression from esophageal thermal asymptomatic lesion to perforation complicating atrial fibrillation ablation: A single-center registry. Circ Arrhythm Electrophysiol. 2017 Aug;10(8):e005233.
112. Kapur S, Barbhaiya C, Deneke T, Michaud GF. Esophageal injury and atrioesophageal fistula caused by ablation for atrial fibrillation. Circulation. 2017 Sep;136(13):1247-1255.
113. Zellerhoff S, Ullerich H, Lenze F, Meister T, Wasmer K, Mönnig G, et al. Damage to the esophagus after atrial fibrillation ablation: Just the tip of the iceberg? High prevalence of mediastinal changes diagnosed by endosonography. Circ Arrhythm Electrophysiol. 2010 Apr;3(2):155-159.
114. Kennedy R, Good E, Oral H, Huether E, Bogun F, Pelosi F, et al. Temporal stability of the location of the esophagus in patients undergoing a repeat left atrial ablation procedure for atrial fibrillation or flutter. J Cardiovasc Electrophysiol.´ 2008 Apr;19(4):351-355.
115. Yamashita K, Quang C, Schroeder JD, DiBella E, Han F, MacLeod R, et al. Distance between the left atrium and the vertebral body is predictive of esophageal movement in serial MR imaging. J Interv Card Electrophysiol. 2018 Jul;52(2):149-156.
116. Starek Z, Lehar F, Jez J, Scurek M, Wolf J, Kulik T, et al. Esophageal positions relative to the left atrium; data from 293 patients before catheter ablation of atrial fibrillation. Indian Heart J. 2018;70(1):37-44.